Sequential Monte Carlo methods for probabilistic forecasts and uncertainty assessment in hydrologic modeling

by

Seong Jin NOH

2012

Sequential Monte Carlo methods for probabilistic forecasts and uncertainty assessment in hydrologic modeling

by

Seong Jin NOH

A Dissertation

submitted in partial fulfillment of the requirement

for the degree of Doctor of Philosophy

Dept. of Urban and Environmental Engineering

Kyoto University, Japan

2012

To my family

Abstract

In this thesis, we develop methodology and a software framework to apply the sequential Monte Carlo (SMC) methods for hydrologic modeling and demonstrate applicability of proposed methods in various case studies. The SMC methods are a Bayesian learning process in which the propagation of all uncertainties is carried out by a suitable selection of randomly generated particles without any assumptions about the nature of the distributions. Unlike the conventional Kalman filter-based methods that are basically limited to the linear updating rule and the assumption of Gaussian distribution errors, SMC filters have the advantage of being applicable to non-linear, non-Gaussian, state-space models.

Chapter 2 reviews the basic theory of Bayesian filtering and various data assimilation (DA) methods such as Kalman filtering, variational assimilation and the sequential Monte Carlo methods.

Chapter 3 proposes a dual updating scheme of state and parameter (DUS) based on the SMC methods to estimate both state and parameter variables of a lumped hydrologic model. The applicability of the DUS is illustrated using the implementation of the storage function model. The forecast provided by the DUS is superior to that of state only updating and deterministic modeling in terms of the model accuracy criteria, a scatter diagram, and simulated hydrographs. A significant reduction of parameter uncertainty is observed for all parameters, and estimated parameter distributions show good conformity with off-line optimum.

Chapter 4 proposes an improved particle filtering approach to consider different response times of internal state variables in a hydrologic model. The proposed method adopts a lagged filtering approach to aggregate model response until the uncertainty of each hydrologic process is propagated. A distributed hydrologic model, water and energy transfer processes (WEP), is implemented for hindcasting of streamflow at the Katsura catchment, Japan via two particle filters:

the lagged regularized particle filter (LRPF) and the sequential importance resampling (SIR) particle filter. The LRPF shows consistent forecasts regardless of the process noise assumption, while the SIR has different values of optimal process noise and shows sensitive variation of confidence intervals.

Chapter 5 presents performance assessment of ensemble Kalman filtering (EnKF) and particle filtering (PF) for short-term streamflow forecasting with a distributed hydrologic model. For both EnKF and PF, sequential data assimilation is performed within a lag-time window to account for lag and response times for internal hydrologic processes in a hydrologic model. Proposed methods are applied to two catchments in Japan and Korea to assess the performance of the methods. The forecasting accuracy of both filters is improved when sufficient lag times are provided. EnKF is sensitive to lag times and exhibits limited forecasting ability with short lead times, while PF exhibits more stable forecasting ability for the range of lead times examined.

Chapter 6 develops a hydrologic modeling framework for data assimilation, namely MPI-OHyMoS. While adapting object-oriented features of the original OHyMoS, MPI-OHyMoS allows users to easily build a probabilistic hydrologic model with data assimilation. In this software framework, PF is available for any hydrologic models considering various sources of uncertainty originated from input forcing, parameters and observations. Ensemble simulations are parallelized by the message passing interface (MPI), which can take advantage of a high performance computing (HPC) system. Structure and implementation processes of DA via MPI-OHyMoS are illustrated using a simple lumped model. MPI-OHyMoS is applied for the uncertainty assessment of a distributed hydrologic model in both synthetic and real experiment cases. In the synthetic experiment, dual state-parameter updating results in a reasonable estimation of parameters to cover synthetic true values within their posterior distributions. In the real experiments, The DUS via MPI-OHyMoS results in a reasonable agreement to the observed hydrograph with reduced uncertainty of parameters.

Keywords: *Sequential Monte Carlo methods, particle filtering, data assimilation, dual state-parameter updating scheme, distributed hydrologic model, ensemble Kalman filtering, MPI-OHyMoS, uncertainty assessment*

Declaration of authorship

I declare that this thesis titled ‘Sequential Monte Carlo methods for probabilistic forecasts and uncertainty assessment in hydrologic modeling’ is, the result of my own investigations, except where specifically indicated in the text, and has not been submitted, either in part or whole, for a degree at this or any other University.

Seong Jin Noh

Acknowledgement

The research in the thesis was conducted under the full-time PhD course in Hydrology and Water Resources Research Laboratory, Kyoto University. This thesis was guided and improved by committee members, Prof. Michiharu Shiiba, my supervisor, Associate Prof. Yasuto Tachikawa and Prof. Kaoru Takara. In retrospect of my PhD course, I was a very lucky man encouraged by all the people around me. I came to realize that I could not acknowledge all their helps and supports within this limited section. Instead of just mentioning their names, I would like to express my deepest gratitude to all the people to help me and my family stay in Japan and study in excellent research environment. The relationship with them is the priceless treasure that I found during my PhD course. I’ll try my best to keep and strengthen this relationship wherever I go. Especially, I would like to express my gratitude to you, now reading my thesis. I wish that my research could be a guide to inspire you with another interesting idea as I have always been inspired from you.
Thank you all!

Contents

List of figures

List of tables

Abbreviations

ASIR	Auxiliary sequential importance resampling
DA	Data assimilation
DEM	Digital elevation map
DUS	Dual updating scheme of state and parameter
EKF	Extended Kalman filter
EnKF	Ensemble Kalman filtering
EnSRF	Ensemble square root filter
KF	Kalman filtering
HPC	High performance computing
OHyMoS	Object-oriented hydrological modeling system
LRPF	lagged regularized particle filter
MCMC	Markov chain Monte Carlo
MISE	Mean integrated square error
MPI	Message passing interface
MPI-OHyMoS	MPI based OHyMoS
PDF	Probability density function
PF	Particle filtering
RPF	Regularized particle filter
SF	Storage function
SIR	Sequential importance resampling
SIS	Sequential importance sampling
SMC	Sequential Monte Carlo
SPMD	Single-program multiple-data
VAR	Variational assimilation
WEP	Water and energy transfer processes

Chapter 1

Introduction

1.1 Background

Identification and minimization of uncertainty are key issues in the hydrologic prediction. Uncertainty in the modeling process can be categorized into three main sources: measurement, parameter, and structural uncertainties (Smith et al., 2008). The measurement uncertainty comes not only from the inaccuracy of the observation equipment but also from incommensurability arising from the differences in temporal and spatial scales between models and data (Beven, 2009). Parameter and structural uncertainties are originated from simplified conceptualization of complex hydrologic processes in hydrologic modeling or inadequate model structures that cannot be properly parameterized in the calibration processes with limited observations.

Data assimilation (DA) is a way to integrate information from a variety of sources to improve model accuracy, considering the uncertainty in both the measurement and modeling system. There have been considerable advances in hydrologic data assimilation for streamflow prediction (e.g., Kitanidis and Bras, 1980; Georgakakos, 1986; Vrugt et al., 2006; Clark et al., 2008; Seo et al., 2003, 2009). DA methods can be divided into two groups: off-line and on-line methods. In general, off-line methods such as GLUE (Beven and Binley, 1992), DREAM (Vrugt et al., 2008) and other Monte Carlo methods use all measurement information to find global optimum in the calibration period. On the other hand, on-line methods based on the state-space approach estimate sequentially the state

of a dynamic system using a sequence of measurement at each time step (Ristic et al., 2004). These on-line or sequential DA methods, the main concern of this thesis, have a significant advantage over traditional time-series techniques for real-time forecasts and explicit handling of predictive uncertainties.

For linear and Gaussian dynamics, Kalman filtering (KF) is the optimal data assimilation method (Kalman, 1960). For a nonlinear system, the extended Kalman filter (EKF) has been applied, but the EKF could lead to unstable results when the nonlinearity in a system is severe. The ensemble Kalman filtering (EnKF), introduced by Evensen (1994), is a Monte Carlo approximation to traditional KF. EnKF uses an ensemble of forecasts to estimate background error covariances (Whitaker and Hamill, 2002). The advantage of EnKF over the EKF is that it does not require the development of the linearized state-space formulation of the hydrological model (Clark et al., 2008). However, the posterior probability density of hydrologic states in a model is often non-Gaussian and cannot be adequately characterized by the first two moments (Leisenring and Moradkhani, 2011). In addition, as EnKF actively updates states, it does not explicitly comply with the principle of conservation of mass (Salamon and Feyen, 2010).

Another approach to data assimilation is variational assimilation (VAR), which has achieved widespread application in weather and oceanographic prediction models. Although variational methods are more computationally efficient than KF-based methods, the derivation of the adjoint model needed for minimisation of a cost function is difficult, especially in the case of non-linear, high dimensional hydrological applications (e.g., Liu and Gupta, 2007).

Among data assimilation techniques, the sequential Monte Carlo (SMC) methods are a Bayesian learning process in which the propagation of all uncertainties is carried out by a suitable selection of randomly generated particles without any assumptions about the nature of the distributions. Unlike the various Kalman filter-based methods that are basically limited to the linear updating rule and the assumption of Gaussian distribution errors, the SMC methods have the advantage of being applicable to non-linear, non-Gaussian, state-space models. Since their introduction in 1993 (Gordon et al., 1993), the application of these powerful and

versatile methods has been increasing in various areas, including pattern recognition, target tracking, financial analysis, and robotics (Ristic et al., 2004; del Moral, 2004; Cappé et al., 2005). In recent years, these methods have received considerable attention in hydrology and earth sciences (e.g., Moradkhani et al., 2005a; Weerts and El Serafy, 2006; Zhou et al., 2006; van Delft et al., 2009; van Leeuwen, 2009; Karssenberg et al., 2010; Noh et al., 2011a, 2011b, 2012). However, potentials of these versatile methods have not been fully explored in hydrologic community. In recent times the SMC methods have been implemented for low numbers of lumped or semi-lumped hydrologic models in the limited forecasting mode. Development and evaluation of elaborate schemes for dual state-parameter updating or spatially distributed hydrologic modelling have been limited. Open software frameworks for the SMC methods are required indeed.

1.2 Objectives

The main objectives of this thesis are as follows:

1. Development of a dual updating scheme of state and parameter (DUS) based on the SMC methods to estimate both state and parameter variables of a lumped hydrologic model. For the estimation of uncertain model parameters, a kernel smoothing method is used in the DUS.

2. Development of a robust particle filtering approach for considering different response times of internal state variables in a distributed hydrologic model. The regularized particle filter is used to preserve sample diversity under the lagged filtering approach.

3. Comparison of performance of ensemble Kalman filtering (EnKF) and particle filtering (PF) for short-term streamflow forecasting using a distributed hydrologic model. For both filters, sequential data assimilation is

performed within a lag-time window to account for lag and response times for internal hydrologic processes in a hydrologic model.

4. Development of a hydrologic modeling framework for data assimilation: MPI-OHyMoS. In this software framework, sequential data assimilation based on particle filtering is available for any hydrologic models considering various sources of uncertainty originated from input forcing, parameters and observations. MPI-OHyMoS allows user to easily build a probabilistic hydrologic model with data assimilation, while adapting object-oriented features of the original OHyMoS.

It should be noted that the objective of this thesis is not limited to simple implementation of the SMC methods for hydrologic modeling. As hydrologic models have non-linear, non-Gaussian properties, the SMC methods could be one of potential alternatives. However, due to unique features of hydrologic modeling, such as delayed response of hydrologic processes and aggregation of uncertainty in routing processes, new methodology and framework are required to improve applicability of versatile SMC methods in hydrologic modeling. Therefore, the higher goal of this thesis is development of methodology to properly apply the SMC methods for probabilistic forecasts and uncertainty assessment in hydrologic modeling.

1.3 Outline of the thesis

This thesis consists of a series of seven closely related chapters to achieve objectives described in the previous section.

Chapter 2 reviews the basic theory of Bayesian filtering and various data assimilation methods such as KF, VAR and the SMC methods.

Chapter 3 proposes a dual updating scheme of state and parameter (DUS) based on the SMC methods to estimate both state and parameter variables of a lumped

hydrologic model. We introduce a kernel smoothing method for the robust estimation of uncertain model parameters in the DUS. The applicability of the dual updating scheme is illustrated using the implementation of the storage function model at the Katsura catchment located in Kyoto, Japan.

Chapter 4 proposes an improved particle filtering approach to consider different response times of internal state variables in a hydrologic model. The proposed method adopts a lagged filtering approach to aggregate model response until the uncertainty of each hydrologic process is propagated. The regularization with an additional move step based on the Markov chain Monte Carlo (MCMC) methods is also implemented to preserve sample diversity under the lagged filtering approach. A distributed hydrologic model, namely water and energy transfer processes (WEP), is implemented for hindcasting of streamflow at the Katsura catchment, Japan via two particle filters: the lagged regularized particle filter (LRPF) and the sequential importance resampling (SIR) particle filter.

Chapter 5 presents performance assessment of EnKF and PF for short-term streamflow forecasting with a distributed hydrologic model, WEP. To mitigate the drawbacks of conventional filters, the ensemble square root filter (EnSRF) and the regularized particle filter (RPF) are implemented. For both the EnSRF and the RPF, sequential data assimilation is performed within a lag-time window to account for lag and response times for internal hydrologic processes in a hydrologic model. Proposed methods are applied to two catchments in Japan and Korea to assess the performance of the methods.

Chapter 6 develops a hydrologic modeling framework for data assimilation, namely MPI-OHyMoS. While adapting object-oriented features of the original OHyMoS, MPI-OHyMoS allows user to easily build a probabilistic hydrologic model with data assimilation. In this software framework, sequential data assimilation based on particle filtering is available for any hydrologic models considering various sources of uncertainty originated from input forcing, parameters and observations. Ensemble simulations are parallelized by the message passing interface (MPI), which can take advantage of a high

performance computing (HPC) system. We apply this software framework for uncertainty assessment of lumped and distributed hydrologic models in synthetic and real experiment cases.

Finally, **Chapter 7** presents conclusions of the thesis.

Chapter 2

Data assimilation methods

2.1 Introduction

Data assimilation (DA) methods are used to improve the predictions of a dynamic model using observations (van Velzen, 2010). Broadly speaking, DA methods may be divided into sequential and variational ones. In sequential methods such as Kalman filtering (KF) and the sequential Monte Carlo (SMC) methods, states are updated by assimilating observations sequentially. This analysis is performed for each time step when new measurements become available. Its impact depends on the uncertainties in both the observations and model states (Rakovec et al., 2012). Variational assimilation (VAR) rather minimizes a cost function over a simulation time window. At the beginning, a first-guess model is constructed, which is afterwards updated by creating an adjoint model which propagates backwards in time and incorporates the mismatch between the model and observations (Liu and Gupta, 2007). In the least squares sense, sequential and variational assimilation methods attempt to essentially solve the same minimization problem and, if the model dynamics is linear, are essentially equivalent (Li and Navon, 2001; Seo et al., 2003) and provide optimal solutions. However, if the non-linearity of the system is severe, the non-Gaussianity of the true posterior density will be more pronounced (e.g., it can be bimodal or heavily skewed). In such cases the performance of conventional KF and VAR methods will be degraded significantly (Ristic et al., 2004). On the other hand, the SMC methods, known as particle filtering (PF), do not need any assumptions about the

nature of the distributions representing the posterior probability density function (PDF) via particles with weights. Therefore, the SMC methods have the advantage of being applicable to non-linear, non-Gaussian, state-space models (Gordon et al., 1993; Arulampalam et al., 2002; Del Moral, 2004; Andrieu et al., 2010). Although the basic SMC methods had been introduced in the 1950, they were ignored due to the degeneracy problem of plain sequential importance sampling and the modest computing power. With the inclusion of the resampling step (Gordon et al., 1993) and parallel computing, research activity has dramatically increased, resulting in many improvements of the SMC methods and their numerous applications (Ristic et al., 2004).

In this chapter, we briefly describe the theory of Bayesian filtering and several data assimilation methods such as KF, VAR for optimal solution in linear, Gaussian cases and the SMC methods for suboptimal solution in non-linear, non-Gaussian cases. The performance evaluation criteria used within this thesis are summarized in the last section.

2.2 Bayesian filtering theory

The problem of filtering is to estimate sequentially the state of a dynamic system (e.g., hydrologic model) using a sequence of noisy measurements (e.g., streamflow, soil moisture) made on the system. To make inferences about a dynamic system, we use probabilistic state-space formulation and the Bayesian approach for updating of information on receipt of new measurements. In the Bayesian filtering, one attempts to construct the posterior PDF of the state, based on all available information, including the sequence of received measurements (Arulampalam et al., 2002).

To define the problem of Bayesian filtering, consider a general dynamic state-space model, which is described as follows:

$$x_k = f(x_{k-1}, u_k) + \omega_k \tag{2-1}$$

$$y_k = h(x_k) + \nu_k \tag{2-2}$$

where x_k is the n_x-dimensional vector denoting the system state at time k. The operator $f:\Re^{n_x}\to\Re^{n_x}$ expresses the system transition of the state x_{k-1} in response to the forcing data u_k. y_k is the measurement. $h:\Re^{n_x}\to\Re^{n_y}$ expresses the measurement function. $\Re$ is a set of real numbers. ω_k and v_k represent the model error and the measurement error, respectively, whose covariances are W_k and V_k. The objective of filtering is to recursively estimate x_k base on the set of all available measurements $y_{1:k} = \{y_i, i = 1, \ldots, k\}$. Thus, it is required to construct the PDF $p(x_k \mid y_{1:k})$ (Arulampalam et al., 2002). If the initial PDF $p(x_0 \mid y_0) \equiv p(x_0)$ is available as prior information, the PDF $p(x_k \mid y_{1:k})$ may be obtained recursively in two stages: prediction and update.

Suppose that the PDF $p(x_{k-1} \mid y_{1:k-1})$ at time $k-1$ is available. The prediction stage involves using the system transition Eq. (2-1) to obtain the prediction probability density of the state at time k via the Chapman-Kolmogorov equation

$$p(x_k \mid y_{1:k-1}) = \int p(x_k \mid x_{k-1}) p(x_{k-1} \mid y_{1:k-1}) dx_{k-1} \tag{2-3}$$

In the above equation, a Markov process of order one has been used as $p(x_k \mid x_{k-1}, y_{1:k-1}) = p(x_k \mid x_{k-1})$. The probabilistic model of the state evolution is constructed by the system transition and the model error ω_k in Eq. (2-1).

When a measurement becomes available at time step, updating stage is carried out via Bayes' rule

$$\begin{aligned} p(x_k \mid y_{1:k}) &= p(x_k \mid y_k, y_{1:k-1}) \\ &= \frac{p(y_k \mid x_k, y_{1:k-1}) p(x_k \mid y_{1:k-1})}{p(y_k \mid y_{1:k-1})} \\ &= \frac{p(y_k \mid x_k) p(x_k \mid y_{1:k-1})}{p(y_k \mid y_{1:k-1})} \end{aligned} \tag{2-4}$$

Where the normalizing constant

$$p(y_k \mid y_{1:k-1}) = \int p(y_k \mid x_k) p(x_k \mid y_{1:k-1}) dx_k \tag{2-5}$$

depends on the likelihood function $p(y_k \mid x_k)$, defined by the measurement model and the error v_k in Eq. (2-2).

The recurrence relations of Eqs. (2-3) and (2-4) are the basis for the optimal Bayesian solution. However, solutions do exist in a restrictive set of cases including KF and VAR. In most practical situation, if the system and measurement models are nonlinear and non-Gaussian, it is not possible to construct the posterior PDF of the current state x_k given the measurement $y_{1:k} = \{y_i, i = 1, \ldots, k\}$ analytically. In this case, suboptimal solutions can be found by the sequential Monte Carlo methods.

2.3 Kalman filtering

KF assumes that the posterior probability density at every time step is Gaussian and hence exactly and completely characterized by two momentums, its mean and covariance (Ristic et al., 2004). In a linear and Gaussian case Eqs. (2-1) and (2-2) can be rewritten as:

$$x_k = F_{k-1}x_{k-1} + \omega_k \qquad \omega_k \sim N(0, W_k) \tag{2-6}$$

$$y_k = H_k x_k + \nu_k \qquad \nu_k \sim N(0, V_k) \tag{2-7}$$

where F_{k-1} and H_k represent matrices defining the linear functions. Random noises ω_k and ν_k are mutually independent zero-mean white Gaussian, with covariances W_k and V_k, respectively.

KF consists of prediction and updating stages. In the prediction stage, means and covariances of states $\hat{x}_k$ and P_k are estimated as follows:

$$\hat{x}_k = F_{k-1}\hat{x}_{k-1} \tag{2-8}$$

$$P_k = W_{k-1} + F_{k-1}P_{k-1}F_{k-1}^T \tag{2-9}$$

In the updating stage, means and covariance are adjusted as follows:

$$\hat{x}_k^{up} = \hat{x}_k + K_k(y_k - H_k\hat{x}_k) \tag{2-10}$$

$$P_k^{up} = (I - K_k H_k)P_k \tag{2-11}$$

where

$$K_k = P_k H_k^T (H_k P_k H_k^T + V_k)^{-1} \tag{2-12}$$

is the Kalman gain. The Kalman filter recursively computes the mean and covariance of the Gaussian posterior $p(x_k \mid y_{1:k})$. This is the optimal solution to the Bayesian filtering problem if linear and Gaussian assumptions hold.

In non-linear cases, the extended Kalman filter (EKF) may be used as suboptimal solution. In the EKF, non-linear operators, f and h, in Eqs. (2-1) and (2-3) are linearized by $\hat{F}$ and $\hat{H}$ as follows:

$$\hat{F}_{k-1} = \left[\nabla_{\hat{x}_{k-1}} f_{k-1}^T(\hat{x}_{k-1})\right]^T \tag{2-13}$$

$$\hat{H}_k = \left[\nabla_{\hat{x}_k} h_k^T(\hat{x}_k)\right]^T \tag{2-14}$$

where

$$\nabla_{x_k} = \left[\frac{\partial}{\partial x_k^i} \cdots \frac{\partial}{\partial x_k^{n_x}}\right]^T \tag{2-15}$$

In the EKF, prediction and updating stages are conducted by Eqs. (2-8) to (2-12) using Jacobians $\hat{F}_{k-1}$ and $\hat{H}_k$ evaluated at $\hat{x}_{k-1}$ and $\hat{x}_k$, respectively. Note that the EKF approximates $p(x_k \mid y_{1:k})$ to be Gaussian. Ensemble Kalman filtering, an efficient alternative for non-linear cases, will be discussed in Chapter 5.

2.4 Variational assimilation

Another approach to data assimilation is variational assimilation (VAR). VAR is also defined in linear and Gaussian operators shown in Eqs. (2-6) and (2-7). The goal of VAR is to find the initial state x_{k-1}^{up} that minimizes the object function:

$$J(x_{k-1}^{up}) = (x_{k-1}^{up} - x_{k-1})^T (P_k)^{-1} (x_{k-1}^{up} - x_{k-1}) + (y_k - H_k x_{k-1}^{up})^T V_k^{-1} (y_k - H_k x_{k-1}^{up}) \tag{2-16}$$

3D-VAR is a data assimilation method that computes the analysis by minimizing Eqs. (2-16). The gradient of the criterion of Eq. (2-16) is given by

$$\nabla J(x_{k-1}^{up}) = 2(P_k)^{-1} (x_{k-1}^{up} - x_{k-1}) + 2H_k^T V_k^{-1} (y_k - H_k x_{k-1}^{up}) \tag{2-17}$$

The minimization problem is solved by performing a number of iterations of a minimization algorithm such that

$$\nabla J(x_{k-1}^{up}) < \varepsilon \tag{2-18}$$

for some predefined tolerance ε (van Velzen, 2010).

4D-VAR is a non-sequential data assimilation method taking all measurements into account in a given time window. However, the adjoint operators required for the minimization function are difficult to construct especially in the case of non-linear, high dimensional applications. Detailed description of VAR can be found in Evensen (2009) and van Velzen (2010).

2.5 Sequential Monte Carlo methods

2.5.1 Sequential importance sampling

As mentioned before, if the system and measurement models are non-linear and non-Gaussian, it is not possible to construct the posterior PDF of the current state x_k given the measurement $y_{1:k} = \{y_i,\ i = 1, \ldots, k\}$ analytically in the Bayesian filtering. When the analytic solution is intractable, an optimal solution can be approximated by the SMC methods (Ristic et al., 2004).

The SMC filters are a set of simulation-based methods that provide a flexible approach to computing posterior distribution without any assumptions being made about the nature of the distributions. The key idea of the SMC methods is to represent the posterior PDF by a set of random samples with associated weights and to compute estimates based on these samples and weights.

Sequential importance sampling (SIS) is the basic framework for most SMC algorithms. In SIS, the marginal posterior density at time k can be approximated as follows:

$$p(x_k \mid y_{1:k}) \approx \sum_{i=1}^{n} w_k^i \delta(x_{0:k} - x_{0:k}^i) \tag{2-19}$$

where $x_{0:k}^i$ and w_k^i denotes whole trajectory of the i^{th} particle and its weight, respectively, and $\delta(\cdot)$ denotes the Dirac delta function. The weights are normalized such that $\sum_{i=1}^{n} w_k^i = 1$ and chosen using the principle of importance sampling. Usually we cannot draw samples x_k^i from $p(\cdot)$ directly. Assume we sample directly form a importance function $q(\cdot)$. Then the weights are

$$w_k^i \propto \frac{p(x_{0:k}^i \mid y_{1:k})}{q(x_{0:k}^i \mid y_{1:k})} \tag{2-20}$$

If the importance function is chosen to factorize such that

$$q(x_{0:k} \mid y_{1:k}) = q(x_k \mid x_{0:k-1}, y_{1:k}) q(x_{0:k-1} \mid y_{1:k-1}) \tag{2-21}$$

then one can augment old particle $x_{0:k-1}^i$ by $x_k \sim q(x_k \mid x_{0:k-1}, y_{1:k})$ to get new particles $x_{0:k}^i$. The weight update equation can then be shown to be

$$w_k^i = w_{k-1}^i \frac{p(y_k \mid x_k^i) p(x_k^i \mid x_{k-1}^i)}{q(x_k^i \mid x_{0:k-1}^i, y_{1:k})} \tag{2-22}$$

Furthermore, if $q(x_k \mid x_{0:k-1}, y_{1:k}) = q(x_k \mid x_{k-1}, y_{1:k})$, then the importance density becomes only dependent on the state and the measurement. The modified weight is then

$$w_k^i \propto w_{k-1}^i \frac{p(y_k \mid x_k^i) p(x_k^i \mid x_{k-1}^i)}{q(x_k^i \mid x_{k-1}^i, y_k)} \tag{2-23}$$

and the posterior filtered density can be approximated as

$$p(x_k \mid y_{1:k}) \approx \sum_{i=1}^{n} w_k^i \delta(x_k - x_k^i) \tag{2-24}$$

The choice of importance density is one of the most critical issues in the design of the SMC methods. The most popular choice is the transitional prior:

$$q(x_k^i \mid x_{k-1}^i, y_k) = p(x_k^i \mid x_{k-1}^i) \tag{2-25}$$

By substituting Eq. (2-25) into Eq. (2-23), the weight updating becomes:

$$w_k^i \propto w_{k-1}^i p(y_k \mid x_k^i) \tag{2-26}$$

With these particles and associated weights, the estimated state vector $\hat{x}_k^{up}$ is the weighted mean of particles as:

$$\hat{x}_k^{up} = \sum_{i=1}^{n} w_k^i x_k^i \tag{2-27}$$

As the number of samples becomes large, this Monte Carlo characterization becomes an equivalent representation to the usual functional description of the posterior PDF, and the SIS filter approaches the optimal Bayesian estimator (Ristic et al., 2004). A common problem with the SIS algorithm is the degeneracy phenomenon, in which after a few iterations, all but one particle will have negligible weight.

2.5.2 Sequential importance resampling

The degeneracy phenomenon can be reduced by performing the resampling step whenever a significant degeneracy is observed. Thus, the sequential importance resampling (SIR) particle filter is derived from the SIS algorithm by performing the resampling step at every time index. The idea of resampling is simply that particles with very low weights are abandoned, while multiple copies of particles are kept with the uniformly weighted measure $\{x_k^i, n^{-1}\}$, which still approximates the posterior PDF, $p(x_k \mid y_{1:k})$ (van Leeuwen, 2009). Resampling is one of the key issues in the SMC filters, and various resampling approaches have been introduced in the literature, such as multinomial resampling, residual resampling, stratified resampling, and systematic resampling. Applications of resampling techniques in hydrologic modeling are reviewed in Chapter 4. Basic resampling methods such as multinomial, stratified, systematic, and residual resampling are described in Appendix A.

A graphical representation of SMC is illustrated in Fig. 2-1. At the top we start with a uniformly weighted random measure. Then we use the received measure y_t to compute its importance weight of each particle. If necessary, a resampling step is executed to select important particles with a uniform weight. If the number of particles is n, the weight is $1/n$. The last step is a prediction introducing process noise.

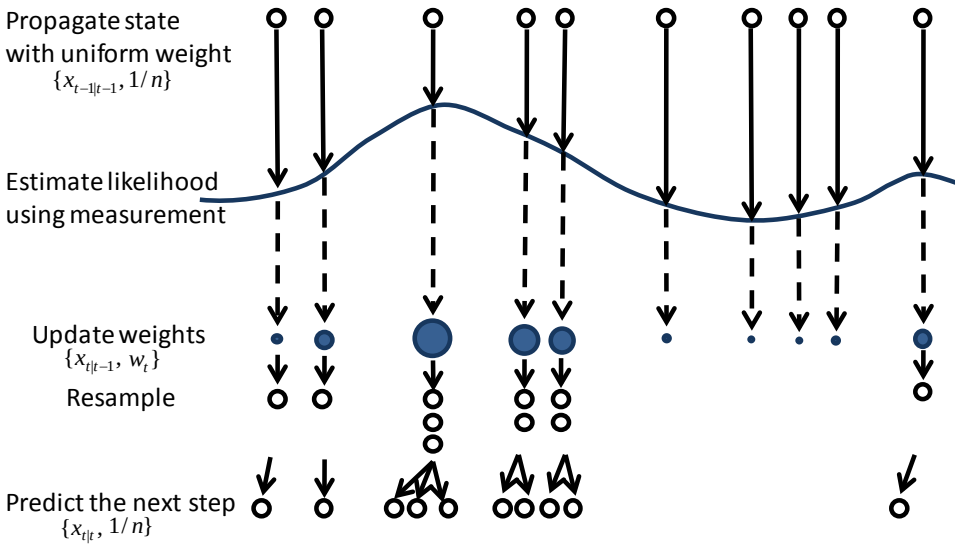

Fig. 2-1 A single cycle of SMC.

2.5.3 Various versions of SMC

Several variants of the SMC methods have been proposed in the literature to overcome the degeneracy and sample impoverishment and to improve selection of importance density. The sequential importance resampling (SIR) filter, described in the previous section, has the advantages of easy evaluation and sampling of importance weights. Most of hydrologic applications are performed by the SIR filter. However, the importance sampling density of the SIR filter is independent of measurements. Thus, the SIR filter is sensitive to outliers of ensembles. Furthermore, performing the resampling step at every iteration may result in a rapid loss of particle diversity. The auxiliary SIR (ASIR) filter, proposed by Pitt and Shephard (1999), performs the resampling step at the previous time step, attempting to mimic the optimal importance density. The regularized particle filter (RPF) uses continuous approximation of the posterior density to improve the sample diversity in the resampling step. A more detailed description and application of the RPF is presented in Chapter 4. It is worth noting that these filters can be (and often are) combined (Ristic et al., 2004).

2.6 Performance evaluation criteria

The statistics to be used for assessment of model performance in this thesis are summarized. These are Nash-Sutcliffe efficiency (NSE) and root mean square error (RMSE), which can be expressed as:

$$NSE = 1 - \frac{\sum_{k=1}^{T}\left(y_k - y_{sim_k}\right)^2}{\sum_{k=1}^{T}\left(y_k - \bar{y}\right)^2} \tag{2-28}$$

$$RMSE = \sqrt{\frac{\sum_{k=1}^{T}\left(y_k - y_{sim_k}\right)^2}{T}} \tag{2-29}$$

where y is observation, $\bar{y}$ is the mean of observation, y_{sim_k} is the forecasted streamflow at the measurement site, and T is the total number of time steps.

Chapter 3

Dual state-parameter updating scheme on a conceptual hydrologic model using sequential Monte Carlo filters

Abstract *This chapter proposes a dual updating scheme of state and parameter (DUS) based on SMC methods to estimate both state and parameter variables of a hydrologic model. We introduce a kernel smoothing method for the robust estimation of uncertain model parameters in the DUS. The applicability of the dual updating scheme is illustrated using the implementation of the storage function model on a middle-sized Japanese catchment. The forecast provided by the dual state-parameter updating scheme is superior to that of state only updating and deterministic modeling in terms of the model accuracy criteria, a scatter diagram, and simulated hydrographs. A significant reduction of parameter uncertainty is observed for all parameters, and estimated parameter distributions show good conformity with off-line optimum. We also compare performance results of the DUS combined with various SMC methods, such as sequential importance resampling (SIR), auxiliary sequential impoprtance resampling (ASIR) and the regularized particle filter (RPF).*

3.1 Introduction

Identification and minimization of uncertainty are key issues in the hydrologic prediction. Data assimilation is a way to integrate information from a variety of sources to improve model accuracy, considering the uncertainty in both the measurement and the modeling system. Among data assimilation techniques, the sequential Monte Carlo (SMC) methods are a Bayesian learning process in which the propagation of all uncertainties is carried out by a suitable selection of randomly generated particles without any assumptions about the nature of the distributions. Unlike the various Kalman filter-based methods that are basically limited to the linear system equation and the assumption of Gaussian distribution errors, the SMC filters have the advantage of being applicable to non-linear, non-Gaussian state-space models. Since their introduction in 1993 (Gordon et al., 1993), the application of these powerful and versatile methods has been increasing in various areas, including pattern recognition, target tracking, financial analysis, and robotics. Only in recent years has the application of these methods been included in hydrology research (Moradkhani et al., 2005a; Smith et al., 2008; Salamon and Feyen, 2009).

In the practical use of hydrologic models, estimated states are highly sensitive to the uncertainty of model parameters. Furthermore, there is no guarantee that parameters calibrated from previous data are the optimum in the current prediction. Therefore, updating state variables based on inappropriate parameters will likely increase uncertainty in the forecasting of hydrologic models. In this respect, sequential estimates of the parameters and state variables are needed to enable the model to generate accurate forecasts.

In this chapter, we propose a dual updating scheme of state and parameter (DUS) based on the SMC filters for the estimation of both the state and parameter variables of a hydrologic model (Noh et al., 2011b). A kernel smoothing method is introduced for the robust estimation of uncertain model parameters in the DUS. We illustrate its

applicability for hydrologic forecasting at the Katsura River catchment in Japan using a conceptual hydrologic model.

This chapter is organized in the following way. Section 3-2 outlines the Bayesian filtering theory; the sequential Monte Carlo filters, known as particle filters, which are based on the sequential importance sampling (SIS); and parameter inference approaches in SMC. In Section 3-3, the case study demonstrating the applicability of the SMC filters is presented. The SMC filters are applied for real-time forecasting of river discharge using the storage function (SF) model. Sequential data assimilation is performed by two different schemes via the SMC filters: state only updating and dual state-parameter updating. Comparisons of the performance results of various SMC filters are presented. Section 3-4 summarizes the methodology and the analysis results.

3.2 Methodology

3.2.1 Sequential importance sampling (SIS)

Sequential Monte Carlo (SMC) filters are a set of simulation-based methods that provide a flexible approach to computing the posterior distribution without any assumptions about the nature of the distributions. As discussed in Chapter 2, the key idea of SMC is based on point mass ("particle") representations of probability densities with associated weights as (Arulampalm et al., 2002):

$$p(x_t \mid y_{1:t}) \approx \sum_{i=1}^{n} w_t^i \delta(x_t - x_t^i) \tag{3-1}$$

where x_t^i and w_t^i denote the i^{th} posterior state ("particle") and its weight, respectively, and $\delta(\cdot)$ denotes the Dirac delta function. The weight is updated as:

$$w_t^i \propto w_{t-1}^i p(y_t \mid x_t^i) \tag{3-2}$$

where $p(y_t \mid x_t^i)$ is the likelihood of each particle x_t^i. The SIS algorithm is a Monte Carlo method that forms the basis for most SMC filters. A common problem with the SIS algorithm is the degeneracy phenomenon: after a few iterations, all but one

particle will have negligible weight. The degeneracy phenomenon can be reduced by performing the resampling step whenever a significant degeneracy is observed. A more detailed description of the SMC filters is presented in Chapter 2.

3.2.2 Variants of SMC filters

Several variants of SMC filters have been proposed in the literature to overcome the degeneracy and sample impoverishment and to improve selection of importance density. The sequential importance resampling (SIR) filter is derived from the SIS algorithm by performing the resampling step at every time index. The auxiliary SIR (ASIR) filter performs the resampling step at the previous time step, attempting to mimic the optimal importance density. The regularized particle filter (RPF) was suggested as a method to improve the sample diversity. A more detailed description of RPF is presented in Chapter 4. It is worth noting that these filters can be (and often are) combined (Ristic et al., 2004).

3.2.3 Parameter inference

Identification of parameter uncertainty is essential to obtain unbiased data assimilation. To handle inference of the unknown parameters, the concept of "artificial evolution" can be applied. That means that the parameter vector θ is fluctuated at each time step, adding an independent, zero-mean normal increment as follows:

$$\theta_t = \theta_{t-1} + \zeta_t \qquad \zeta_t \sim N(0, s^2 V_{t-1}^{\theta}) \tag{3-3}$$

where ζ_t is random noise, V_{t-1}^{θ} is the variance of parameter particles at time t-1 before resampling, and s is a small tuning parameter. The drawback of this approach is that estimated posterior distribution of parameters becomes more diffuse compared to the actual ones (Moradkhani et al., 2005a). Kernel smoothing (Liu and West, 2001) is one remedy for this problem and is accomplished by determining the covariance of parameters based on particles from previous time points. The smooth kernel density can be a mixture of Gaussian densities as follows:

$$P(\theta_t \mid y_{1:t-1}) \sim \sum_{i=1}^{n} w_{t-1}^{i} N(\theta_t \mid m_{t-1}^{i}, h^2 V_{t-1}^{\theta}) \tag{3-4}$$

where h is the variance reduction parameter. The kernel locations m_{t-1}^{i} are specified by a shrinkage rule forcing the particles to be closer to their mean:

$$m_{t-1}^{i} = a\theta_{t-1}^{i} + (1-a)\bar{\theta}_{t-1} \text{ with } a = \sqrt{1-h^2} \tag{3-5}$$

where $\bar{\theta}_{t-1}$ is mean of parameter at time t-1. It can be verified that the mixture probability in Eq. (3-4) has a covariance matrix V_{t-1}^{θ} and that it does not increase over time (Liu and West, 2001). Several issues related with parameter estimation are discussed in Appendix C. A dual state-parameter updating scheme with kernel smoothing via the SIR particle filter can be summarized in Fig. 3-1.

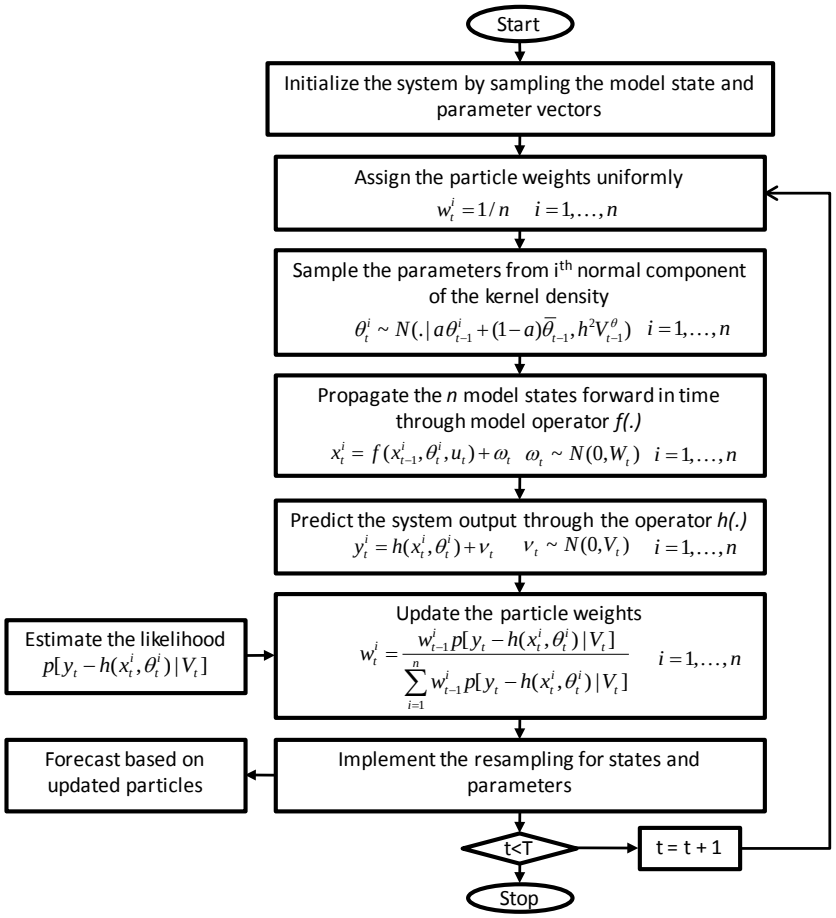

Fig. 3-1 Flowchart of the dual state-parameter updating scheme with kernel smoothing via the SIR particle filter.

3.3 Implementation

3.3.1 Study area

The SMC filters were applied to the Katsura River catchment (Fig. 3-2) to improve the river flow forecasting. This catchment is located in Kyoto, Japan, and covers an area of 1,100 km^2 (887 km^2 at the Katsura station). There are 13 rainfall observation stations and 6 river flow observation stations. The Hiyoshi dam is located upstream, and the outflow record from that reservoir has been considered to be input data in a hydrologic model.

Fig. 3-2 The Katsura River catchment.

3.3.2 Hydrological model and simulation condition

The storage function (SF) model (Kimura, 1961) is one of the most commonly used conceptual hydrologic models for flood prediction due to its simple numerical procedure and its proper regeneration of nonlinear characteristics of flood runoff. The state-space form of the SF model adapted in this catchment is as follows:

$$\frac{ds(t)}{dt} = r_e(t - T_L) - \left(\frac{s(t)}{k}\right)^{1/p} + \omega_t \tag{3-6}$$

$$q_{sim}(t) = \frac{A_{down}}{3.6}\left(\frac{s(t)}{k}\right)^{1/p} + q_{dam}(t - T_{dam}) \tag{3-7}$$

$$q_t = q_{sim}(t) + v_t \tag{3-8}$$

where s is catchment storage (mm), t is time (hr), A_{down} is the downstream area from the dam (km^2), q_{sim} is simulated river discharge (m^3/s), q_t and q_{dam} are observed discharge at the Katsura gauging station and at the Hiyoshi dam (m^3/s), T_L and T_{dam} are the lag time parameters of catchment and outflow from the dam reservoir (hr), and k and p are model parameters. ω_t and v_t are the state and the measurement error, respectively. Effective rainfall r_e is estimated as follows:

$$r_e = r \times f^* \text{ with } f^* = \begin{cases} 1 & r_{accum} \geq R_{sa} \\ f & r_{accum} < R_{sa} \end{cases} \tag{3-9}$$

where r is rainfall (mm/hr), f is the runoff coefficient, r_{accum} is the accumulated rainfall amount (mm), and R_{sa} is the saturation amount (mm). Areal mean values of hourly observed rainfall from the 13 gauging stations were used as model input. Six model parameters, including k, p, T_L, T_{dam}, f and R_{sa}, have been estimated from the events of 2004. In the state only updating scheme, pre-calibrated parameter values were used. On the other hand, the dual state-parameter updating scheme has been performed on five model parameters, excluding T_{dam}, which showed stable values compared to others. Both simulations were performed by the SIR particle filter with 3,000 particles. Covariance of the error of system (W_t) and measurement (V_t) were assumed to be 4 mm and 10% of the current observed discharge, respectively.

3.3.3 State only updating scheme

Fig. 3-3 shows the simulation results of state only updating via the SIR particle filter compared to observations and a deterministic prediction. In this scheme, particles are resampled in each observation time step, and catchment storage (s) is perturbed according to the system noise. While updated river discharge using a state only updating scheme shows good conformity between observation and simulation (Fig.

3-3(c)), a forecast based on the same particles does not reproduce the river flow properly compared to a deterministic prediction (Fig. 3-3(d)). To compare off-line optimal parameters with those calibrated from the past event (Table 3-1), several parameters show quite different values. In this respect, it can be inferred that state updating based on inappropriate parameters may be one of the causes misleading the forecast.

3.3.4 Dual state-parameter updating scheme

In the dual state-parameter updating scheme, initial values of each parameter have been set to uniform distribution with widths that cover deviations of pre-calibrated parameter distributions. In other words, true static values of parameters are assumed to be located within these initial distributions. Inference of five parameters (e.g., k, p, T_L, f and R_{sa}) was performed by the kernel smoothing method in the DUS. The value of kernel smoothing parameter a in Eq. (3-5) was set as 0.95.

Fig. 3-4 illustrates the simulation results of the dual state-parameter updating. Compared with the state only updating case, a forecast by the dual updating scheme shows better conformity with observations (Fig. 3-4(d)). Furthermore, the unexpected drawdown of hydrograph in the rising part (Fig. 3-3(d)) is not shown in the dual updating case. Traces of the catchment storage s present different patterns in Fig. 3-3(b) and Fig. 3-4(b), whereas updated discharge hydrographs show similar traces in both cases.

Table 3-1 Parameter information.

Model parameters	Pre-calibrated from 2004 events	Off-line optimum from 2007 events	Initial range for dual updating
k (-)	17.0	30.0	10.0~40.0
p (-)	0.6	0.66	0.4~0.9
T_L (hr)	3.8	6.0	3.0~7.0
f (-)	0.33	0.65	0.1~0.8
R_{sa} (mm)	82.0	105.0	50.0~150.0
T_{dam} (hr)	4.0	4.0	4.0

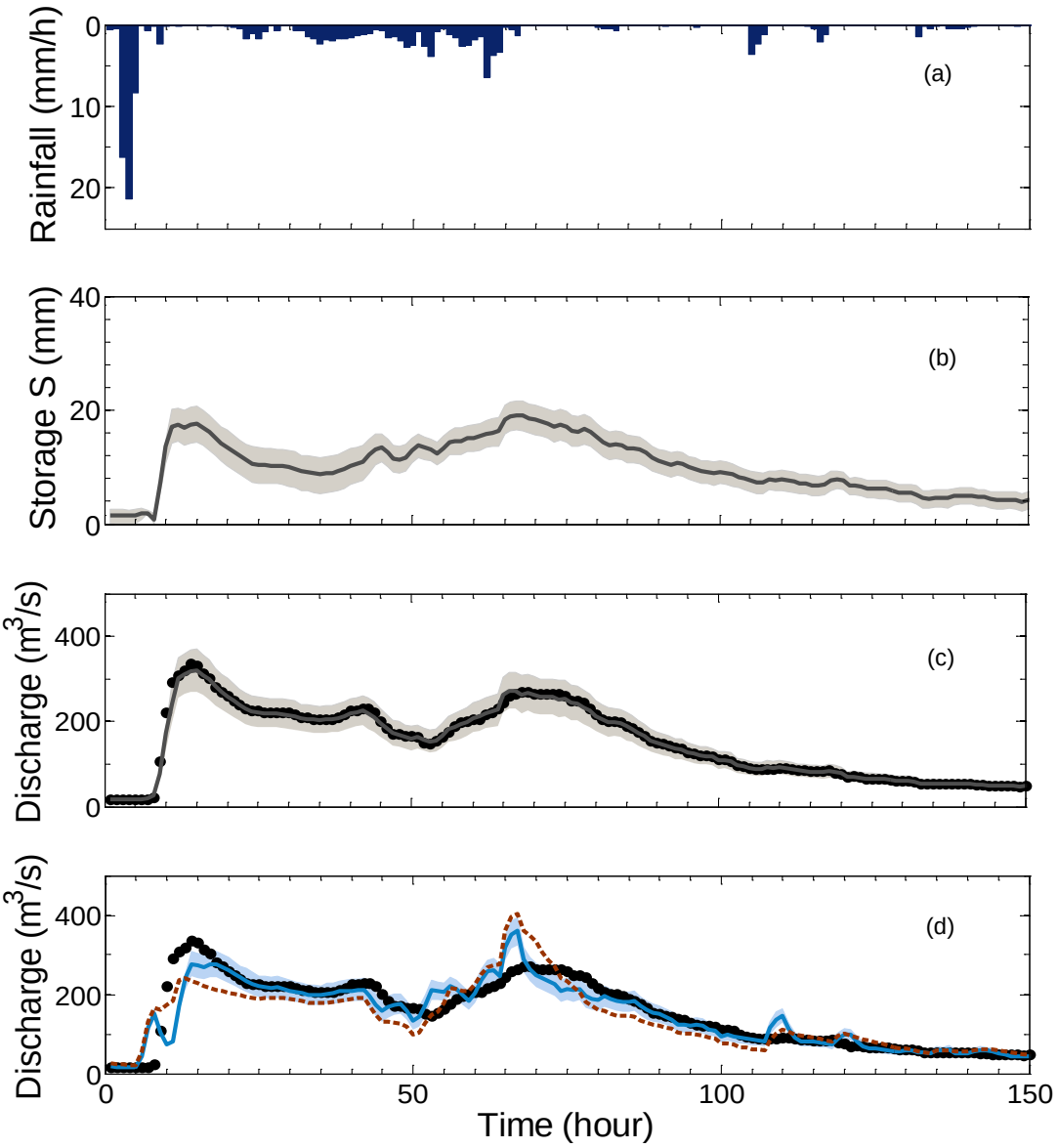

Fig. 3-3 Results of the state only updating via the SIR particle filter from 11 to 16 July 2007. (a) Hourly precipitation. (b) Catchment storage. (c) Updated river discharge. (d) 3-hour-lead forecasted river discharge. Black dots represent observed discharge. Blue line and area represent mean value and 95% confidence interval, respectively. Dashed line represents a deterministic modeling case.

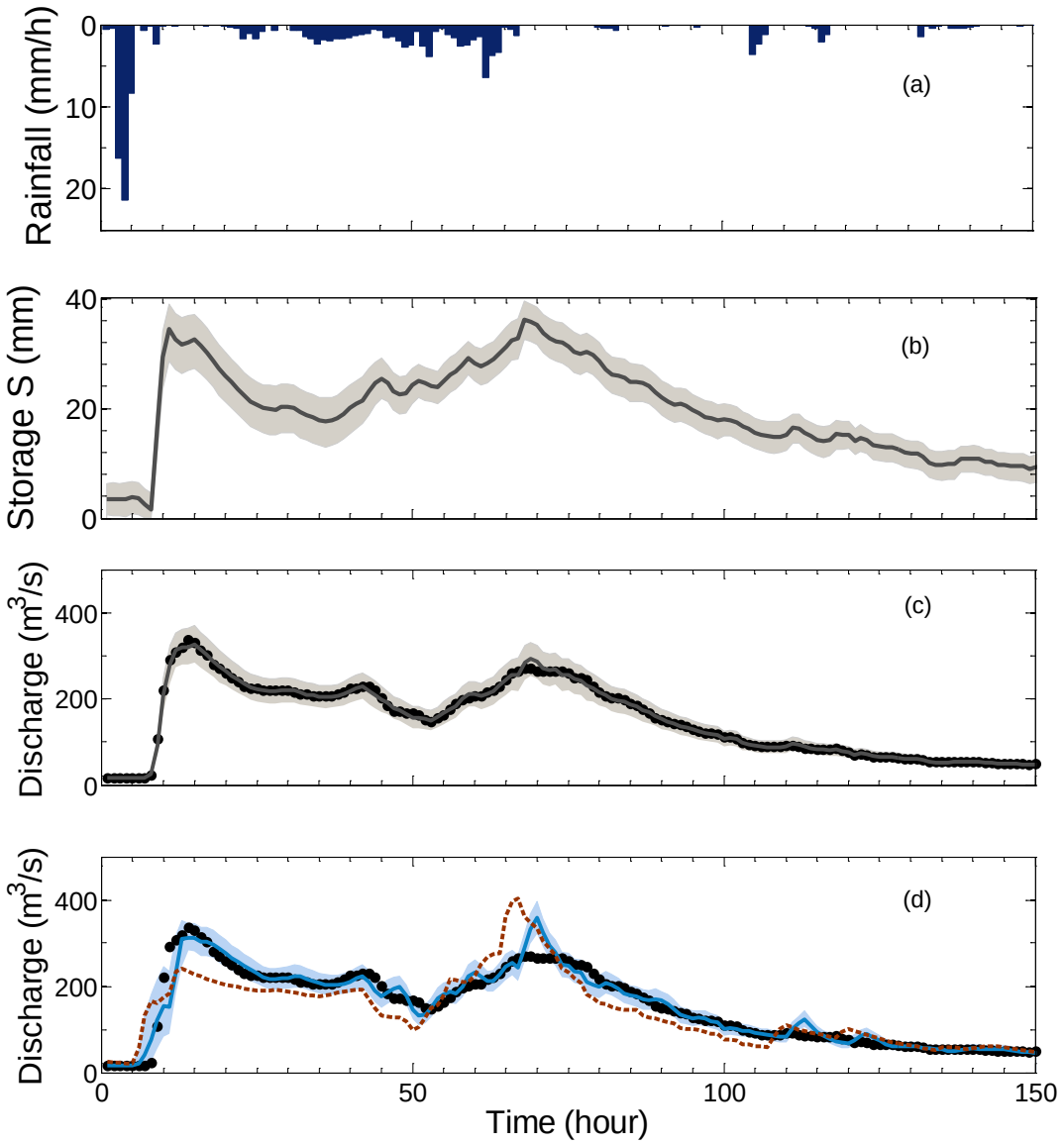

Fig. 3-4 Results of the dual state-parameter updating via the SIR particle filter from 11 to 16 July 2007. (a) Hourly precipitation. (b) Catchment storage. (c) Updated river discharge. (d) 3-hour-lead forecasted river discharge. Black dots represent observed discharge. Blue line and area represent mean value and 95% confidence interval, respectively. Dashed line represents a deterministic modeling case.

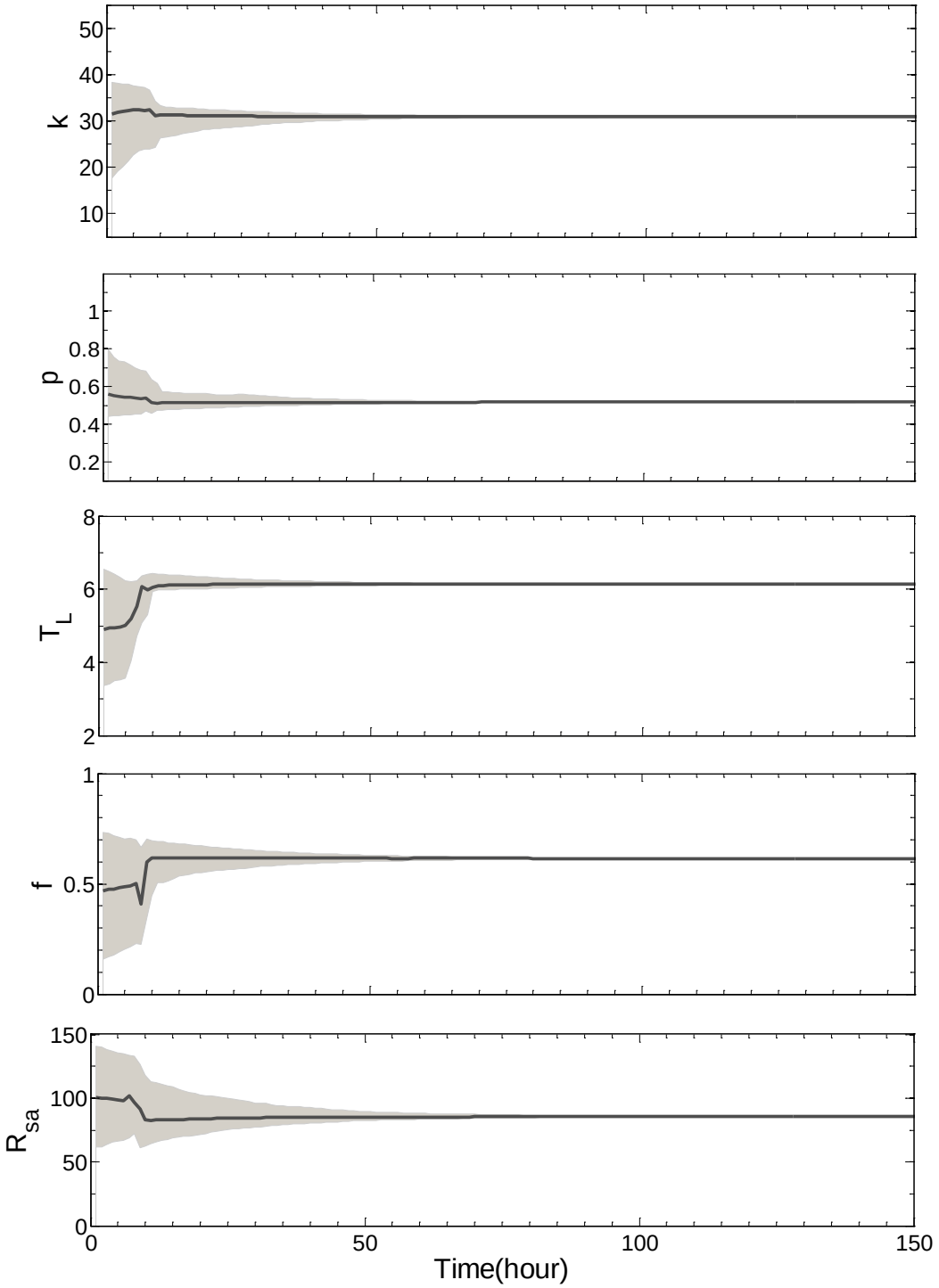

Fig. 3-5 Traces of parameter *k*, *P*, T_L, *f*, R_{sa} of the SF model using dual state-parameter updating of the SIR particle filter from 11 to 16 July 2007. Black lines represent median value, and gray area represents 95% confidence interval.

Fig. 3-5 presents the traces of parameter distribution. One can observe a significant reduction of parameter uncertainty for all parameters after the first flood peak. In comparison with the off-line optimum (Table 3-1), estimated parameters show similar ranges, especially in parameter k, T_L and f.

It is worth noting that when the artificial evolution is applied for parameter inference instead of kernel smoothing in the dual updating scheme, estimated parameters present more diffusive distributions and unstable inference is produced resulting in different posterior distributions at each simulation. However, inference from kernel smoothing presents relatively consistent results because there is less uncertainty of parameters.

In the scatter diagram shown in Fig. 3-6, the dual state-parameter updating scheme presents enhanced simulation results in the overall flow regime from high flow to low flow. Additionally, the model accuracy criteria shown in Table 3-2 confirm that the DUS is superior to other simulations.

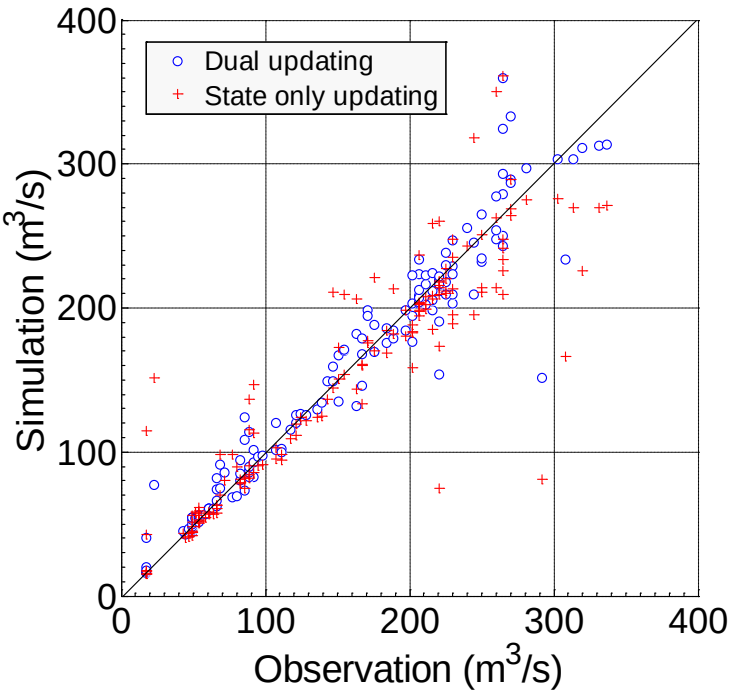

Fig. 3-6 Scatter diagram of simulation results. Cross dots represent results of state only updating. Circle dots represent results of dual state-parameter updating.

Table 3-2 Statistics on model accuracy.

	Deterministic	State only updating	Dual updating
RMSE (m^3/s)	44.6	36.4	20.4
NSE	0.73	0.82	0.94

3.3.5 Comparison of various SMC filters

Several different versions of the SMC filters, such as SIR, ASIR, and RPF with the MCMC move step, were implemented under the same simulation conditions. The Markov chain Monte Carlo (MCMC) move step of RPF, which is used for improving sample diversity in the resampling step, is based on the Metropolis-Hastings algorithm (Robert and Casella, 1999). The dual state-parameter updating scheme has been adapted in all the cases with 3,000 particles. A comparison of the simulated discharge hydrograph is illustrated in Fig. 3-7. There is no significant difference in the estimated 3-hour-ahead forecasting via three SMC filters.

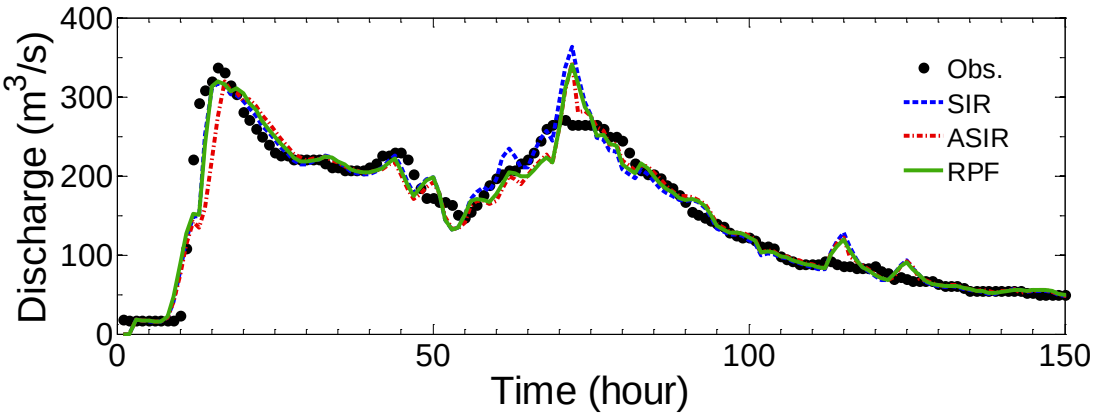

Fig. 3-7 Forecasted river discharge (3 hour ahead) by three SMC filters from 11 to 16 July 2007. Black dots represent observed discharge.

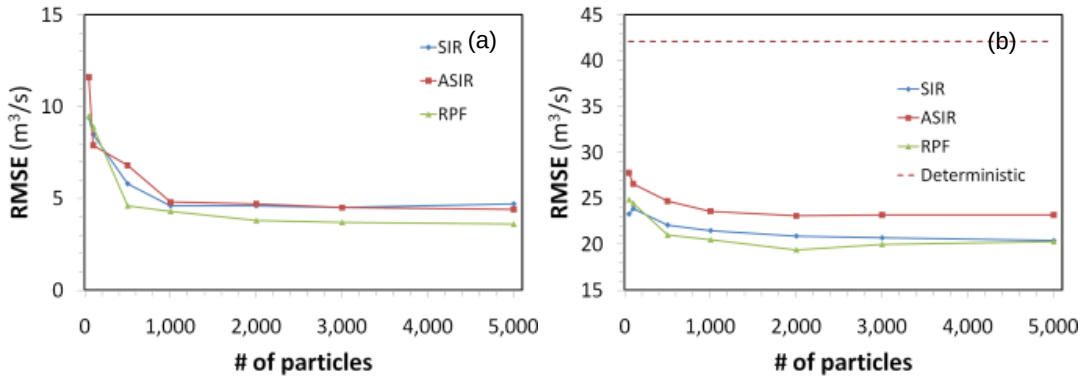

Fig. 3-8 Sensitivity analysis of the effects of particle numbers on the prediction accuracy. (a) Updated river discharge. (b) Forecasted river discharge.

Although three SMC filters reproduce river discharge properly in the first flood peak (1~30 hours) and the recession part, all the SMC methods overestimate the discharge during 65-80 hours. Uncertainty of forcing data (e.g., rainfall) and no consideration of spatial heterogeneity in the SF model are plausible reasons.

Sensitivity analysis was performed concerning the effects of particle numbers on the prediction accuracy (Fig. 3-8). RMSE statistics of simulated discharge show stabilized accuracy in both updating and forecasting via three SMC filters when the number of particles exceeds 1,000. In terms of forecasting accuracy, SIR and the RPF show similar RMSE statistics, while ASIR presents a slightly higher number of errors than others. Researchers also stated in a previous study (Ristic et al., 2004) that if the importance density of ASIR does not characterize the transitional prior $p(x_t \mid x_{t-1}^i)$ for some reason (e.g., process noise is large), the use of ASIR can even degrade the performance. The simulation time for 1,000 particles is less than 2 min in three SMC filters, which is short enough to be applied for real-time forecasting.

3.4 Conclusions

The sequential Monte Carlo (SMC) filters were applied to a conceptual hydrologic model, the storage function model, using state only updating and the dual state-parameter updating scheme. The river discharge forecast via the SMC filters was

compared with observations. The forecast provided by the dual state-parameter updating scheme was superior to that of state only updating and deterministic modeling in terms of the model accuracy criteria, a scatter diagram, and simulated hydrographs. In the dual state-parameter updating scheme, parameter inference was performed by the kernel smoothing method. A significant reduction of parameter uncertainty was observed for all parameters after the first flood peak, and estimated parameter distributions showed good conformity with off-line optimum. Performance results of SIR and the RPF showed similar forecasting accuracy, while ASIR resulted in a slightly higher number of errors than others. However, RMSE statistics of three SMC filters presented stable results when the number of particles was over 1,000.

The SMC filters are applicable to more complex hydrologic models, such as process-based and spatially distributed hydrologic models, in which it is difficult to use the conventional data assimilation methods. We will examine the performance of the SMC filters on a distributed hydrologic model in the following chapter.

Chapter 4

Applying sequential Monte Carlo methods into a distributed hydrologic model

Abstract *In this chapter, we propose an improved particle filtering approach to consider different response times of internal state variables in a hydrologic model. The proposed method adopts a lagged filtering approach to aggregate model response until the uncertainty of each hydrologic process is propagated. The regularization with an additional move step based on the Markov chain Monte Carlo (MCMC) methods is also implemented to preserve sample diversity under the lagged filtering approach. A distributed hydrologic model, water and energy transfer processes (WEP), is implemented for hindcasting of streamflow at the Katsura catchment, Japan via two particle filters: the lagged regularized particle filter (LRPF) and the sequential importance resampling (SIR) particle filter. The LRPF shows consistent forecasts regardless of the process noise assumption, while SIR has different values of optimal process noise and shows sensitive variation of confidence intervals, depending on the process noise. Improvement of the LRPF forecasts compared to SIR is particularly found for rapidly varied high flows due to preservation of sample diversity from the kernel, even if particle impoverishment takes place.*

4.1 Introduction

Data assimilation (DA) is a way to integrate information from a variety of sources to improve prediction accuracy, taking into consideration of the uncertainty in both the measurement system and the prediction model. There have been considerable advances in hydrologic DA for streamflow prediction (e.g., Kitanidis and Bras, 1980; Georgakakos, 1986; Vrugt et al., 2006; Clark et al., 2008; Seo et al., 2003, 2009; Liu et al., 2012). State-space filtering methods based on variations of Kalman filtering (KF) approach have been proposed and implemented because of their potential ability to explicitly handle uncertainties in hydrologic predictions. However, the KF approaches for a non-linear system such as the extended Kalman filter (EKF) have limitations in the practical application due to their instability for strong non-linearity and the high computational cost of model derivative equations, especially for high-dimensional state-vector problems such as spatially distributed models. To cope with the drawbacks of the EKF, ensemble Kalman filtering (EnKF) was introduced by Evensen (1994). EnKF is computationally efficient because it has no need for model covariance estimation, but it is still based on the assumption that all probability distributions involved are Gaussian. Further reviews of Kalman filter-based applications for hydrologic models are shown in Vrugt et al. (2006), Moradkhani et al. (2005b, 2008), and Evensen (2009).

Another approach to DA is variational assimilation (VAR), which has achieved widespread application in weather and oceanographic prediction models. In hydrologic investigations, VAR is implemented for estimating spatial soil-moisture distributions by Reichle et al. (2001) and for assimilating potential evaporation and real-time observations of streamflow and precipitation to improve streamflow forecasts by Seo et al. (2003, 2009). Although variational methods are more computationally efficient than KF-based methods, the derivation of the adjoint model needed for minimisation of a cost function is difficult, especially in the case of non-linear, high dimensional hydrological applications (e.g., Liu and Gupta, 2007).

Among DA techniques, the sequential Monte Carlo (SMC) methods, known as the particle filters, are a Bayesian learning process in which the propagation of all uncertainties is carried out by a suitable selection of randomly generated particles without any assumptions being made about the nature of the distributions (Gordon et al., 1993; Musso et al., 2001; Arulampalam et al., 2002; Johansen, 2009). Unlike the various Kalman filter-based methods that are basically limited to the linear correction step and the assumption of Gaussian distribution errors, SMC methods have the advantage of being applicable to non-Gaussian state-space models. The application of these powerful and versatile methods has been increasing in various areas, including pattern recognition, target tracking, financial analysis, and robotics.

In recent years, these methods have received considerable attention in hydrology and earth sciences (e.g., Moradkhani et al., 2005a; Weerts and El Serafy, 2006; Zhou et al., 2006; van Delft et al., 2009; van Leeuwen, 2009; Karssenberg et al., 2010). Since their first introduction to the rainfall-runoff model of Moradkhani et al. (2005a), Weerts and El Serafy (2006) compared ensemble Kalman filtering and particle filtering for state updating of hydrological conceptual rainfall-runoff models. The SMC methods have also been applied to parameter estimation and uncertainty analysis of hydrological models. Smith et al. (2008) evaluate structural inadequacy in hydrologic models, Qin et al. (2009) estimate both soil moisture and model parameters, and Rings et al. (2010) implement hydrogeophysical parameter estimation. Uncertainty of a distributed hydrological model is analyzed by Salamon and Feyen (2009, 2010), and dual state-parameter updating of a conceptual hydrologic model is applied to flood forecasting by Noh et al. (2011b). The diversity of assimilated data and models has been increasing; a snow water equivalent prediction model (Leisenring and Moradkhani, 2010) and assimilation with remote sensing-derived water stages (Montanari et al., 2009) have been investigated. However, the framework to deal with the delayed response, which originates from different time scales of hydrologic processes, routing and spatial heterogeneity of catchment characteristics, and forcing data, especially in a distributed hydrologic model, has not been thoroughly addressed in hydrologic DA. Furthermore,

alternative methods proposed in the literature to mitigate loss of sample diversity (e.g., Musso et al., 2001; Arulampalam et al., 2002), which may cause collapse of the filtering system, have not been studied in hydrology.

In this chapter, we apply the particle filters for a distributed hydrologic model in support of short-term hydrologic forecasting (Noh et al., 2011a). A lagged particle filtering approach is proposed to consider different response times of internal states in a distributed hydrologic model. The regularized particle filter with the Markov chain Monte Carlo (MCMC) move step is also adopted to improve sample diversity under the lagged filtering approach. A process-based distributed hydrologic model, WEP (Jia and Tamai, 1998; Jia et al., 2001, 2009), is implemented for sequential DA through state updating of internal hydrologic variables. Particle filtering is parallelized and implemented in the multi-core computing environment via the open message passing interface (MPI).

This chapter is organized thus: Section 4-2 explains the SMC filtering theory and a lagged filtering approach with an additional regularization step to reflect different responses of internal processes in sequential DA. Section 4-3 presents the case study results, demonstrating the applicability of the proposed particle filtering approach. The lagged regularized particle filter (LRPF) and the sequential importance resampling (SIR) particle filter are evaluated for hindcasting of streamflow in the Katsura River catchment using the WEP model. Section 4-4 summarizes the results and conclusions.

4.2 Method of SMC filters

In this section, we briefly describe the theory of Bayesian filtering and sequential Monte Carlo (SMC) filtering for its suboptimal solution in non-linear and non-Gaussian cases. We describe several variants of SMC filters, including sequential importance resampling (SIR) and regularized particle filter (RPF), which are based on sequential importance sampling (SIS). Detailed descriptions of sequential Monte Carlo methods can be found in Chapter 2.

4.2.1 Basic particle filtering and resampling methods

In SMC filters, the posterior probability density function (PDF) of the current state x_k given the measurement is represented by use the weight that can be updated as:

$$w_k^i \propto w_{k-1}^i p(y_k \mid x_k^i) \tag{4-1}$$

where $p(y_t \mid x_t^i)$ is likelihood of each particle x_t^i. As discussed in Chapter 2, sequential updating of the weight may lead to degeneracy problem, in which after a few iterations, all but one particle will have negligible weight. A suitable measure of the degeneracy is the effective sample size n_{eff} estimated as (Kong et al., 1994):

$$n_{eff} = \frac{1}{\sum_{i=1}^{n} (w_k^i)^2} \tag{4-2}$$

If the weights is uniform (i.e., $w_k^i = 1/n$ for i = 1, ..., n), then $n_{eff} = n$. If all but one particle have 0 weight, then $n_{eff} = 1$. The ratio of the effective particle number n_{ratio} is estimated as follows:

$$n_{ratio} = \frac{n_{eff}}{n} \tag{4-3}$$

The maximum of n_{ratio} is 1 when the weights are uniform. Small n_{ratio} indicates a severe degeneracy and vice versa. n_{ratio} is used as an indicator of degeneracy because it can be used easily regardless of the particle number.

The degeneracy phenomenon can be reduced by performing the resampling step whenever a significant degeneracy is observed. Thus, the SIR particle filter is derived from the SIS algorithm by performing the resampling step at every time index. The idea of resampling is simply that particles with very low weights are abandoned, while multiple copies of particles are kept with the uniformly weighted measure $\left\{x_k^i, n^{-1}\right\}$, which still approximates the posterior PDF, $p(x_k \mid y_{1:k})$ (van Leeuwen, 2009). Resampling is one of the key issues in the SMC filters, and various resampling approaches have been introduced in the literature, such as multinomial resampling, residual resampling, stratified resampling, and systematic resampling. A comparative analysis and review of resampling approaches can be found in Douc et

al. (2005) and van Leeuwen (2009). Systematic resampling, also known as stochastic universal sampling, is often preferred due to its computational simplicity and good empirical performance. It has also been shown that systematic resampling has the lowest sampling noise (Kitagawa, 1996). Hence, we use systematic resampling for all particle filtering cases in this chapter. It is worth noting that there are several choices in resampling methods, and the proper method may be different, depending on the characteristics of hydrologic models. See Weerts and El Serafy (2006), Rings et al. (2010), and Salamon and Feyen (2009) for residual resampling; see also Salamon and Feyen (2010) and Moradkhani et al. (2005a) for systematic resampling. Although the SIR method has the advantage that the importance weights are easily evaluated, because resampling is applied at each iteration, this filter may lead to a sudden loss of diversity in particles and is sensitive to outliers (Ristic et al., 2004). Basic resampling methods such as multinomial, stratified, systematic, and residual resampling are described in Appendix A. The effective parallel programming method of resampling is discussed in Appendix B.

4.2.2 Regularized particle filter

The positive effects of the resampling step are to automatically concentrate particles in regions of interest of the state-space and to reduce particle degeneracy. However, the particles resampled from high weights are statistically selected many times. This leads to another problem, known as sample impoverishment, which means a loss of diversity among the particles because the resultant sample will contain many repeated points (Ristic et al., 2004). Some systematic techniques have been proposed to solve the problem of sample impoverishment. An alternative solution is to introduce the regularization step when the sample impoverishment becomes severe. The regularized particle filter (RPF) is based on regularization of the empirical distribution associated with the particle system using the kernel method (Musso et al., 2001). The main idea of the RPF consists of changing the discrete approximation of posterior distribution to a continuous approximation, so the resampling step is changed into simulating an absolutely continuous distribution, hence producing a

new particle system with *n* different particle locations. The concept of discrete and continuous approximation of particle density is illustrated in Fig. 4-1. If the weights are concentrated on the limited number of particles, the resampling in the discrete approximation (e.g., the SIR particle filter) may lead to a poor representation of the posterior density, while a continuous approximation in regularized measure improves the diversity in the resampling step.

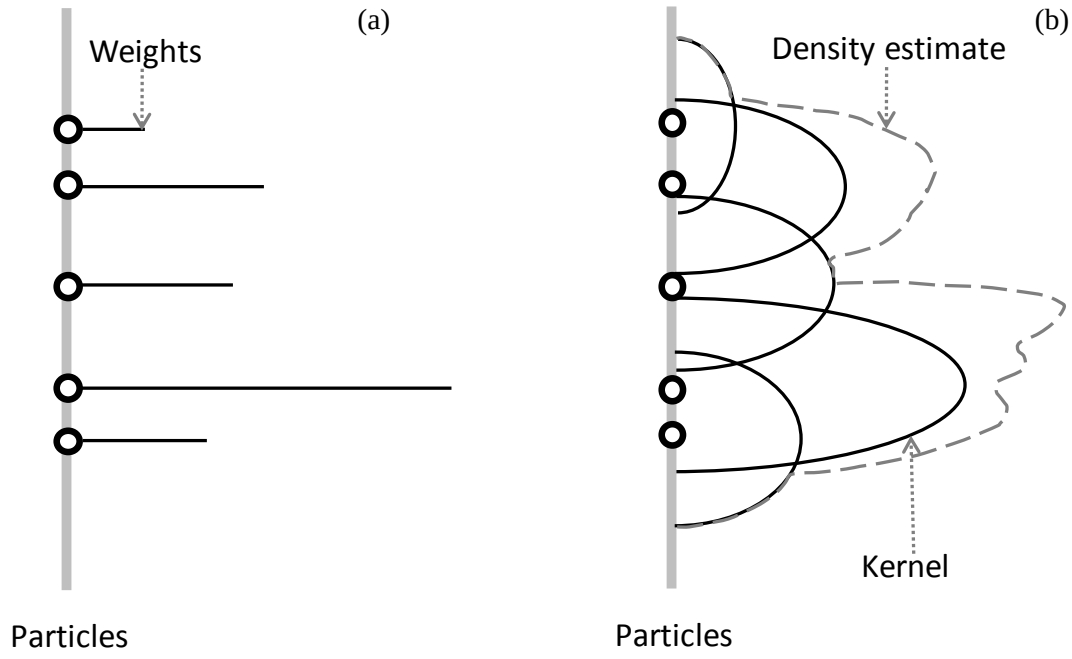

Fig. 4-1 The concept of discrete and continuous approximation of particle density: (a) weighted empirical measure, and (b) regularized measure by kernel. Adapted from Musso et al. (2001).

In the RPF, posterior particles are drawn from the approximation

$$p(x_k \mid y_{1:k}) \approx \sum_{i=1}^{n} w_k^i K_h(x_k - x_k^i) \tag{4-4}$$

where

$$K_h(x) = \frac{1}{h^{n_x}} K\left(\frac{x}{h}\right) \tag{4-5}$$

is the rescaled kernel density $K(\cdot)$, $h>0$ is the bandwidth, and n_x is the dimension of the state vector *x*. The kernel density is a symmetric probability density function on $\Re^{n_x}$, such that

$$K>0,\quad \int K(x)dx=1,\quad \int xK(x)dx=0,\quad \int \|x\|^2 K(x)dx<\infty. \tag{4-6}$$

The kernel $K(\cdot)$ and bandwidth *h* are chosen to minimise the mean integrated square error (MISE) between the true posterior density and the corresponding regularized weighted empirical measure in Eq. (4-4), which is defined as

$$MISE(\hat{p})=\mathrm{E}[\int[\hat{p}(x_k|y_{1:k})-p(x_k|y_{1:k})]^2 dx_k] \tag{4-7}$$

where $\hat{p}(\cdot|\cdot)$ denotes the approximation to $p(x_k|y_{1:k})$ given by the right-hand side of Eq. (4-4). In the special case of equally weighted samples, $w^i=1/n$ for *i* = 1, ..., *n*, the optimal choice of the kernel is the Epanechnikov kernel,

$$K_{opt}=\begin{cases}\frac{n_x+2}{2c_{n_x}}(1-\|x\|^2) & if\ \|x\|<1\\ 0 & otherwise\end{cases} \tag{4-8}$$

where c_{n_x} is the volume of the unit sphere of $\Re^{n_x}$. It is worth noting that the use of kernel approximation becomes increasingly less appropriate as n_x (dimensionality of the state) increases. The optimal bandwidth with unit covariance matrix is

$$h_{opt}=A\cdot n^{-\frac{1}{n_x+4}}\quad with\ A=[8c_{n_x}^{-1}(n_x+4)\left(2\sqrt{\pi}\right)^{n_x}]^{\frac{1}{n_x+4}} \tag{4-9}$$

The RPF differs from SIR only in additional regularization steps when sample impoverishment happens. The key step is

$$x_k^{i\,*}=x_k^i+h_{opt}D_k\varepsilon^i \tag{4-10}$$

where $x_k^{i\,*}$ is a new particle generated from kernel density, D_k is estimated from L_k, which is the empirical covariance matrix such that $D_kD_k^T=L_k$, and ε^i is the random noise from the kernel. Note that the calculation of the empirical covariance matrix L_k is carried out prior to the resampling and is therefore a function of both the x_k^i

and w_k^i. n_x is the dimension of the state vector x and c_{n_x} is the volume of the unit sphere of $\Re^{n_x}$ given by

$$c_{n_x} = \frac{\pi^{n_x/2}}{\Gamma(n_x/2+1)} \tag{4-11}$$

where Γ is the gamma function.

The theoretical disadvantage of the RPF is that its samples are no longer guaranteed to asymptotically approximate those from the posterior. This can be mitigated by including the Markov chain Monte Carlo (MCMC) move step (Gilks and Berzuini, 2001) based on the Metropolis-Hastings algorithm (Robert and Casella, 1999). The key idea is that a resampled particle is moved to a new state, according to Eq. (4-10), only if $u \le \alpha$, where $u \sim U[0,1]$ and α is the acceptance probability. Otherwise, the move is rejected.

$$\alpha = \begin{cases} \min\left\{1, \dfrac{p(y_k \mid x_k^{i*})}{p(y_k \mid x_k^i)}\right\} & \text{if } p(y_k \mid x_k^i) \neq 0 \\ 1 & \text{otherwise} \end{cases} \tag{4-12}$$

In above, α becomes 1.0 when the likelihood of new particle is greater than that of the previous particle. That means that the MCMC move step contributes to screening bad particles in the regularization step, thus ensuring that particles asymptotically approximate samples from the posterior.

A single cycle of the RPF with the MCMC move step is illustrated in Fig. 4-2. The basic procedure of the RPF is the same with SIR before resampling. After the resampling step, entirely new samples are drawn from the continuous kernel. If a new particle is rejected in the MCMC move step, the particle resampled before regularization is used. Therefore, the efficiency of the RPF depends on how many particles are preserved in the MCMC move step. Although this approach is frequently found to improve performance with a less rigorous deviation, the RPF has not been introduced in hydrologic DA.

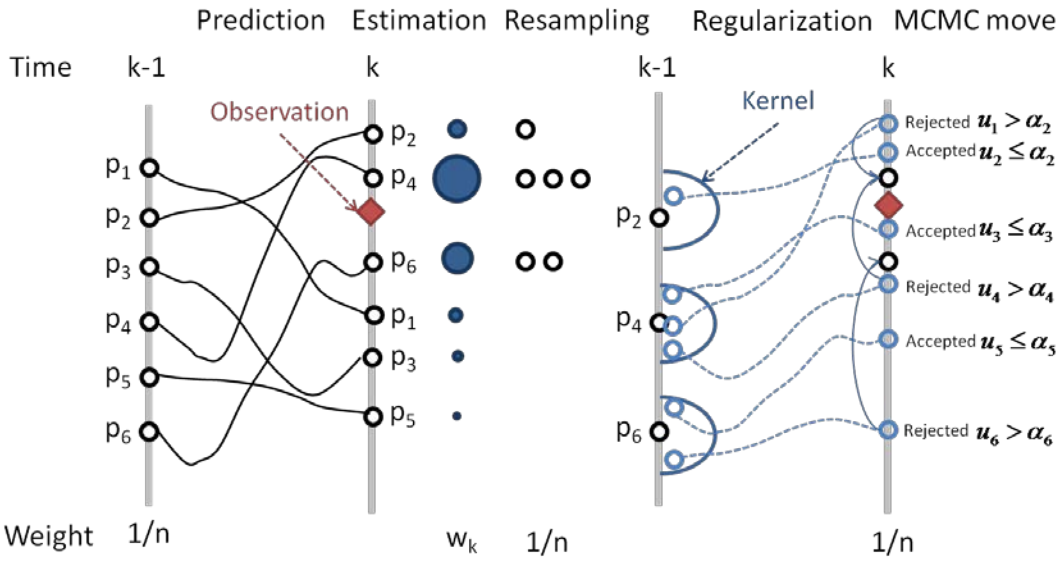

Fig. 4-2 A single cycle of a regularized particle filter.

4.2.3 Particle filter with lag time approach

Many hydrological processes operate—in response to precipitation—at similar length scales, but the time scales are delayed (Blöschl and Sivapalan, 1995). In a distributed hydrologic model, there are many types of state variables, and each variable interacts with others based on different time scales. For example, in catchment modelling, internal state variables may refer to two-dimensional distribution of soil moisture content, evapotranspiration, and overland flow; and an observable state may refer to streamflow flux at the monitoring sites. There is a time lag until the changes of soil moisture distribution affect infiltration and sub-surface/surface runoff processes and generated runoff is routed as streamflow into the measurement site. Hydrologic components in a hydrologic model have usually different time scales, which need to be considered in the data assimilation process.

As stated by Salamon and Feyen (2010), this response time is usually greater than the high-frequency discharge measurements. One simple approach is to use delayed updating, which utilizes longer time intervals before updating state variables. However, delayed updating leads to omitting large quantities of measurement information, and a fixed delay assumption may result in inappropriate estimation,

because a response time always changes, depending on the current spatial distributions of the state and forcing variables. Furthermore, when system behaviour is relatively fast (e.g., hourly based hydrologic or hydraulic modelling cases), delayed updating may lead to missing proper timing of assimilation. That can make it hard to implement sequential data assimilation techniques into hydrologic modelling. Thus, we propose the lagged regularized particle filter (LRPF), not only for considering different catchment responses, but also for using whole measurement information for data assimilation.

Fig. 4-3 shows an example of the LRPF. Here, k is the current time step, and j is the lag time required for responses of internal state variables to be transmitted into the observable variables. Note that it is better to set the lag time j large enough to cover plausible ranges because the system response is time-variant.

The assimilation window of the lagged filtering is defined from k-j to k time step. The procedure of the lagged filtering is as follows: 1) To have prediction at the time step k, simulation starts from the time step k-j. 2) When particles arrive at the current time k, the lagged weights are estimated according to the measurement. 3) Resampling is executed according to the lagged weights. Note that state variables at the time step k-j+1 are resampled simultaneously with those at the current time step. 5) If the effective particle number n_{eff} is less than the threshold ($n_{eff} < n_{thr}$), the regularization step is executed from the time step k-j with new particle members generated from kernel. 6) When each particle arrives in the current time step k, acceptance probability α is calculated according to the lagged likelihood, as shown in Eq. (16). If a particle is rejected ($u > \alpha$), state variables before regularization will be used without kernel perturbation. 7) For the next time step k+1, simulation starts from time step k-j+1 and follows the same procedure as from 1) to 6). In this way, sequential data assimilation procedure is implemented at every time step without loss of measurement information. Compared to conventional particle filtering, an additional procedure needed in the lagged regularized particle filtering is only that state variables at the time step k-j+1 should be stored and resampled according to lagged weights.

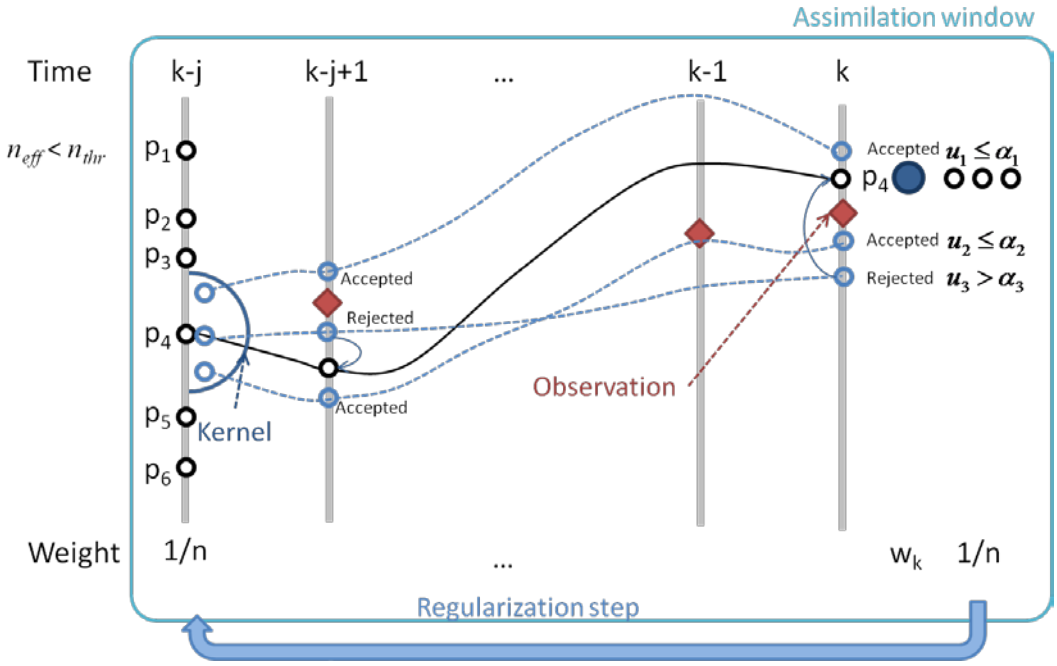

Fig. 4-3 Particle traces in the regularization step under the lagged filtering approach.

Lagged weight, w_{lag}^{i} , and lagged likelihood, L_{lag}^{i} , can be calculated through various methods, including the aggregation of the past weight. However, in this chapter, the weight and likelihood at the last time step k (w_k^i , L_k^i) are simply used as lagged weight and likelihood, respectively. Note that the use of weights without aggregation can show better results in cases of short-term forecasting.

Fig. 4-4 summarises one cycle of the algorithm of the RPF with the Markov chain Monte Carlo (MCMC) move step under the lagged filtering approach. The procedure connected with the dashed line means the regularization step. It is worth mentioning that the regularization step can be executed not just in the sample impoverishment, but also in the particle collapse case, which means all particles have negligible weights that fall outside the measurement PDF. In this case, the regularization step is used effectively for re-initialization of the particle system.

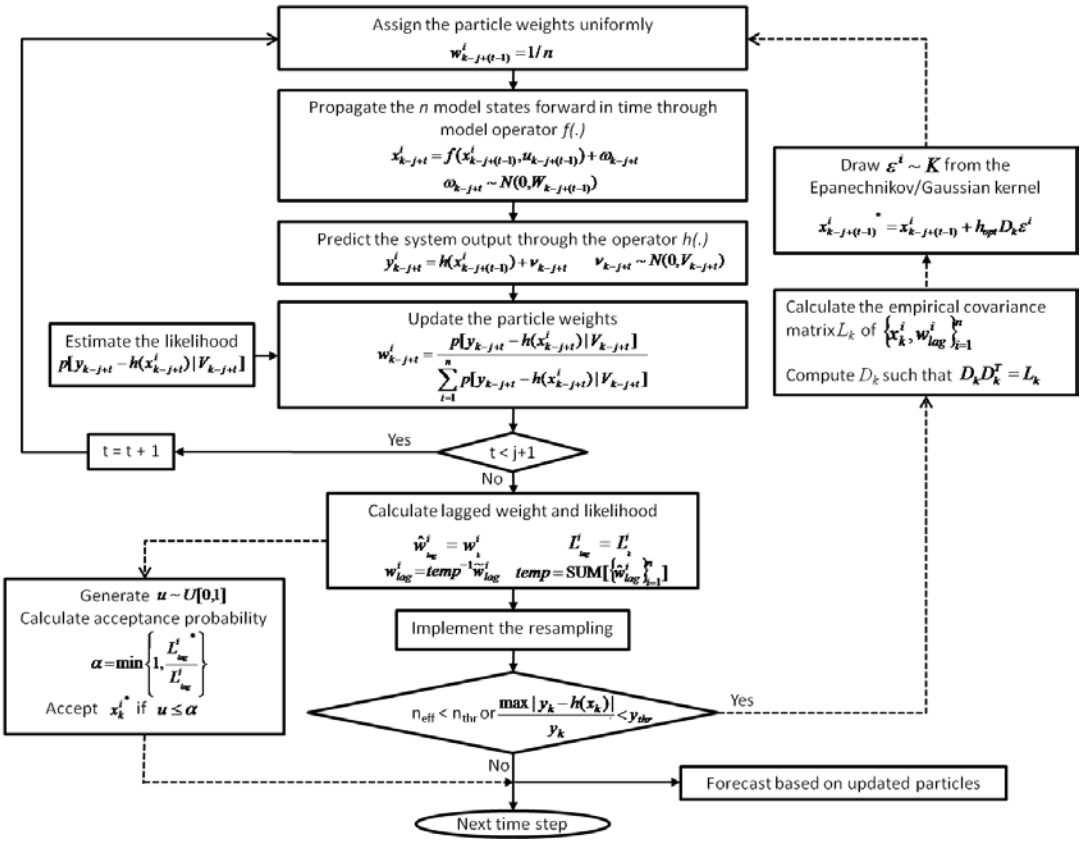

Fig. 4-4 The flow diagram of the regularized particle filter with the MCMC move step in the lagged filtering approach.

4.3 Implementation

4.3.1 Study area

The SMC methods are applied to the Katsura River catchment (Fig. 4-5) to show the applicability of the proposed particle filtering approach. This catchment is located in Kyoto, Japan, and covers an area of 1,100 km^2 (887 km^2 at the Katsura station). Topography in the catchment is characterized by a mountainous upstream in the north and a flatter plain in the south. The elevation in the catchment ranges from 4 to 1,158 m, with an average of about 325 m. The land use consists of forest (76.7%), agricultural area (9.3%), residential area (7.5%), water body (2.0%), public area (2.7%), vacant land (1.2%), and road (0.6%), respectively. There are 13 rainfall

observation stations, 1 meteorological observation station, and 4 river flow observation stations. Annual precipitation and temperature are about 1,422 mm and 16.2 ℃ in Kyoto city (2001~2010). Precipitation is concentrated in the summer season from May to September. The Hiyoshi dam is located upstream. The controlled outflow record from the dam reservoir is given as inflow to the hydrologic model, and the model simulates rainfall-runoff processes for the downstream of the dam.

4.3.2 Hydrological model and particle filtering

The hydrologic model used is the water and energy transfer processes (WEP) model, which was developed for simulating spatially variable water and energy processes in catchments with complex land covers (Jia and Tamai, 1998; Jia et al., 2001). State variables of WEP include soil moisture content, surface runoff, groundwater tables, discharge and water stage in rivers, heat flux components, etc. (Fig. 4-6). The spatial calculation unit of the WEP model is a square or rectangular grid. Runoff routing on slopes and in rivers is carried out by applying a one-dimensional kinematical wave approach from upstream to downstream. The WEP model has been applied in several watersheds in Japan, Korea, and China with different climate and geographic conditions (Jia et al., 2001, 2009; Kim et al., 2005a, 2005b; Qin et al., 2008).

The model setup uses 250 m grid resolution and an hourly time step. We use hourly observed rainfall from 13 observation stations organized by the Ministry of Land, Infrastructure, Transport and Tourism in Japan (http://www1.river.go.jp/) and hourly observed meteorological data including air temperature, relative humidity, wind speed, and duration of sunlight from the Kyoto station, which is organized by Japan Meteorological Agency (http://www.jma.go.jp/jma/index.html). The nearest neighbour interpolation method is used for representation of spatial distribution of rainfall. An SRTM 90 m digital elevation map (DEM) is adopted (http://srtm.csi.cgiar.org/) and converted to 250 m resolution. Soil distribution is obtained from the website of the Food and Agriculture Organization of the United Nations (http://www.fao.org/nr/land/soils/en/).

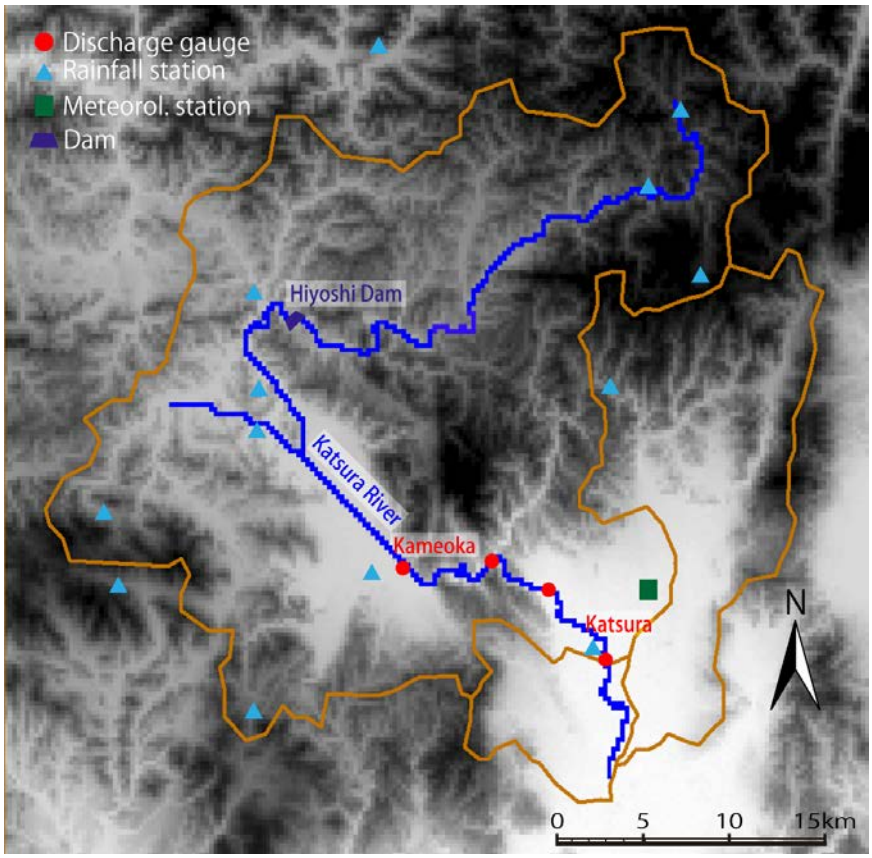

Fig. 4-5 The Katsura River catchment.

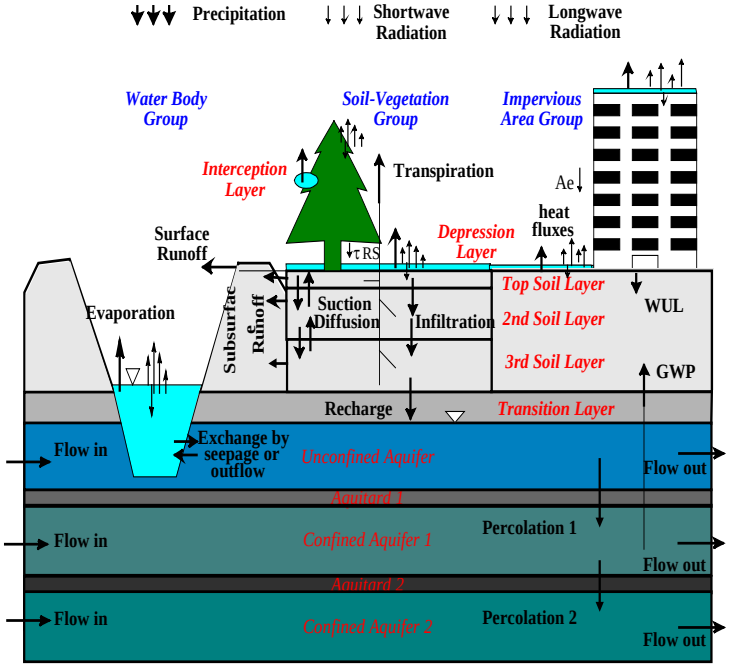

Fig. 4-6 Schematic view of WEP model structure. Adapted from Jia et al. (2009).

Physical property of soil is derived from soil texture information using the ROSETTA model (Schaap et al., 2001). However, the saturated hydraulic conductivity of several soils is roughly adjusted for the data period of 2007, since soil property estimated from large-scale soil maps varies greatly. For other parameters related to aquifers and vegetation, we apply parameter ranges from the earlier studies mentioned above. No flux boundary condition is specified at the catchment boundary for the groundwater flow. Artificial water use is approximately estimated as 3 m^3s^{-1} and subtracted directly from simulated discharge at the Katsura station.

Ensemble simulation of 192 particles is conducted on a multi-processing computer (96 cores in the supercomputing system of Kyoto University) via parallel-computing techniques of open MPI (http://www.open-mpi.org/). The parallel programming code is written using a single-program multiple-data (SPMD) approach, which means the same modelling procedure with different state variables. A master process aggregates particle statistics and controls resampling/regularization steps. Message passing commands of MPI is used effectively to transfer spatially distributed state variables from one particle to another in the resampling step.

4.3.3 Process and measurement error models

The Particle filters perform suboptimal estimation of the system states by considering the uncertainty in both the measurement and modelling systems. Therefore, the choice of the error models is crucial to obtaining a better estimation (Weerts and El Serafy, 2006). Another important point is to choosing hidden state variables for filtering. Since there are numerous state variables in a distributed hydrologic model, it is not practical to consider the uncertainty of all state variables with a limited number of particles. Therefore, it is necessary to choose a limited number of state variables, which process error of the modelling system is aggregated in, and is easily updated by observable variables. In this chapter, we select soil moisture content and overland flow in each grid as hidden state variables and streamflows at the Katsura station as an observable variable for data assimilation.

Global multipliers are introduced to perturb state variables stochastically and effectively. In the case of soil moisture content, the total soil moisture depth at the previous time step S_{k-1} is aggregated for three soil layers within the catchment as:

$$S_{k-1} = \sum_{l=1}^{3} \sum_{j=1}^{m} \theta_j^l d_j^l \tag{4-13}$$

where θ_j^l and d_j^l are the volumetric soil moisture content (m^3/m^3) and the soil depth (m) in each layer, and l and m represent the number of soil layers and the total number of grids within the catchment, respectively. Then, process noise of the soil moisture content w_{soil_k} is added to the aggregated state variable S_{k-1} as:

$$\hat{S}_k = S_{k-1} + w_{soil_k} \tag{4-14}$$

w_{soil_k} is assumed as Gaussian distribution $N(0, \sigma_{soil_k}^2)$ having a heteroscedastic standard deviation as:

$$\sigma_{soil_k} = \alpha_{soil} S_{k-1} + \beta_{soil} \tag{4-15}$$

In the above, α_{soil} and β_{soil} are adaptable parameters that can be obtained from sensitivity analysis. Although proper tuning of these adaptable parameters is important, their optimum value changes according to different data periods, which is another source of uncertainty in data assimilation. We will discuss the effects of adaptable parameters, especially α_{soil}, on two different particle filters later. The value of β_{soil} is set as 50 mm for the whole simulation. When the process error of soil moisture content w_{soil_k} is generated for each particle, the perturbed states of soil moisture $\hat{\theta}_j^l$ are calculated using multiplicative factor γ_s as follows:

$$\gamma_s = \frac{\hat{S}_k}{S_{k-1}} \tag{4-16}$$

$$\hat{\theta}_j^l = \gamma_s \theta_j^l \tag{4-17}$$

In the above equations, if perturbed soil moisture at each grid and layer $\hat{\theta}_j^l$ becomes greater or smaller than the physical limitation, $\hat{\theta}_j^l$ is adjusted at its maximum (i.e.,

porosity) or minimum (i.e., wilting point). It is also worth noting that non-linearity of the distributed hydrologic model can alleviate loss of spatial diversity in the perturbation process, which is one of the disadvantages of global multipliers. For example, even if the same noise is applied, the spatial pattern of state variables can become different due to antecedent soil moisture and the non-linear system response for that. Similar noise definition for soil moisture has been applied for state updating of a distributed hydrologic model in the study of Kim et al. (2007).

The perturbation of overland flow is also applied in a multiplicative way as:

$$\hat{q}_{ov_j} = (1 + w_{ov_k})\, q_{ov_j} \tag{4-18}$$

where q_{ov_j} and $\hat{q}_{ov_j}$ are overland flow with and without process noise w_{ov_k}, respectively, which is assumed as a Gaussian distribution $N(0, \sigma^2_{ov_k})$. The standard deviation of overland flow noise σ_{ov_k} is parameterized as follows:

$$\sigma_{ov_k} = c_{ov} 10^{\alpha_{ov} \exp(-y_{sim\,k-1} / \beta_{ov})} \tag{4-19}$$

where α_{ov} and β_{ov} are adaptable parameters with settings of -10 and 5 m^3/s, respectively, as obtained from sensitivity analysis. $y_{sim\,k-1}$ is the simulated discharge of data assimilation at the previous time step. c_{ov} is the constant coefficient. The value of c_{ov} is estimated through the sensitivity analysis and set as 0.02 for the whole simulation. This formulation was originally proposed by Seo et al. (2009) to enhance the forecast in periods of low flow. Eq. (4-19) specifies progressively smaller uncertainty if the simulated flow falls below the threshold, β_{ov} (m^3/s). We adopt this error formulation because an error of overland flow routing is expected to decline in low flow periods.

The measurement error of the discharge is assumed as a Gaussian distribution $N(0, \sigma^2_{obs_k})$ similar to previous studies (Georgakakos, 1986; Weerts and El Serafy, 2006; Salamon and Feyen, 2010). The standard deviation of the measurement error is chosen as:

$$\sigma_{obs_k} = \alpha_{obs} y_k + \beta_{obs} \tag{4-20}$$

In the above equation, α_{obs} is set as 0.1, which means 10% of the measurement error, and the constant coefficient β_{obs} is applied as 5 m^3/s to consider uncertainty in periods of low flow such as artificial water use and dam reservoir control. The uncertainty of forcing data is not considered in this chapter to make it easy to evaluate the difference of each particle filter. Fifteen percent of perturbation from the uniform distribution is applied for the initial soil moisture condition.

4.3.4 Results and discussion

We implement two kinds of particle filters, SIR and the LRPF, for the hindcasting of streamflow using the WEP model. The resampling step is implemented in both SIR and the LRPF. An additional regularization step is executed only in the LRPF when sample impoverishment occurs or the ensemble mean falls outside 20% of the observed discharge. Simulation periods and observation are shown in Table 4-1. Hourly observed discharges at the Katsura station are used for the data assimilation, and observation at the Kameoka station is used for comparison. A five-day warm-up period is added before the data assimilation starts.

Table 4-1 Simulation periods and observed flow.

Simulation period	Max. observed flow at Katsura (m^3s^{-1})	Data availability at each location	
		Katsura	Kameoka
1 Jun.-31 Jul. 2007	336.9	O	X
1 Aug.-30 Oct. 2004	2276.7	O	O
1 Jun.-31 Aug. 2003	361.6	O	O

Deterministic simulation results and 6-hour-lead forecasts of each particle filter at the Katsura station for the years 2007, 2004, and 2003 are shown in Figs. 4-7, 4-8, and 4-9, respectively. The lag time of 8 hours is applied in the LRPF. The applied values of α_{soil} are 0.05 for 2007 and 0.03 for 2004 and 2003. The forecasted streamflow via two particle filters shown in Figs. 4-7, 4-9 indicates good conformity between observation and simulation, while the deterministic modeling shows significant underestimation, especially in the high flood period. Ninety percent of

confidence intervals of SIR are larger than those of the LRPF, although the same error assumption is used. Compared with results of other years, the differences of confidence intervals between two filters are small in the year of 2004, shown in Fig. 4-8, since the deterministic modeling results show better agreement with observation, relatively. Elapsed simulation time for the year of 2007 is about 11 hours in SIR and 16 hours in the LRPF for a 2-month period simulation with 24-hour-lead forecast at every time step, respectively.

Various ranges of process noise, α_{soil}, are simulated for each particle filter to assess the effects of process noise on the forecast. The mean and 90% confidence intervals of 6-hour-lead forecasts for varying parameter value of α_{soil} are illustrated in Fig. 4-10. In the case of SIR, confidence intervals of forecast widen rapidly, and the ensemble mean becomes unstable when the value of α_{soil} increases. On the other hand, those of the LRPF show stable results regardless of the process noise.

Fig. 4-11 illustrates streamflow forecast of varying lead times via the LRPF and SIR. Two particle filters show different patterns, especially in the rising limb of the hydrograph from 1000 to 1010 time step. When the lead time becomes shorter, forecasts via the LRPF show better results compared to SIR. Conversely, two particle filters show similar forecasts from 1050 to 1180 time step, and the varying pattern is relatively smooth. When the observed flows change sharply, even if the heteroscedastic error assumption is applied, the process error becomes too small in a moment for the prior distribution to cover the observation distribution, which leads to sample impoverishment. In the case of the LRPF, new particles, generated from the kernel and selected in the lagged time window, mitigate the loss of sample diversity, while the recovery of particle diversity needs more time steps in the case of SIR.

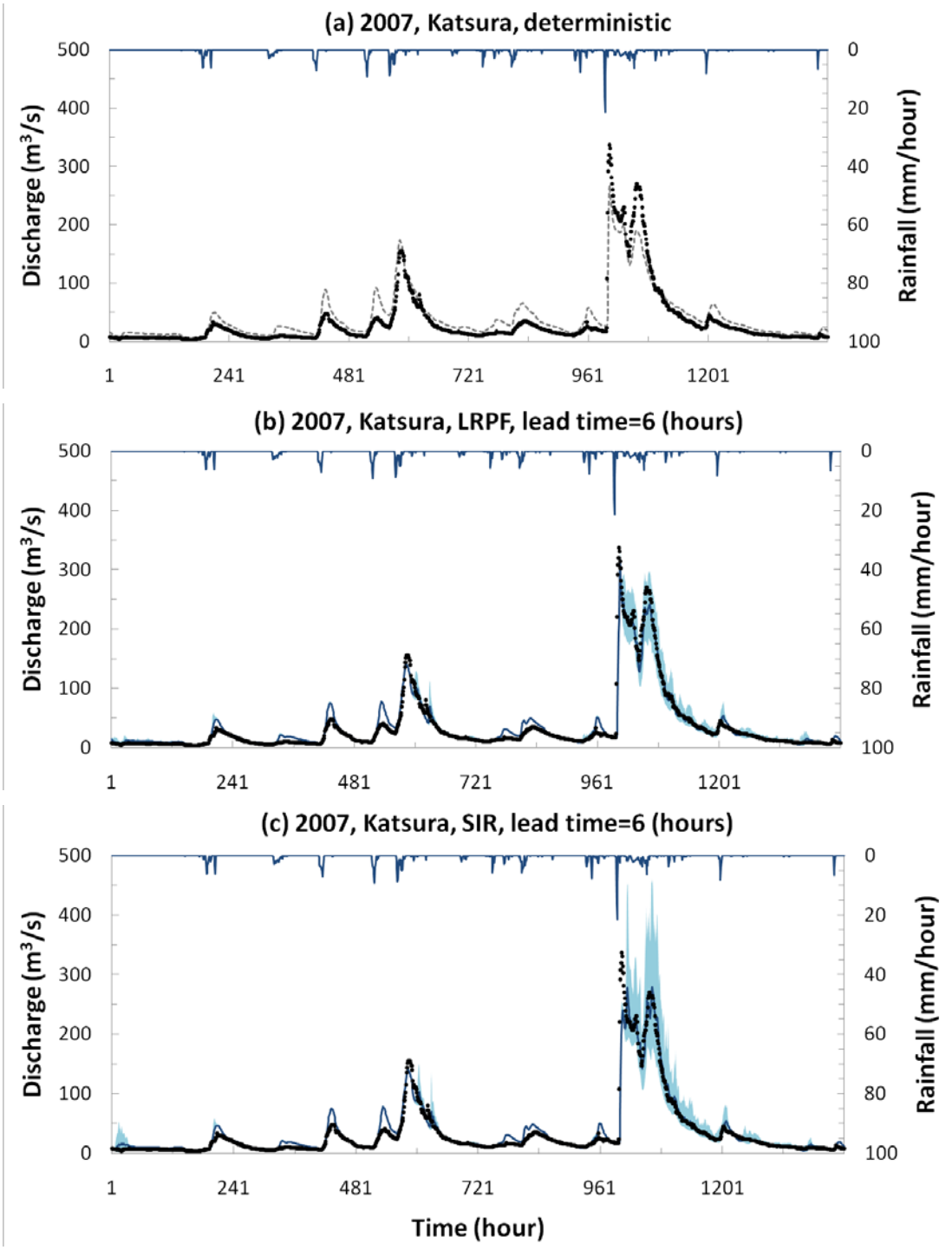

Fig. 4-7 Observed versus 6-hour-lead forecasts at the Katsura station via the LRPF and SIR (1 Jun.-31 Jul. 2007): (a) a deterministic modeling case; (b) the LRPF; and (c) SIR. The blue line and area represent the mean value and 90% confidence intervals, respectively. A gray dashed line represents a deterministic modeling case. The black dots represent observed discharge.

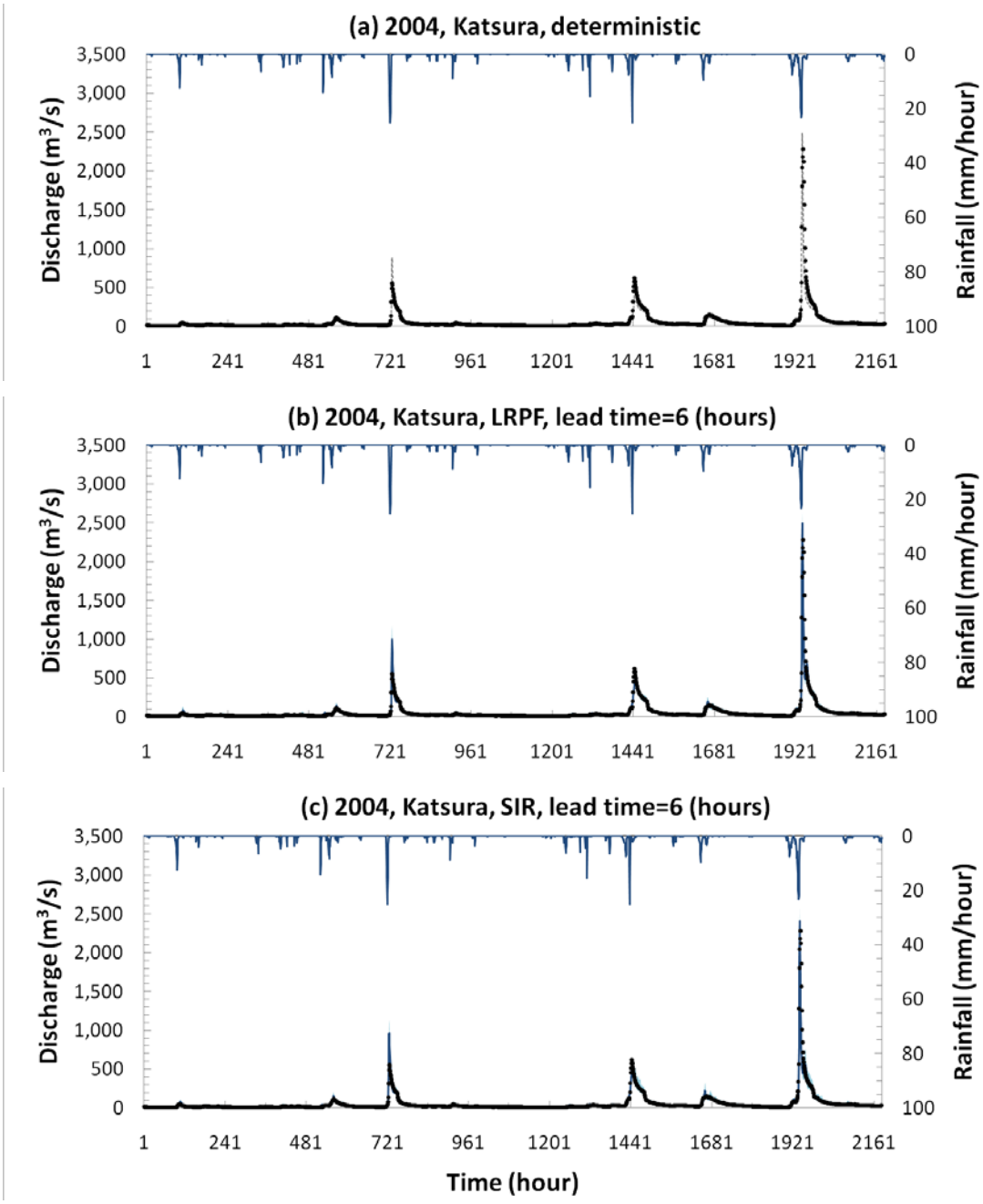

Fig. 4-8 Observed versus 6-hour-lead forecasts at the Katsura station via the LRPF and SIR (1 Aug.-30 Oct. 2004): (a) a deterministic modeling case; (b) the LRPF; and (c) SIR. The blue line and area represent the mean value and 90% confidence intervals, respectively. A gray dashed line represents a deterministic modeling case. The black dots represent observed discharge.

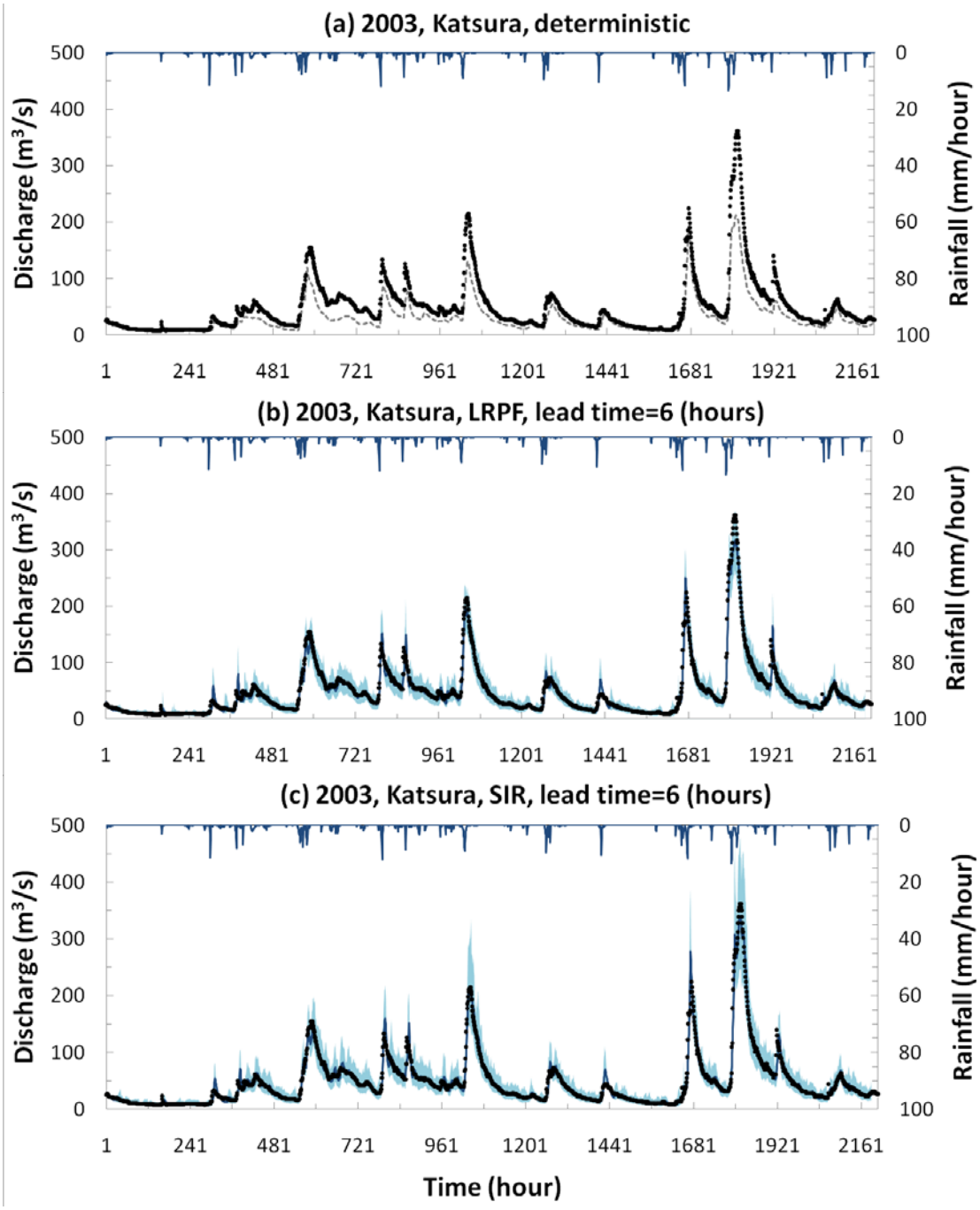

Fig. 4-9 Observed versus 6-hour-lead forecasts at the Katsura station via the LRPF and SIR (1 Jun.-31 Aug. 2003): (a) a deterministic modeling case; (b) the LRPF; and (c) SIR. The blue line and area represent the mean value and 90% confidence intervals, respectively. A gray dashed line represents a deterministic modeling case. The black dots represent observed discharge.

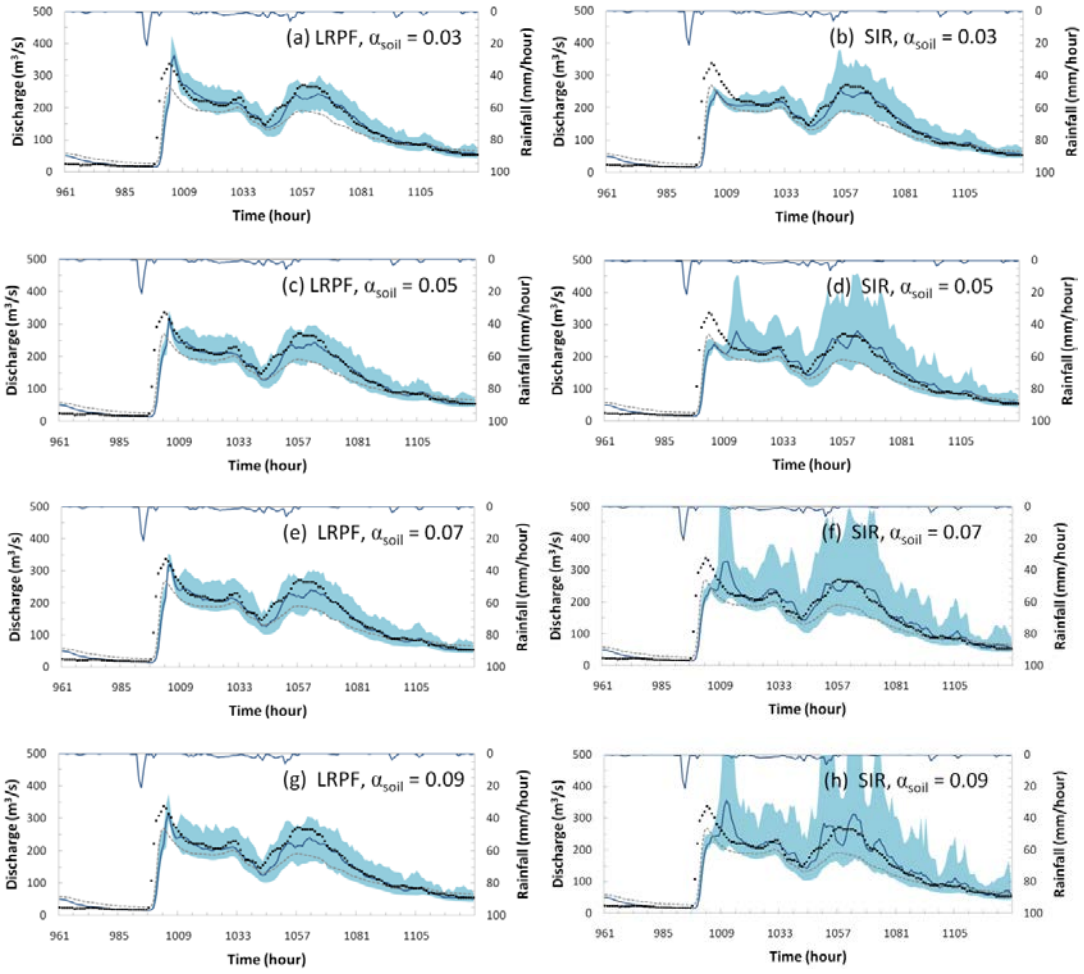

Fig. 4-10 Observed versus 6-hour-lead forecasts at the Katsura station via the LRPF and SIR for varying parameter values of the process error variance, α_{soil} (11 to 17 July 2007). The blue line and area represent the mean value and 90% confidence intervals, respectively. A gray dashed line represents a deterministic modeling case. The black dots represent observed discharge.

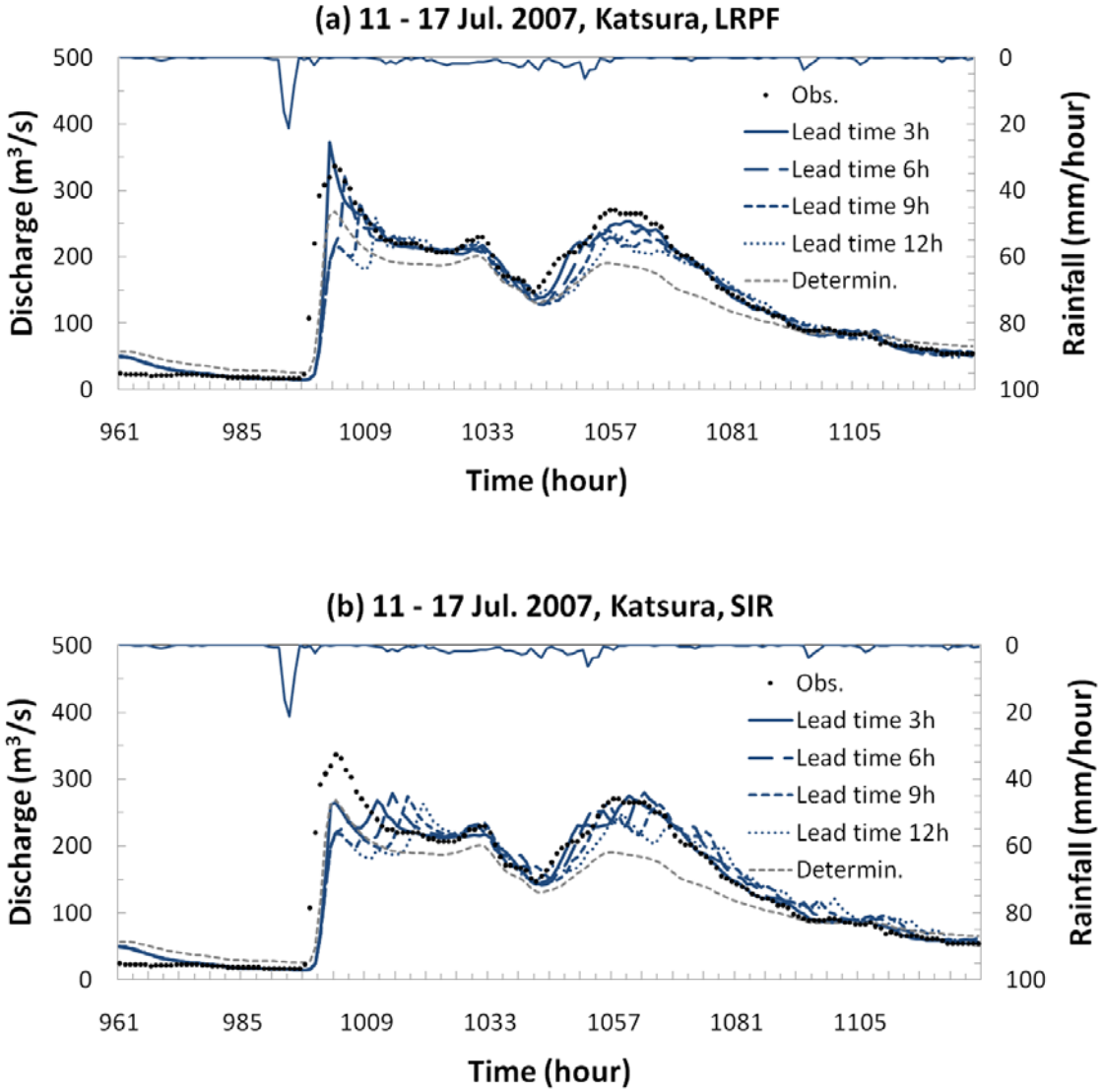

Fig. 4-11 Observed versus forecasts of varying lead times at the Katsura station via the LRPF and SIR with α_{soil} of 0.05 (11 to 17 July 2007): (a) the LRPF; and (b) the SIR particle filter. The blue lines represent forecasts of varying lead times. A gray dashed line represents a deterministic modeling case. The black dots represent observed discharge.

Fig. 4-12 shows the sensitivity of the lag time of the LRPF and process noise parameter, α_{soil}, for each particle filter are estimated for varying lead times in the year of 2007 using Nash-Sutcliffe efficiency. When the lag time is larger than 4 hours, the difference of Nash-Sutcliffe efficiency (NSE) for varying lead times becomes negligible, as shown in Fig. 4-12(a). Eight hours of the lag time are applied to the other simulations by the LRPF. NSE scores for varying lead times show different behaviours for each particle filter (Fig. 4-12(b)). While NSE of the LRPF shows a consistent behaviour regardless of error assumption, with all the red lines overlapping along the lead time, that of SIR changes according to the values of α_{soil}. Overall, the LRPF shows improved NSE for any range of α_{soil}. NSE shows rather significant differences between the two particle filters when plotted for the high flows (not shown).

Fig. 4-13 shows NSE of each particle filter for varying lead times in the years 2004 and 2003. Overall, LRPF forecasts show less variation compared to SIR forecasts, except the forecast of 2003 at Kameoka. Similarly to the year 2007 (Fig. 4-12(b)), NSE scores of SIR in 2004 and 2003 drop sharply when the process error α_{soil} increases. Although NSE scores of the LRPF show less change than does SIR, NSE differences of the LRPF of 2003 increase according to the lead time. Relatively excessive perturbation in the regularization step for the smoothly varied flood events may be one potential reason. However, differences of NSE appear to be negligible within 8-hour lead times. The forecasts at Kameoka show reduced NSE scores in both particle filters. In the case of 2004, LRPF shows better forecasts within 4-hour lead times, while SIR outperforms for other lead times in 2004 and 2003. Since the H-Q relationship of Kameoka is made with limited data, the Kameoka station appears to have larger uncertainty than does Katsura. Due to the lack of data, more extensive comparison is beyond the scope of this chapter. Nevertheless, we can observe that the statistical stability of the LRPF is superior to that of SIR in terms of confidence intervals and accuracy for uncertain process noise, α_{soil} (not shown), similar to the results of 2007 (Fig. 4-10).

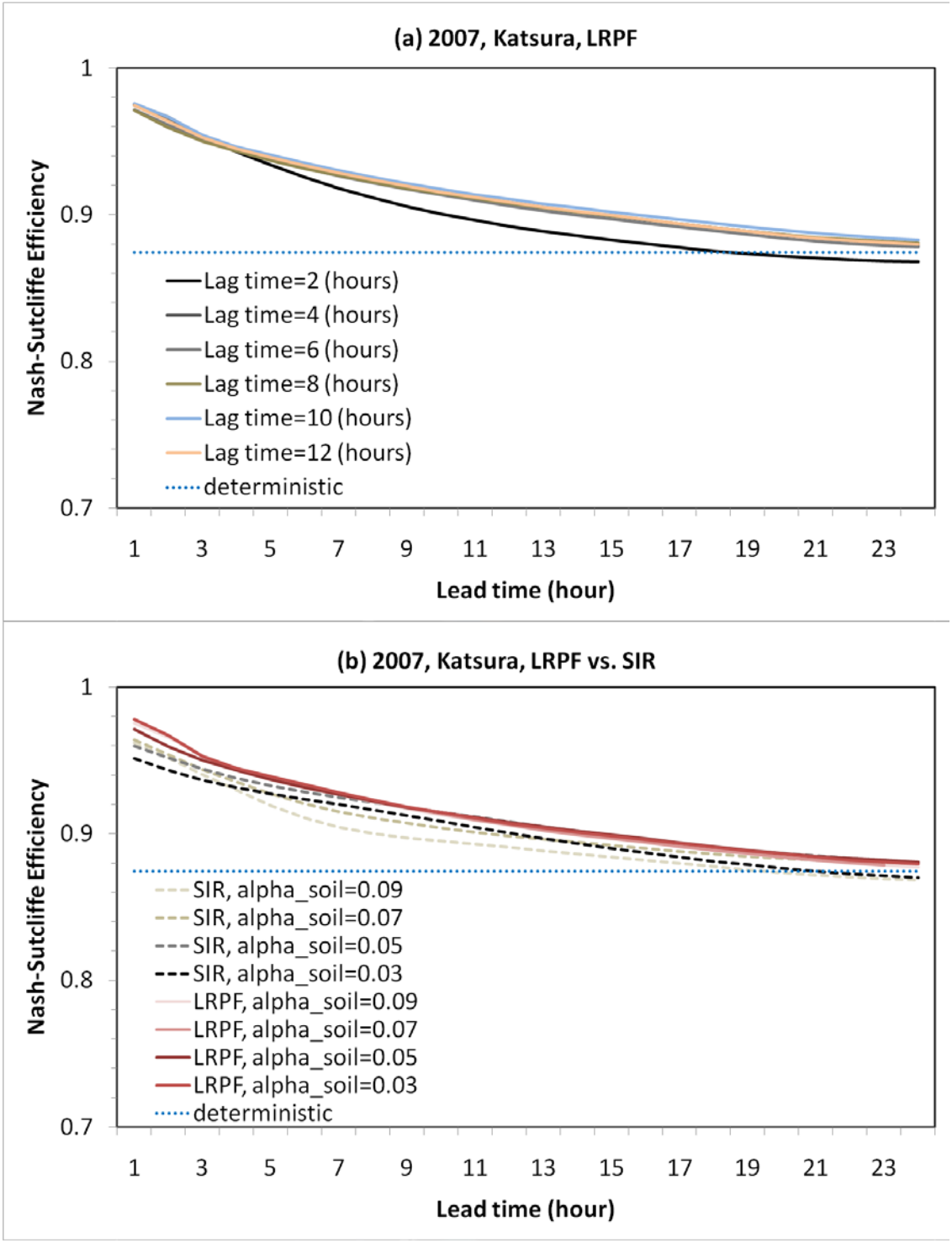

Fig. 4-12 Nash-Sutcliffe model efficiency for varying parameter values of the process error variance, α_{soil} . The red lines represent the lagged regularized particle filter. The dashed lines represent the SIR particle filter. A dotted line represents a deterministic modeling case.

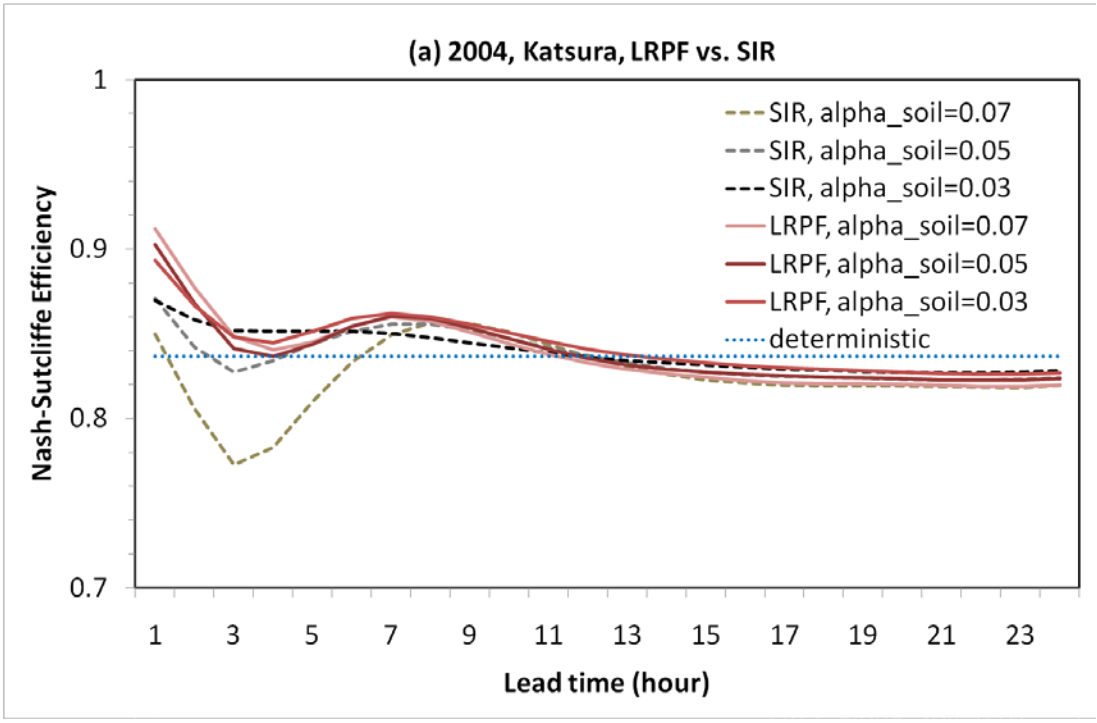
(a) 2004, Katsura, LRPF vs. SIR
Nash-Sutcliffe Efficiency
1
0.9
0.8
0.7
1 3 5 7 9 11 13 15 17 19 21 23
Lead time (hour)
SIR, alpha_soil=0.07
SIR, alpha_soil=0.05
SIR, alpha_soil=0.03
LRPF, alpha_soil=0.07
LRPF, alpha_soil=0.05
LRPF, alpha_soil=0.03
deterministic

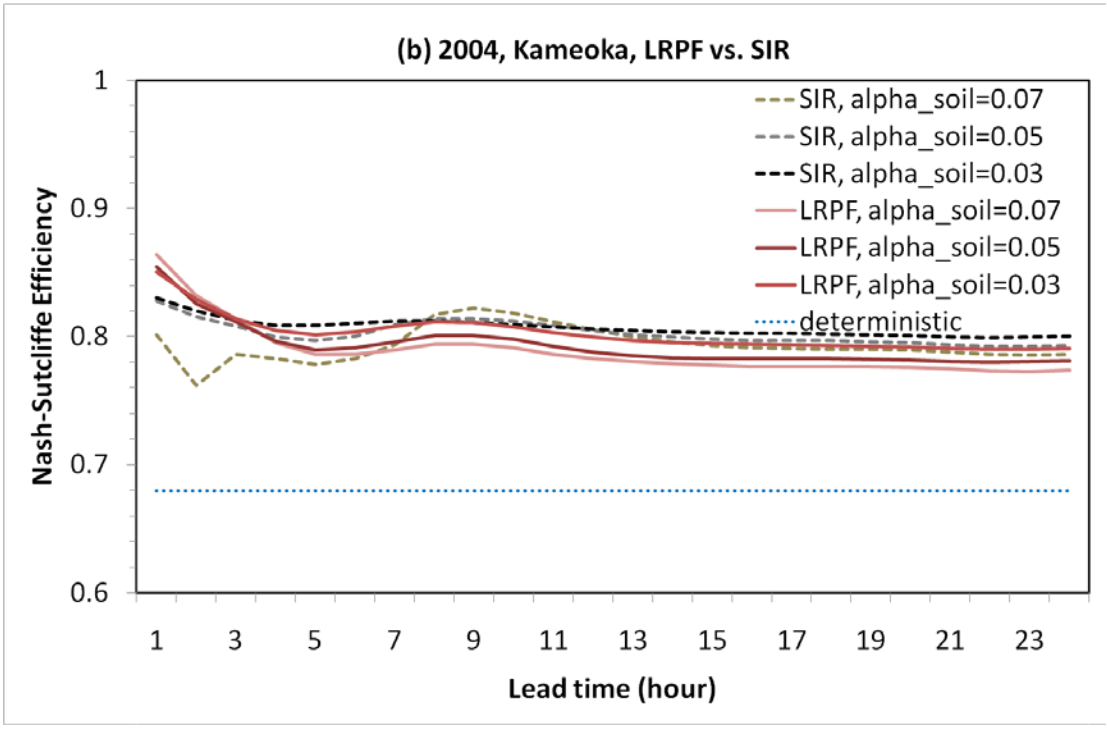
(b) 2004, Kameoka, LRPF vs. SIR
Nash-Sutcliffe Efficiency
1
0.9
0.8
0.7
0.6
1 3 5 7 9 11 13 15 17 19 21 23
Lead time (hour)
SIR, alpha_soil=0.07
SIR, alpha_soil=0.05
SIR, alpha_soil=0.03
LRPF, alpha_soil=0.07
LRPF, alpha_soil=0.05
LRPF, alpha_soil=0.03
deterministic

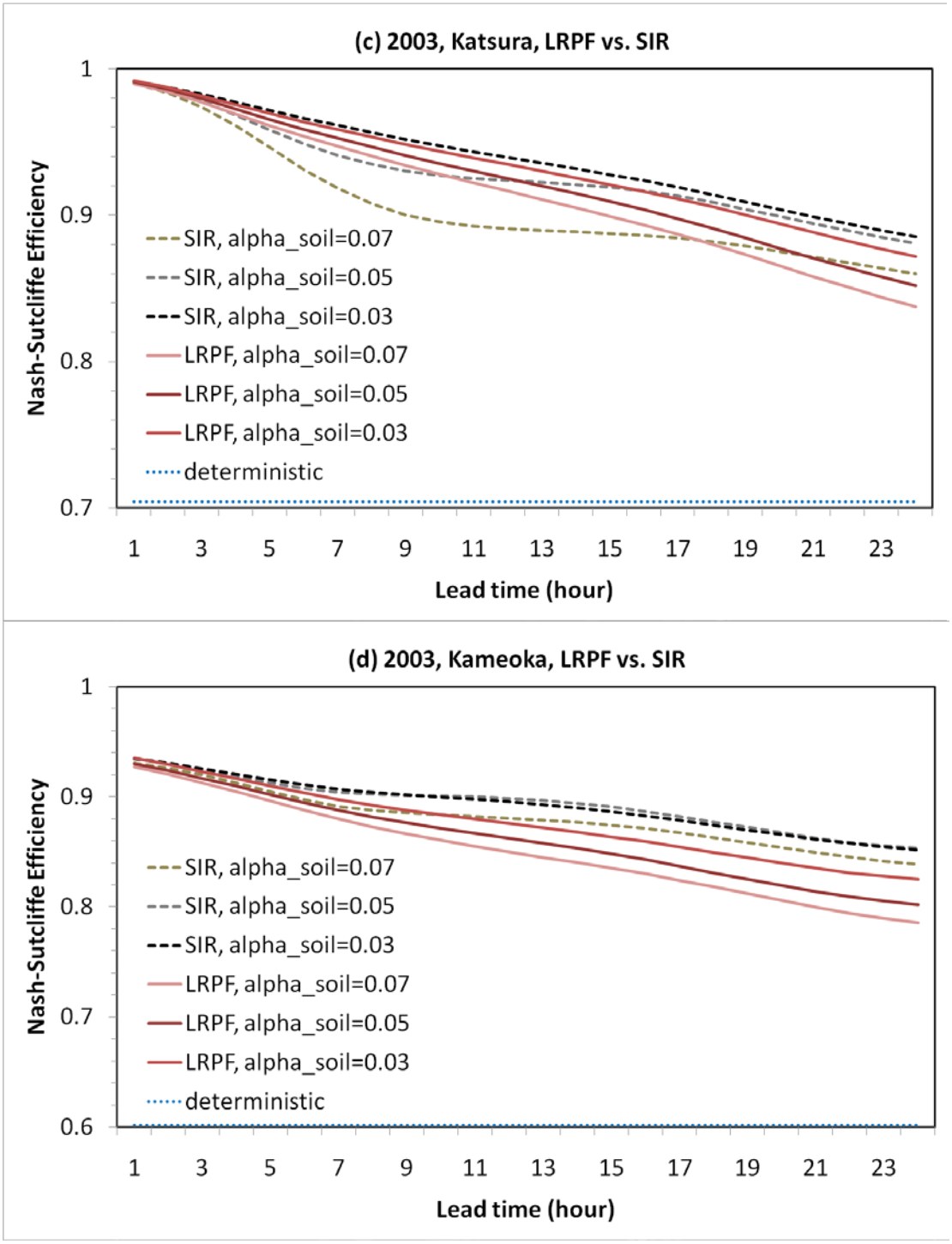

Fig. 4-13 Nash-Sutcliffe model efficiency for varying parameter values of the process error variance, α_{soil} . The red lines represent the lagged regularized particle filter. The dashed lines represent the SIR particle filter. A dotted line represents a deterministic modeling case.

Table 4-2 shows statistics of streamflow forecasts with varying lead times at Katsura including NSE, root mean square error (RMSE) and correlation coefficient (COR) for a given process noise (α_{soil} = 0.03). Statistics shown in Table 4-2 indicate that the LRPF is somewhat better than SIR especially in the years 2007 and 2004. The improvement by the LRPF over SIR is larger for shorter lead times and the high flows (not shown). COR shows high values for both cases in overall periods. It is worth noting that SIR has different optimum values of process noise for data periods, and thus it shows large variation of statistics depending on the process noise (not shown) as the patterns shown in Figs. 4-11 and 4-12.

Table 4-2 Statistics of streamflow forecasts with varying lead times (α_{soil} = 0.03).

Year	Method	Lead time (hour)														
		1			3			6			12			24		
		NSE	RMSE	COR	NSE	RMSE	COR	NSE	RMSE	COR	NSE	RMSE	COR	NSE	RMSE	COR
2007	DET	0.87	16.7	0.96	0.87	16.7	0.96	0.87	16.7	0.96	0.87	16.7	0.96	0.87	16.7	0.96
	LRPF	0.98	7.9	0.99	0.95	11.5	0.98	0.93	13.6	0.97	0.91	16.1	0.95	0.88	18.3	0.94
	SIR	0.96	10.1	0.98	0.95	12.2	0.97	0.93	13.7	0.97	0.91	15.6	0.96	0.88	18.2	0.95
2004	DET	0.84	59.9	0.93	0.84	59.9	0.93	0.84	59.9	0.93	0.84	59.9	0.93	0.84	59.9	0.93
	LRPF	0.89	48.1	0.95	0.85	57.5	0.92	0.86	55.4	0.93	0.84	58.8	0.93	0.83	61.4	0.92
	SIR	0.87	53.2	0.93	0.85	56.8	0.92	0.85	56.9	0.93	0.84	59.7	0.92	0.83	61.1	0.92
2003	DET	0.70	26.9	0.98	0.70	26.9	0.98	0.70	26.9	0.98	0.70	26.9	0.98	0.70	26.9	0.98
	LRPF	0.99	4.4	1.00	0.98	6.7	0.99	0.96	9.4	0.98	0.93	12.6	0.97	0.87	17.6	0.96
	SIR	0.99	4.5	1.00	0.98	6.5	0.99	0.97	9.0	0.98	0.94	12.1	0.97	0.89	16.6	0.96

4.4 Conclusions

A lagged particle filtering approach was proposed as a framework to deal with the delayed response, which originates from different time scales of hydrologic processes in a distributed hydrologic model. The regularized particle filter with the MCMC move step was implemented to preserve sample diversity under the lagged filtering approach. As a process-based distributed hydrologic model, WEP was

implemented to illustrate the strength and weakness of the LRPF compared to SIR for short-term streamflow forecast.

Two particle filters showed significantly improved forecasts compared to deterministic modelling cases in different simulation periods. Various ranges of process noise related to soil moisture were simulated for varying lead times. While SIR has different values of optimal process noise and shows sensitive variation of confidence intervals according to the process noise, the LRPF shows consistent forecasts regardless of the process noise assumption. Due to the preservation of particle diversity by the kernel, the LRPF showed enhanced forecasts, especially when the discharge changed sharply in a short time (the year 2007) and flood peak was high (the year 2004). However, the relatively large perturbation by the kernel could produce negative effects when the flood peak was relatively small and the hydrograph varied smoothly (the year 2003).

The SMC methods have significant potential for high non-linearity problems, especially for process-based distributed models in hydrologic investigation. However, the computational cost and marginal adequacy of the SMC methods for distributed modelling have been bottlenecks to their practical implementation. As shown in this chapter, a particle filtering process can be effectively parallelized and implemented in the multi-core computing environment via a MPI library. The LRPF is expected to be used as one of the frameworks for sequential data assimilation of process-based distributed modelling. The main benefits of the LRPF are the improved forecasts for rapidly varied high floods and the stability of confidence intervals for uncertainty of process noise. More extended implementation for multi-site forecasting and effective sequential estimation of model parameters remain open problems, indeed.

Chapter 5

Ensemble Kalman filtering and particle filtering in a lag-time window for short-term streamflow forecasting with a distributed hydrologic model

Abstract *Performance of ensemble Kalman filtering (EnKF) and particle filtering (PF) is assessed for short-term streamflow forecasting with a distributed hydrologic model, namely, the water and energy transfer processes (WEP) model. To mitigate the drawbacks of conventional filters, the ensemble square root filter (EnSRF) and the regularized particle filter (RPF) are implemented. For both the EnSRF and the RPF, sequential data assimilation is performed within a lag-time window to account for lag and response times for internal hydrologic processes in a hydrologic model. Proposed methods are applied to two catchments in Japan and Korea to assess the performance of the methods. The forecasting accuracy of both the EnSRF and the RPF is improved when sufficient lag times are provided. The EnSRF is sensitive to lag times and exhibits limited forecasting ability with short lead times, while the RPF exhibits more stable forecasting ability for the range of lead times examined. Filtering in a lag-time window also yields improved performance with a limited number of ensembles.*

5.1 Introduction

Flood disaster is the main cause of losses from natural hazards in the world and is responsible for a greater number of damaging events than any other type of natural event that threatens human safety. In recent years, steady increases in flood damage have contributed to a growing interest in the development of flood forecast systems and their operation in real time. Accurate streamflow predictions with a forecast lead time of several hours are of considerable value in mitigating flood damage and addressing operational flood scenarios (Barbetta et al., 2011). However, due to various uncertainties originating from simulation models, observations and forcing data, it is difficult to obtain accurate flood forecasting results for required lead times.

In the past few years, ensemble forecasting techniques based on the sequential data assimilation methods have become increasingly popular, due to their potential ability to explicitly handle the various sources of uncertainty in operational hydrological models (Vrugt et al., 2006). The basic idea of sequential data assimilation is to quantify errors for both the hydrological model and observations and to recursively update hydrological model states in a way that optimally combines model simulations with observations when new observations become available (Clark et al., 2008).

Among the various data assimilation methods, Kalman filtering (KF) is the optimal data assimilation method for linear and Gaussian dynamics (Kalman, 1960). For a nonlinear system, the extended Kalman filter (EKF) has been applied, but the EKF could lead to unstable results when the nonlinearity in a system is severe. The ensemble Kalman filtering (EnKF), introduced by Evensen (1994), is a Monte Carlo approximation to traditional KF. EnKF uses an ensemble of forecasts to estimate background error covariances (Whitaker and Hamill, 2002). The advantage of EnKF over the EKF is that it does not require the development of the linearized state-space formulation of the hydrological model (Clark et al., 2008). A number of previous studies have demonstrated the performance of EnKF in improving hydrological predictions (e.g., Vrugt et al., 2006; Clark et al., 2008; Komma et al., 2008;

Moradkhani et al., 2005b, 2008; Nie et al., 2011; Han et al., 2012; He et al., 2012; McMillan et al., 2012; Li et al., 2012). However, the posterior probability density of hydrologic states in a model is often non-Gaussian and cannot be adequately characterized by the first two moments (Leisenring and Moradkhani, 2011). In addition, as EnKF actively updates states, it does not explicitly comply with the principle of conservation of mass (Salamon and Feyen, 2010).

Particle filtering (PF), also known as the sequential Monte Carlo (SMC) methods, is a Bayesian learning process in which the propagation of all uncertainties is conducted by a suitable selection of randomly generated particles without any assumptions about the nature of the distributions (Gordon et al., 1993; Musso et al., 2001; Arulampalam et al., 2002; Johansen, 2009). Unlike Kalman filter-based methods, PF performs updating on particle weights instead of state variables (Liu and Gupta, 2007), which has the advantage of reducing numerical instability, especially in physically based or process-based models. In addition, PF is applicable to non-Gaussian state-space models. In recent years, applications of these versatile methods have been increasing in hydrology and earth sciences (e.g., Moradkhani et al., 2005a; Weerts and El Serafy, 2006; Zhou et al., 2006; Salamon and Feyen, 2009, 2010; van Delft et al., 2009; van Leeuwen, 2009; Qin et al. 2009; Karssenberg et al., 2010; Dechant and Moradkhani, 2011; Giustarini et al., 2011; Hiemstra et al., 2011; Montzka et al., 2011; Noh et al., 2011a, 2011b, 2012; Frei and Künsch, 2012; Plaza et al., 2012; Pasetto et al., 2012; Vrugt et al., 2012).

Recently, there have been advances in both EnKF and PF that have improved their performance. In conventional EnKF, perturbation of measurements is used to update ensemble members, which is an additional source of uncertainty. The ensemble square root filter (EnSRF) was developed to avoid sampling issues associated with the use of "perturbed observations" in the ensemble update step (Whitaker and Hamill, 2002). In the case of PF, the sequential importance resampling (SIR) particle filter, which is the basic particle filter, may lead to a sudden loss of diversity in particles due to the resampling step (Ristic et al., 2004). In the hydrologic modeling community, mitigation methods for the SIR filter have been suggested that involve

changing resampling methods, such as residual resampling (Weerts and El Serafy, 2006) and using an empirical likelihood function rather than a Gaussian function (Leisenring and Moradkhani, 2011). Another remedy for sample degeneracy is the regularization particle filter (RPF) with the Markov chain Monte Carlo (MCMC) move step, which preserves sample diversity by adding noise from kernels and by selecting importance particles through an additional move step. In a previous study, the RPF was successfully applied to streamflow forecasting with a distributed hydrologic model (Noh et al., 2011b).

There have been attempts to compare the performance of EnKF and PF in the hydrologic modeling community (Weerts and El Serafy, 2006; Zhou et al., 2006; Leisenring and Moradkhani, 2011). PF tends to outperform EnKF when the ensemble size is sufficiently large, as reported for other research fields. However, on the subject of the ensemble size required for operational uses, the performance of filters has been observed to be different for different hydrologic models and filtering methods. Weerts and El Serafy (2006) and Zhou et al. (2006) reported that EnKF outperformed PF when the ensemble size was small, while PF performed better than EnKF even at relatively small ensemble sizes according to results obtained by Leisenring and Moradkhani (2011). In addition, performance assessment was focused on a lumped hydrologic model and the comparison was limited to short ranges of forecast lead times. The comparison of EnKF and PF in a distributed hydrologic model, which is usually highly non-linear and non-Gaussian in its distribution, has not been fully addressed in terms of operational uses such as varying lead times and ensemble sizes.

In this chapter, the performance of the ensemble Kalman filter and the particle filter is assessed for short-term streamflow hindcasting with a distributed hydrologic model. To alleviate the drawbacks of conventional filtering methods resulting from disturbed observations in EnKF and a loss of diversity in PF, the ensemble square root filter and the regularized particle filter are selected. For the EnSRF and the RPF, state variables are analyzed and updated through a lag-time window to consider different response times of internal hydrologic processes in a distributed hydrologic

model. A lag-time window enables filtering processes to consider a time lag in the routing process and use all available measurement information. The proposed methods are applied to two different catchments in Japan and Korea to assess performance of the methods.

In this chapter, Bayesian filtering theory, EnKF and PF, including the EnSRF and the RPF, are outlined below. Procedures for applying the EnSRF and the RPF in a lag-time window are then presented. Experiment setups, including study areas, a distributed hydrologic model, uncertainty assumption of modeling and observation, are presented next. The performance of these two filters for different catchments is analyzed for varying lag-time windows and ensemble numbers. A summary and concluding remarks are provided in the last section.

5.2 Bayesian filtering in a lag-time window

In this section, we briefly explain Bayesian filtering methods such as ensemble Kalman filtering (EnKF) and particle filtering (PF) and then propose a new scheme to apply two filters in a lag-time window.

5.2.1 Ensemble Kalman filtering

EnKF (Evensen, 1994) is a suboptimal estimator, where the error statistics are predicted using Monte Carlo methods. EnKF consists of update and prediction steps. The ensemble means of the hidden and observable states are defined as

$$\bar{x}_k = \frac{1}{n}\sum_{i=1}^{n} x_k^i \tag{5-1}$$

$$\overline{h(x_k)} = \frac{1}{n}\sum_{i=1}^{n} h(x_k^i) \tag{5-2}$$

where x_k^i and $h(x_k^i)$ denote the hidden and observable states of i^{th} ensemble, respectively, and n is the number of ensemble members. If the measurements are a nonlinear combination of state variables, the Kalman gain is calculated as

$$K = P_{xy_k}(P_{yy_k} + V_k)^{-1} \tag{5-3}$$

$$P_{xy_k} = \frac{1}{n-1}\sum_{i=1}^{n}\left(x_k^i - \bar{x}_k\right)\left(h(x_k^i) - \overline{h(x_k)}\right)^T \tag{5-4}$$

$$P_{yy_k} = \frac{1}{n-1}\sum_{i=1}^{n}\left(h(x_k^i) - \overline{h(x_k)}\right)\left(h(x_k^i) - \overline{h(x_k)}\right)^T \tag{5-5}$$

where V_k denotes the variance of the measurement noise (Houtekamer and Mitchell, 2001).

The update equation is calculated according to

$$x_k^{up,i} = x_k^i + K\left(y_k^i - h(x_k^i)\right) \tag{5-6}$$

In conventional EnKF (e.g., Burgers et al. (1998)), y_k^i in Eq. (5-6) represents perturbed observations given by

$$y_k^i = y_k + v_k^i \tag{5-7}$$

where v_k^i is a zero-mean random variable with a normal distribution and variance V_k. The derivation and detailed description of EnKF is given by Evensen (2003) and Oke et al. (2007).

5.2.2 Ensemble square root filter

The perturbed observations in Eqs. (5-6) and (5-7) can have a detrimental effect in that they add noise to the analysis. Whitaker and Hamill (2002) introduced the ensemble square root filter (EnSRF) to provide the correct analysis error covariance without perturbing the observations. With this method, the ensemble is broken into mean and anomaly portions, and updating is performed separately for the ensemble mean and anomalies:

$$\bar{x}_k^{up} = \bar{x}_k + K\left(\bar{y}_k - \overline{h(x_k)}\right) \tag{5-8}$$

$$x_k'^{up,i} = x_k'^i + K'\left(y_k'^i - h(x_k^i)'\right) \tag{5-9}$$

where the prime denotes the deviations of each ensemble from the ensemble mean. The ensemble mean is updated with the traditional gain given by Eq. (5-3), while anomalies are updated with a reduced gain given by

$$K' = P_{xy_k}\left[\left(\sqrt{P_{yy_k}+V_k}\right)^{-1}\right]^T\left[\left(\sqrt{P_{yy_k}+V_k}+\sqrt{V_k}\right)\right]^{-1} \tag{5-10}$$

In Eq. (5-9), $y_k'^i = 0$, which indicates no perturbation of observation in anomalies. Therefore, each ensemble member is updated by

$$x_k^{up,i} = \bar{x}_k^i - K'\left(h(x_k^i)'\right) \tag{5-11}$$

Whitaker and Hamill (2002) showed that the sampling error associated with perturbed observations makes the EnSRF more accurate than EnKF.

5.2.3 Particle filtering

PF is a set of simulation-based methods that provide a flexible approach to computing posterior distributions without any assumptions being made about the nature of the distributions. The key idea of PF is based on point mass ("particle") representations of probability densities with associated weights:

$$p(x_k \mid y_{1:k}) \approx \sum_{i=1}^{n} w_k^i \delta(x_k - x_k^i) \tag{5-12}$$

where x_k^i and w_k^i denote the i^{th} posterior state ("particle") and its weight, respectively, and $\delta(\cdot)$ denotes the Dirac delta function. Weight can be updated as:

$$w_k^i \propto w_{k-1}^i p(y_k \mid x_k^i) \tag{5-13}$$

where $p(y_t \mid x_t^i)$ is the likelihood of each particle x_t^i. A common problem in PF is the degeneracy phenomenon, which can be reduced by performing the resampling step whenever a significant degeneracy is observed. A more detailed description of PF is presented in Chapter 2.

5.2.4 Regularized particle filter

The main idea of the regularized particle filter (RPF) consists of changing the discrete approximation of a posterior distribution to a continuous approximation. With conventional particle filters, the weight of a particle is defined at a discrete point; therefore, the same particles are duplicated in the resampling step. However, the RPF defines particle weights in a continuous mode, which enables a new particle

system with different particle locations in the resampling step, also called the regularization step, as follows:

$$x_k^{i\,*} = x_k^i + h_{opt} D_k \varepsilon^i \tag{5-14}$$

$$h_{opt} = A \cdot n^{-\frac{1}{n_x+4}} \quad with\ A = \left[8 c_{n_x}^{-1} (n_x + 4) \left(2\sqrt{\pi}\right)^{n_x} \right]^{\frac{1}{n_x+4}} \tag{5-15}$$

where $x_k^{i\,*}$ is a new particle generated from kernel density, h_{opt} is the optimal bandwidth with unit covariance matrix, D_k is estimated from L_k, which is the empirical covariance matrix such that $D_k D_k^T = L_k$, and ε^i is the random noise from the kernel.

The theoretical drawback of the RPF is that its samples are no longer guaranteed to asymptotically approximate those from the posterior distribution. This drawback can be mitigated by including the Markov chain Monte Carlo (MCMC) move step (Gilks and Berzuini, 2001) based on the Metropolis-Hastings algorithm (Robert and Casella, 1999). A more detailed description of the RPF is given in Chapter 4.

5.2.5 Filtering in a lag-time window

In catchment hydrology, different types of patterns are often encountered at different time and space scales, and these are associated with different processes (Grayson and Blöschl, 2001). Generally, different hydrologic processes such as groundwater flow, infiltration and streamflow have different temporal scales (e.g., Blöschl and Sivapalan, 1995). In addition, unlike other states, streamflow is an aggregated variable routed from headwater areas. There is a time lag until precipitation is infiltrated, subsurface/surface runoff occurs and generated runoff is routed as streamflow into the measurement site. Therefore, we introduce a lag-time window for filtering processes to consider a time lag in the routing process and different time scales of the hydrologic processes and also to use all of the available measurement information. Figs. 5-1 and 5-2 illustrate a single cycle of EnKF and PF, respectively, in a lag-time window. Here, *k* is the current time step, and *j* is the lag time required for responses of internal state variables to be transmitted into the observable

variables. For simplicity, we assume that an observation becomes available in every time step.

The procedure for applying a lag-time window for the ensemble square root filter is as follows:

1. To have a prediction at the current time step *k*, simulation is initiated at the time step *k*-*j*.
2. At the time step *k*-*j*+1, state variables are stored.
3. When ensembles arrive at the current time *k*, state variables are updated using Eq. (5-9).
4. State variables at the time step *k*-*j*+1 are updated as:

$$x_{k-j+1}^{up,i} = \bar{x}_{k-j+1}^{i} - K'_{k-j+1}\left(h(x_k^i)'\right) \tag{5-16}$$

In a similar manner, the procedure for applying a lag-time window for the regularized particle filter can be defined as follows:

1. To have a prediction at the current time step *k*, simulation is initiated at the time step *k*-*j*.
2. At the time step *k*-*j*+1, state variables are stored.
3. When ensembles arrive at the current time step *k*, the weights of the ensembles are estimated using Eq. (5-13).
4. According to the estimated weights, ensembles are resampled. During the resampling step, all state variables at the time step *k*-*j*+1 and *k* are duplicated together from the highly weighted particles to particles having negligible weights.
5. When a loss of sample diversity occurs, the regularization step is executed, which means that steps 1 to 3 are repeated by newly generated states at time step *k*-*j* using Eq. (5-14) and the acceptability of each ensemble is checked at time step *k* using the MCMC move step.

For both filters, updated or resampled states at the time step k-j+1 are used as initial conditions in the next assimilation window. It is best to set the lag time j to be sufficiently large to cover plausible ranges. The sensitivity of the time lag for each filter will be assessed in the following section.

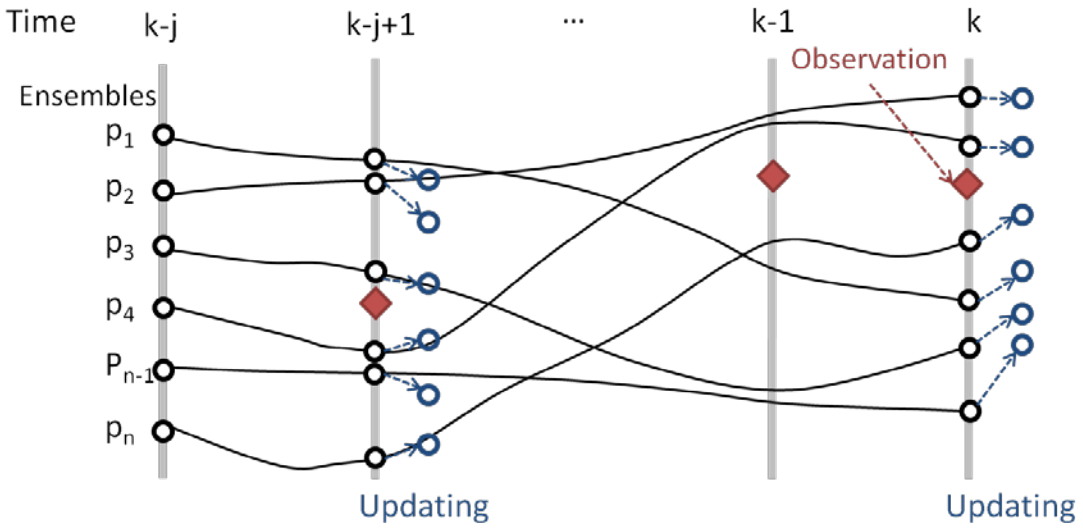

Fig. 5-1 A cycle of the ensemble Kalman filter in a lag-time window.

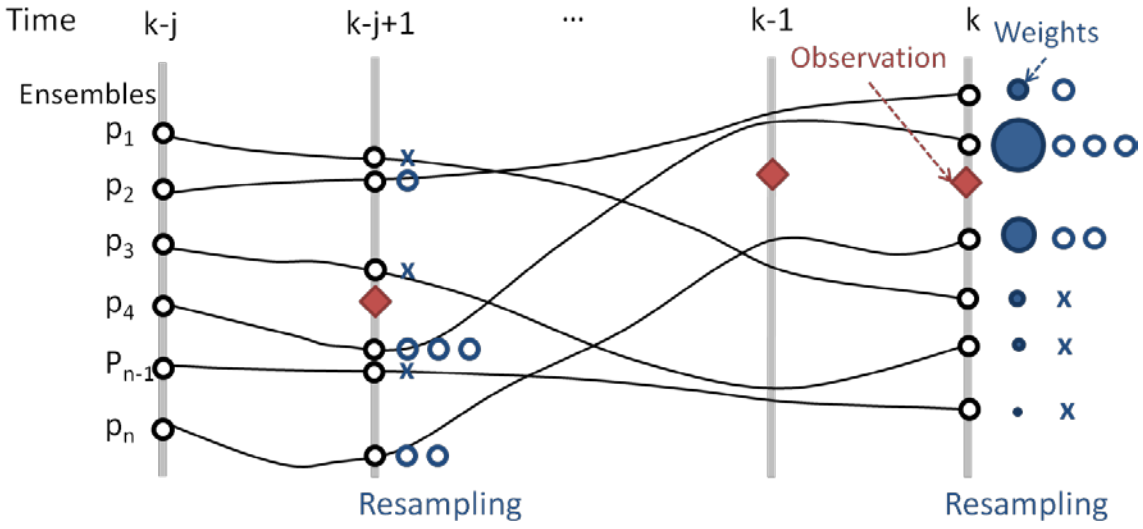

Fig. 5-2 A cycle of the particle filter in a lag-time window.

5.3 Evaluation experiments and results

5.3.1 Hydrological Model

The applied hydrologic model is the water and energy transfer processes (WEP) model, which was developed for simulating spatially variable water and energy processes in catchments with complex land covers (Jia and Tamai, 1998; Jia et al., 2001). A more detailed description of the WEP model is presented in Chapter 4.

5.3.2 Study area and input data

The proposed methods are applied to two small-sized catchments, the Katsura River catchment and the Gyeongancheon catchment, which are located in Japan and Korea, respectively (see Fig. 5-3). The Katsura River catchment in Japan covers an area of 887 km^2, and its dominant land uses are forests (76.7%), agricultural areas (9.3%) and residential areas (7.5%). The grid resolution is 250 m for all distributed input data, including topography, soil, land use, etc. There are 13 rainfall observation stations and 1 meteorological observation station, the hourly data from which are used as model inputs. The Hiyoshi dam is located upstream, and the outflow record from the dam reservoir is used as inflow to the hydrologic model. The soil distribution is obtained from the website of the Food and Agriculture Organization of the United Nations (http://www.fao.org/nr/land/soils/en/).

The Gyeongancheon catchment is located in Gyeonggido, Korea, and covers an area of 565 km^2. The Gyeongancheon stream flows from south to north, joining the Han River, one of the main rivers in Korea. The dominant land uses are forests (78.6%), agricultural areas (16.0%) and residential areas (4.2%). The grid resolution is 200 m. There are 5 rainfall observation stations and 2 meteorological observation stations. The soil distribution is obtained from the National Academy of Agricultural Science of Korea.

Simulation periods and observed rainfall and flow are shown in Table 5-1. Hourly observed discharges at each outlet are used for the data assimilation. The nearest-neighbor interpolation method is used for representation of the spatial distribution of

rainfall. Physical properties of soils are derived from soil texture information using the ROSETTA model (Schaap et al., 2001). For other parameters, such as aquifers and vegetation, we apply parameter ranges identified in the earlier studies mentioned previously.

Table 5-1 Simulation periods and observed flow and rainfall.

Observation station	Simulation period	Max. observed flow (m^3s^{-1})	Total observed rainfall (mm)
Katsura	1 Jun. - 31 Aug. 2003	361	729
Gyeongan	1 Jul. - 31 Sep. 2010	793	1225

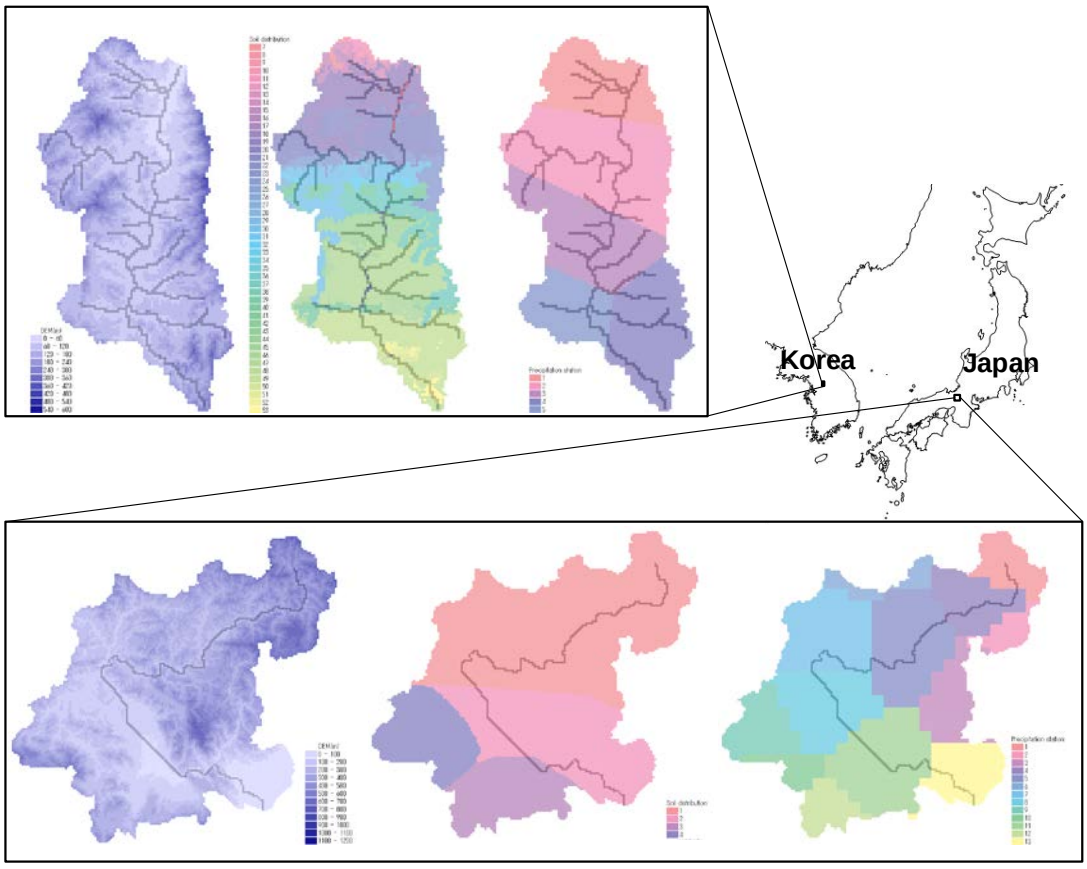

Fig. 5-3 The Gyeongancheon catchment and the Katsura River catchment located in Korea and Japan, respectively: (a) elevation map, (b) soil distribution, and (c) rainfall network for the Gyeongancheon catchment; and (d) elevation map, (e) soil distribution, and (f) rainfall network for the Katsura River catchment.

5.3.3 Noise models for data assimilation

In this chapter, we select soil moisture content as a hidden state variable and streamflow measured at the catchment outlet as an observable variable for data assimilation. Global multipliers are used to perturb state variables for both filters. In the case of the EnSRF, states are aggregated and updated for each rainfall network (see Fig. 5-3). However, a single multiplier is implemented in the RPF because direct updating of states is not required in the particle filters. In this section, we briefly explain how ensembles are perturbed by process noises in both filters. To avoid complexity in notation, we exclude the index *i*, indicating the i^{th} ensemble member, from the equations. The total soil moisture depth at the previous time step S_{k-1} is aggregated for three soil layers within the catchment as follows:

$$S_{k-1} = \sum_{l=1}^{3} \sum_{j=1}^{m} \theta_j^l d_j^l \tag{5-17}$$

where θ_j^l and d_j^l are the volumetric soil moisture content (m^3/m^3) and the soil depth (m) in each layer, and *l* and *m* represent the number of soil layers and the total number of grids within the catchment, respectively. The process noise of the soil moisture content w_{soil_k} is added to the aggregated state variable S_{k-1} as follows:

$$\hat{S}_k = S_{k-1} + w_{soil_k} \tag{5-18}$$

where w_{soil_k} is assumed to follow a Gaussian distribution $N(0, \sigma_{soil_k}^2)$ with a heteroscedastic standard deviation given as follows:

$$\sigma_{soil_k} = \alpha_{soil} S_{k-1} + \beta_{soil} \tag{5-19}$$

In the above equation, α_{soil} and β_{soil} are adaptable parameters that can be obtained from sensitivity analysis. As shown in a previous study (Noh et al. 2011b), the selection of adaptable parameters, α_{soil} and β_{soil}, is not sensitive if a lag-time window is used in PF. Therefore, a value of 0.05 is used for both filters.

The measurement error of the discharge is assumed to follow a Gaussian distribution, $N(0, \sigma_{obs_k}^2)$, as reported in previous studies (Georgakakos, 1986; Weerts and El

Serafy, 2006; Salamon and Feyen, 2010). The standard deviation of the measurement error is chosen as follows:

$$\sigma_{obs_k} = \alpha_{obs} y_k + \beta_{obs} \tag{5-20}$$

In the above equation, α_{obs} is set at 0.1, meaning that 10% of the measurement error and the constant coefficient β_{obs} are applied to estimating the uncertainty in periods of low flow such as artificial water use. Fifteen percent of perturbation from the uniform distribution is applied to the initial soil moisture condition.

5.3.4 Results and discussion

We implement two sequential data assimilation methods, the ensemble square root filter and the regularized particle filter, for hindcasting of streamflow using the WEP model. For both filters, warm-up periods of 120 hours are allowed before the data assimilation starts. The number of ensembles is set as 64 for EnKF and PF, considering the capacity of computing resources and ensemble diversity after the sensitivity analysis. Simulations are conducted for two small catchments in Japan and Korea to demonstrate the applicability of proposed methods for short-term streamflow forecasting.

Fig. 5-4 shows 6-hour-lead forecasts of the EnSRF and the RPF and deterministic simulation results at the Katsura station in Japan from 1 June to 31 August 2003. The blue line and area represent the ensemble mean and 90% confidence intervals, respectively. The dashed gray line represents the deterministic modeling case. The black dots represent observed discharge at the Katsura station. The applied lag times are 10 and 8 hours for the EnSRF and the RPF, respectively. While the deterministic simulation significantly underestimates streamflow, the streamflows forecasted with the two filters agree well with observations, indicating that sequential data assimilation contributes to correcting internal states properly in both filters. Ninety-percent confidence intervals around the EnSRF predictions are larger than those around the RPF predictions, although the same noise assumptions are used.

The effects of a lag-time window on both filters are assessed for various ranges of lag times using Nash-Sutcliffe efficiency (NSE).

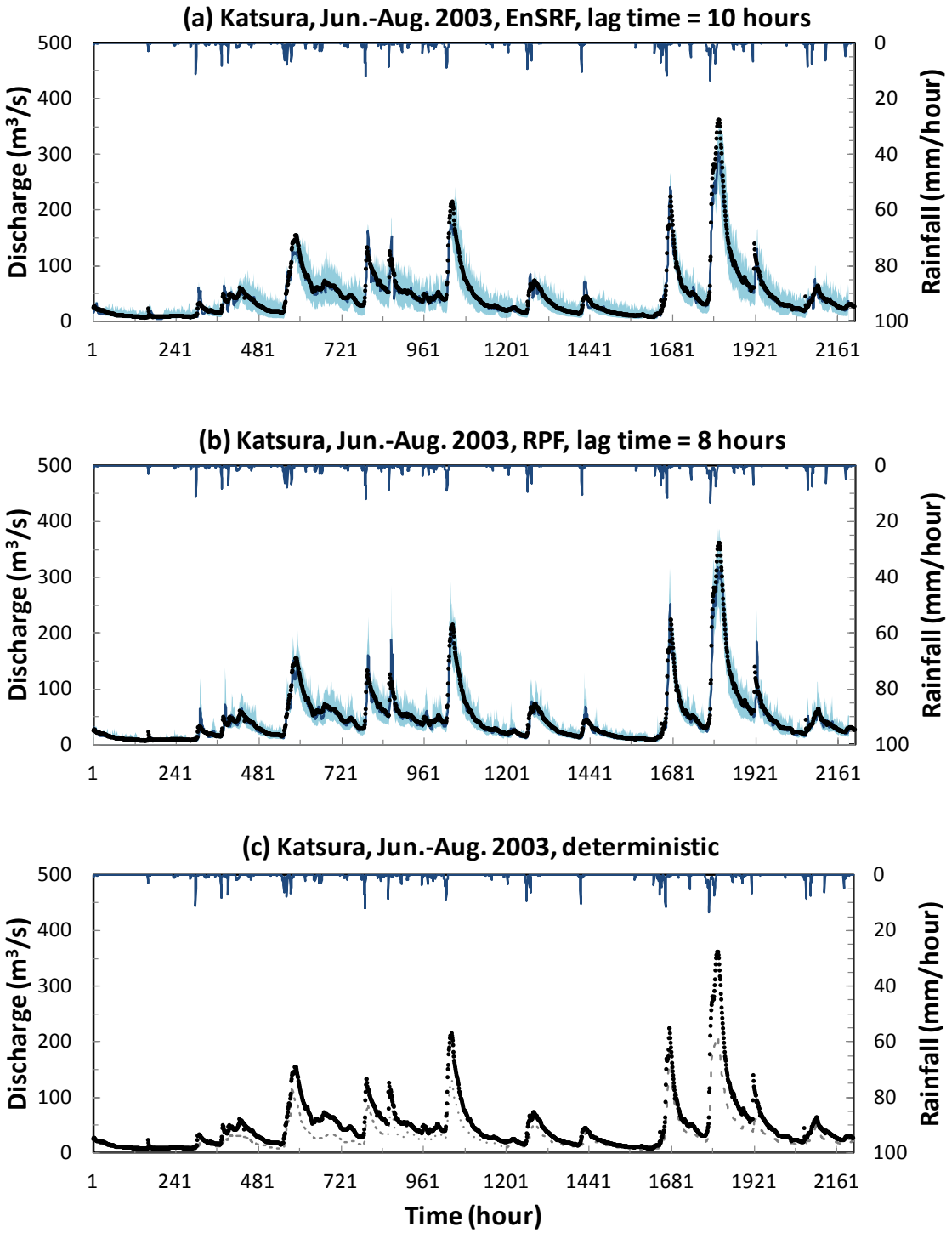

Fig. 5-4 Observed versus 6-hour-lead forecasts at the Katsura station (1 Jun.–31 Aug. 2003): (a) the EnSRF, (b) the RPF, and (c) deterministic modeling.

Fig. 5-5 shows NSE for varying lag-time windows and lead times in the EnSRF and the RPF. The other simulation conditions are the same as those shown in Fig. 5-4. While the forecasts are inferior to the deterministic modeling results without DA when lag-time windows are short, the performance of both filters improves as the lag time increases. Overall, the RPF outperforms the EnSRF for varying lead times when the lag time is greater than 4 hours. There appears to be a threshold value for both filters beyond which prediction performance does not improve. The EnSRF seems to be sensitive to the size of the lag-time window and reaches stable performance when the lag time is approximately 10 hours. The performance of the RPF improves more quickly than that of the EnSRF and becomes stable when the lag time is greater than 8 hours. Different patterns of NSE are also detected in each filter. In the case of the EnSRF, the best performance is achieved with approximately 5 and 7 hours of lag time, while performance decreases with shorter lead times (< 4 hours). The RPF, on the other hand, exhibits the best performance when the lead time is the shortest (1 hour). In this chapter, soil moisture contents are perturbed and updated in a lag-time window. Therefore, even if the hidden states are properly updated by the EnSRF, transition time seems to be required before updating effects appear in the forecast. However, in the case of the RPF, although soil moisture contents are considered as target states, all states, including network variables such as streamflows, are duplicated or renewed in the resampling step.

The effects of varying the length of the lag-time window on a high flood are illustrated in Fig. 5-6. The simulation data are the same as those shown in Fig. 5-5, and the selected flood event, from 8 to 19 August 2003, is the largest that occurred during the simulation period. Without a lag-time window (lag time = 1 hr), both filters show very unstable forecasts in terms of means and confidence intervals, which indicates that ensembles are updated in advance, before the effects of perturbation are transmitted into observation variables. However, as the lag time increases, confidence intervals decrease in size, and the ensemble mean more closely approximates the mean of the observations, demonstrating that the lag-time window may contribute to reduce uncertainty in the prediction.

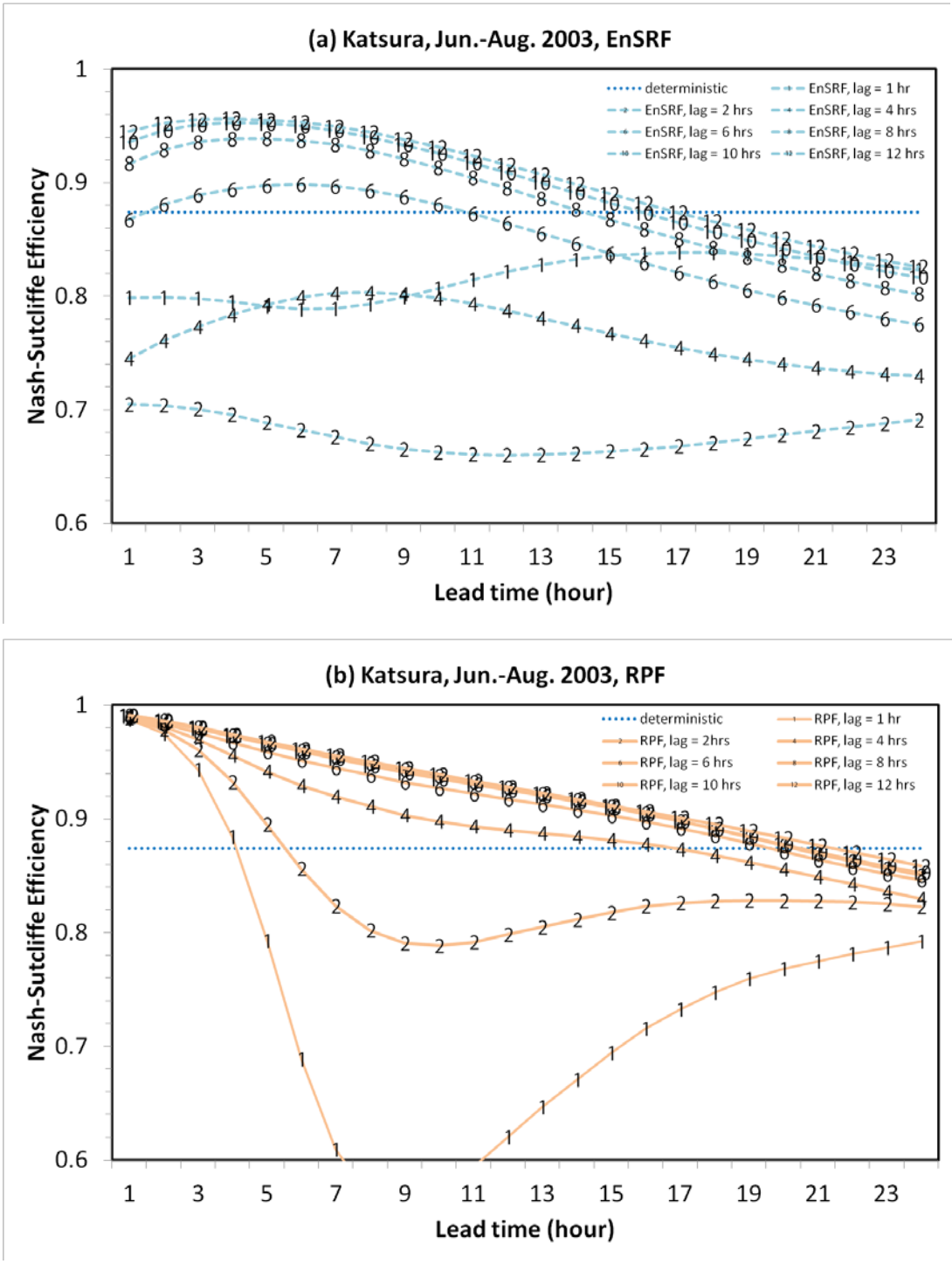

Fig. 5-5 Nash-Sutcliffe model efficiency for varying lag-time windows for the Katsura station: (a) the EnSRF and (b) the RPF.

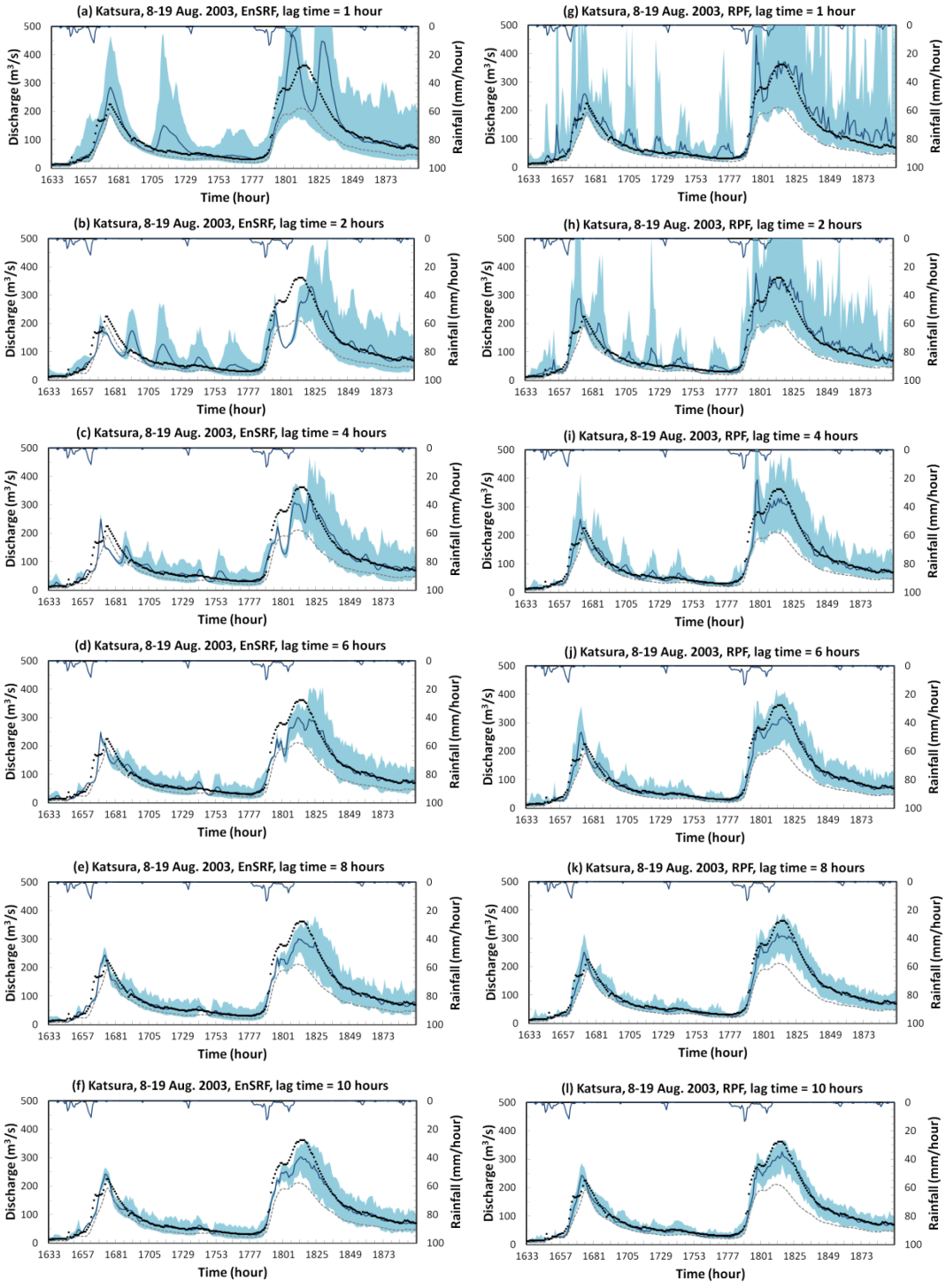

Fig. 5-6 Observed versus 6-hour-lead forecasts at the Katsura station with the EnSRF and the RPF for varying lag-time windows (8 to 19 August 2003): lag times of (a) 1 hr, (b) 2 hrs, (c) 4 hrs, (d) 6 hrs, (e) 8 hrs, and (f) 10 hrs for the EnSRF; lag times of (g) 1 hr, (h) 2 hrs, (i) 4 hrs, (j) 6 hrs, (k) 8 hrs, and (l) 10 hrs for the RPF.

A sensitivity analysis of the ensemble number is illustrated in Fig. 5-7. The model efficiency is assessed by varying particle numbers from 32 to 192 for both filters. The same simulation conditions as shown in Fig. 5-4 are specified. Even when the ensemble number decreases, no significant changes in the performance of either the EnSRF or the RPF are observed, although the confidence intervals increase slightly (not shown). The RPF performs better than the EnSRF even when the number of ensembles is extremely low. From the point of view of operational use, the number of ensembles required for filtering is one of the important criteria for choosing a method. The results show that if both filters are analyzed in a lag-time window, their performance can be improved with a limited number of ensembles.

Application results for the Gyeongancheon catchment in Korea for the period from 1 July to 31 September 2010 are shown in Fig. 5-8. Lag times of 8 and 6 hours for the EnSRF and the RPF, respectively, were determined in the other calibration period (not shown). The deterministic approach exhibits good performance, and 6-hour-lead forecasts obtained with the two filters also agree well with observations. In terms of NSE shown in Fig. 5-9, the two filters yield better results than the deterministic approach for overall lead times. The EnSRF and the RPF yield equivalent predictions for lead times from 5 to 14 hours, while the RPF outperforms the EnSRF for other lead times. A similar trend is observed for NSE; therefore, NSE of the EnSRF decreases when the lead time is decreased for the Katsura River catchment. Similar results were obtained for the Gyeongancheon catchment.

Statistics of streamflow forecasts for the two catchments for varying lead times are shown in Table 5-2. NSE and root mean square error (RMSE, m^3s^{-1}) are estimated, and the best scores are underlined for each lead time. Comparing the results for the two catchments, the forecasts for the Katsura catchment are better than those for the Gyeongancheon catchment. Different magnitudes of uncertainty for rainfall and discharge observations in the two catchments may be among the reasons for this difference. In terms of overall statistics, the RPF yielded predictions equal to or better than the EnSRF in accuracy for both catchments.

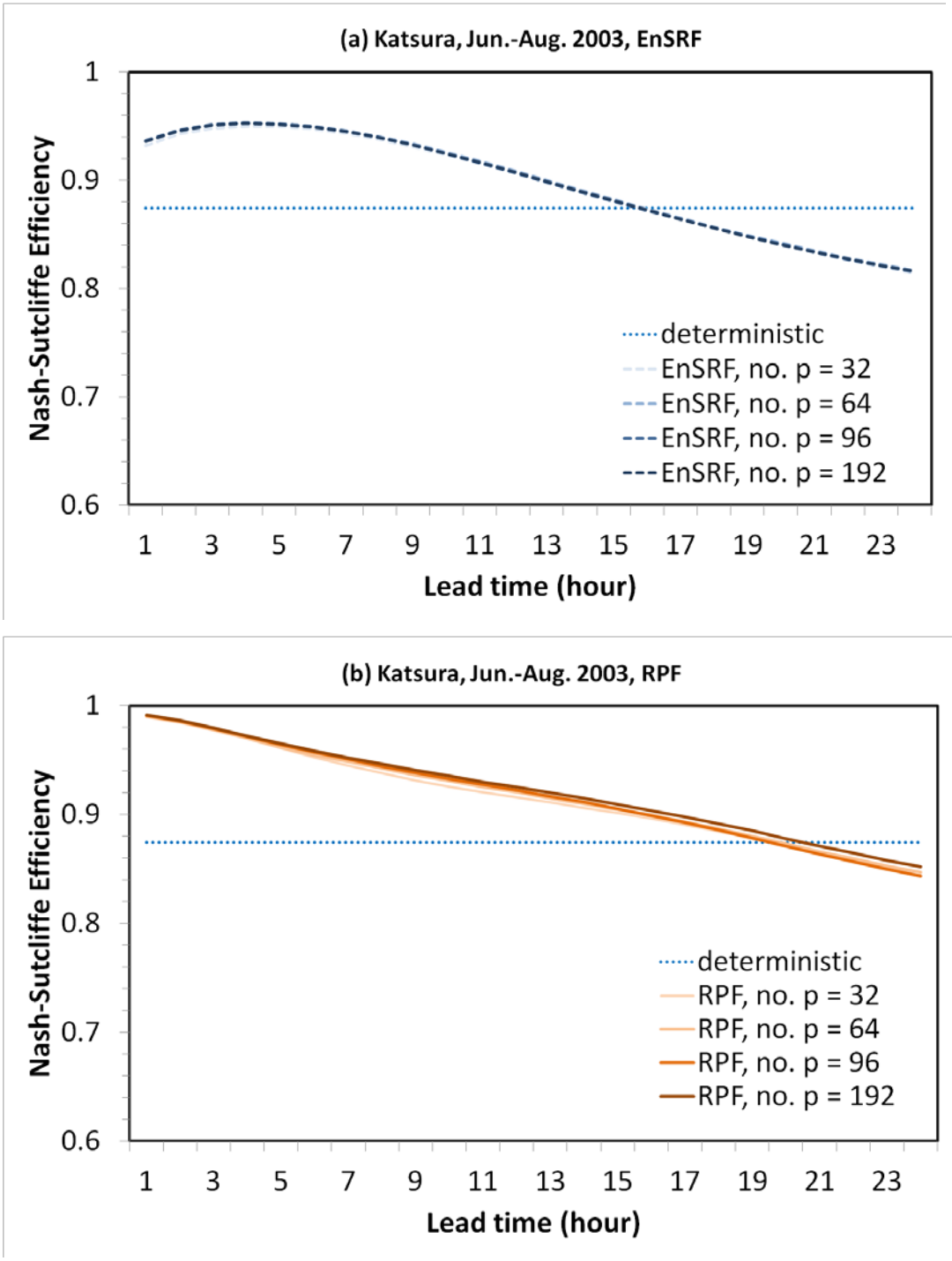

Fig. 5-7 Nash-Sutcliffe model efficiency for varying ensemble numbers for the Katsura station: (a) the EnSRF and (b) the RPF.

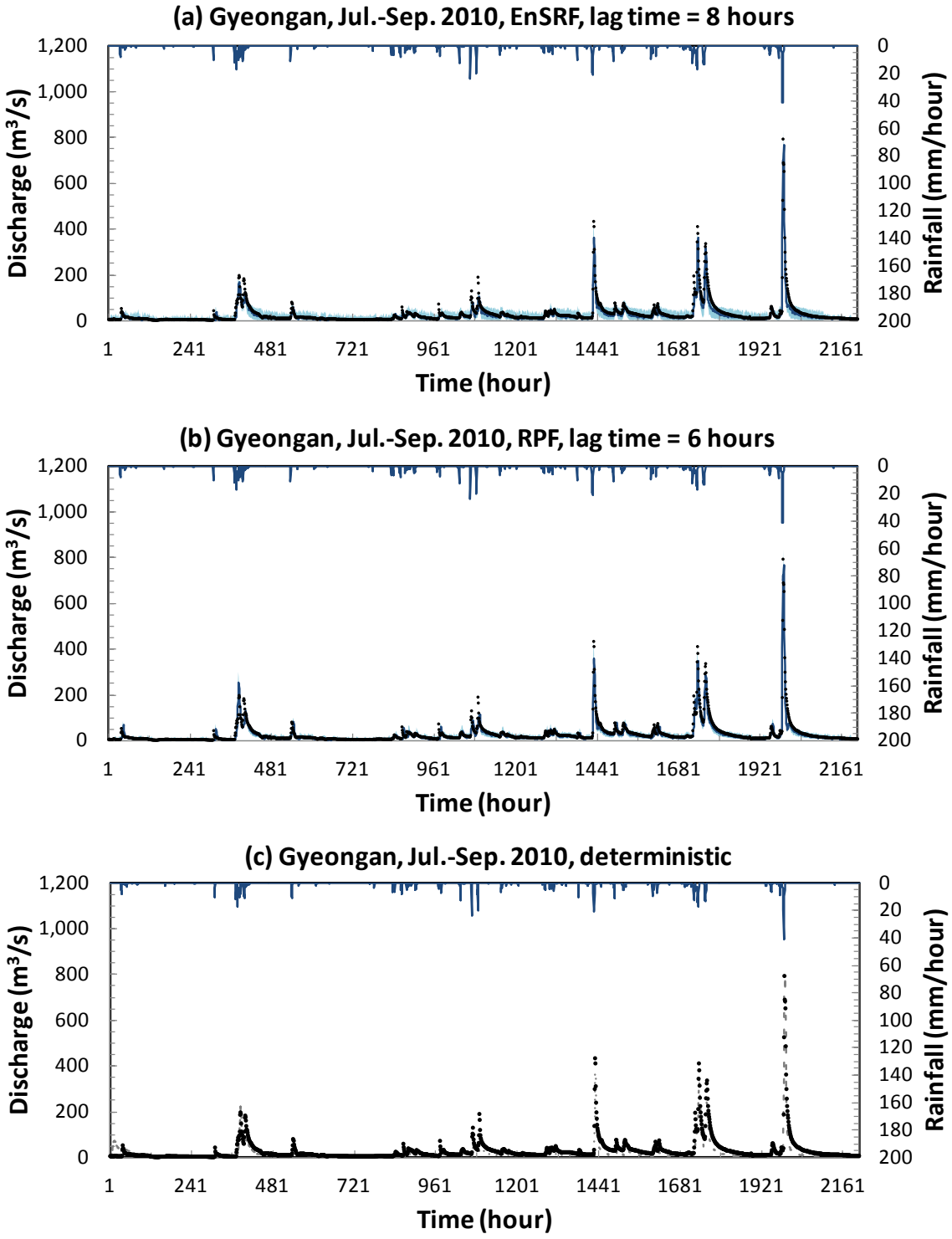

Fig. 5-8 Observed versus 6-hour-lead forecasts for the Gyeongan station (1 Jul.–31 Sep. 2010): (a) the EnSRF, (b) the RPF, and (c) deterministic modeling.

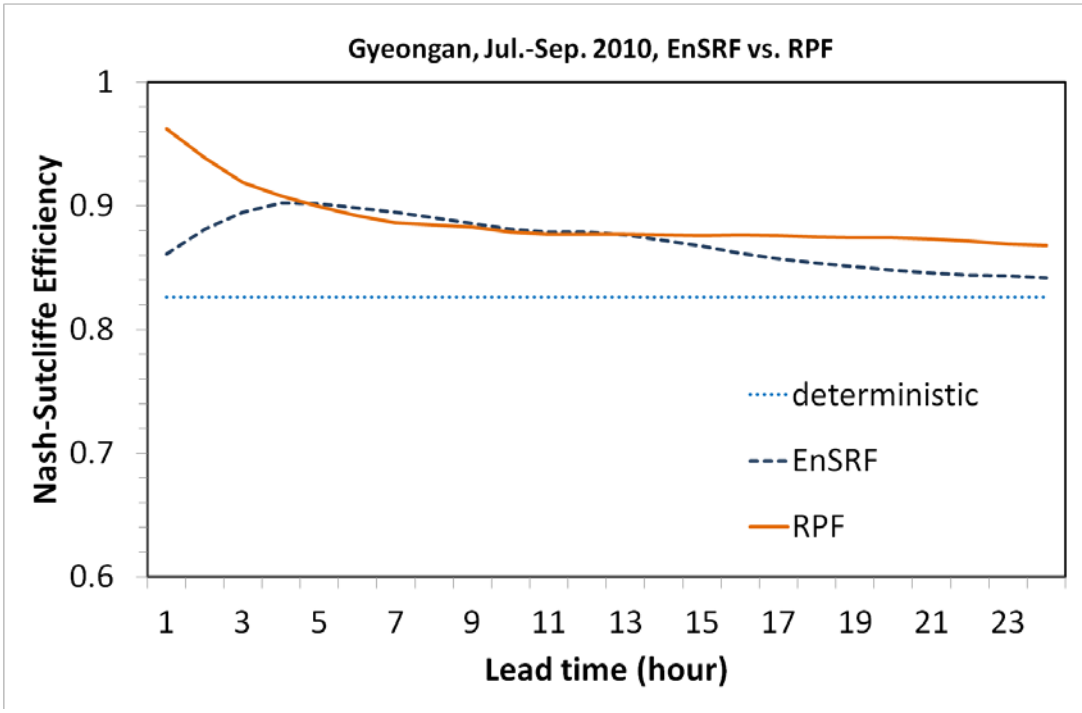

Fig. 5-9 Nash-Sutcliffe model efficiency for the Gyeongan station for the EnSRF and the RPF.

Table 5-2 Statistics of streamflow forecasts in the two catchments.

Catchment	Method	lag time	Lead time (hour)									
			1		3		6		12		24	
			NSE	RMSE	NSE	RMSE	NSE	RMSE	NSE	RMSE	NSE	RMSE
Katsura River catchment	Deterministic	-	0.87	15.7	0.87	15.7	0.87	15.7	0.87	15.7	0.87	15.7
	EnSRF	10	0.94	8.8	0.95	7.7	0.95	7.8	0.91	10.5	0.82	14.9
	RPF	8	0.99	3.3	0.98	4.9	0.96	7.0	0.93	9.4	0.85	13.4
Gyeongancheon catchment	Deterministic	-	0.83	21.6	0.83	21.6	0.83	21.6	0.83	21.6	0.83	21.6
	EnSRF	8	0.86	13.7	0.90	12.7	0.90	11.7	0.88	12.8	0.84	14.6
	RPF	6	0.96	7.2	0.92	9.1	0.89	12.1	0.88	12.9	0.87	13.4

5.4 Conclusions

Two sequential data assimilation methods, the ensemble Kalman filter and the particle filter, have been assessed for short-term streamflow hindcasting with a distributed hydrologic model, WEP. The ensemble square root filter and the

regularized particle filter were implemented to avoid flaws associate with conventional methods. The updating of state variables was performed through a lag-time window to consider lag and response times among internal hydrologic processes in a distributed hydrologic model. The EnSRF and the RPF were applied to two small catchments in Japan and Korea to assess the performance of the two methods. Ensembles perturbed by the noise of variation in soil moisture content were assimilated by streamflows observed at each outlet. In the case of the Katsura River catchment in Japan, in the predictions of both the EnSRF and the RPF improved when the lag time increased. Updated ensembles produced improved streamflow predictions for lead times of up to 15 hours (Fig. 5-5). Without a lag-time window, the predictions became unstable in terms of means and confidence intervals (Fig. 5-6). In the sensitivity analysis of the ensemble number, no significant variation in model efficiency was detected with variation in ensemble number (Fig. 5-7). The results of this chapter indicate that the RPF performed better than the EnSRF even when the number of ensembles was extremely low, but the further study is required. In the case of the Gyeongancheon catchment in Korea, the predictions obtained with the EnSRF and the RPF were equivalent for lead times ranging from 5 to 14 hours, while the prediction accuracy of the RPF was superior to the EnSRF for other lead times.

In both catchments, a lag-time window contributed to improving performance of the EnSRF and the RPF, and the RPF yielded predictions equal to or better than those of the EnSRF in prediction accuracy. In the case of the EnSRF, a decrease in model performance was observed for both catchments when the lead times were short (< 4 hours). The sequential data assimilation methods have significant potential for application to highly non-linear, non-Gaussian problems, such as process-based distributed models. Therefore, further study should be focused on real-time and multi-site data assimilation for hydrologic forecasting for a large-scale catchment, for which a lag-time window may provide an essential framework.

Chapter 6

Development of a hydrological modeling framework for data assimilation with particle filters

Abstract *In this chapter, we develop a hydrologic modeling framework for data assimilation, namely MPI-OHyMoS. While adapting object-oriented features of the original OHyMoS, MPI-OHyMoS allows users to build a probabilistic hydrologic model with DA. In this software framework, sequential DA based on particle filtering is available for any hydrologic models considering various sources of uncertainty originating from input forcing, parameters, and observations. Ensemble simulations are parallelized by the message passing interface (MPI), which can take advantage of a high-performance computing (HPC) system. Structure and implementation processes of DA via MPI-OHyMoS are illustrated using a simple lumped model. This software framework is applied for uncertainty assessment of a distributed hydrologic model in both synthetic and real experiment cases. In the synthetic experiment, dual state-parameter updating results in a reasonable estimation of parameters to cover synthetic true within their posterior distributions. In the real experiments, dual updating with identifiable parameters results in a reasonable agreement to the observed hydrograph with reduced uncertainty of parameters.*

6.1 Introduction

Data assimilation (DA) has received increased attention due to its capability to handle explicitly the sources of uncertainty in various areas. Numerous sophisticated DA algorithms have been proposed from ruled-based, direct-insertion methods, to advanced smoothing and sequential techniques, as well as the variants of these techniques (Liu et al., 2012). In the hydrologic research community, applications of DA have proved promising in improving prediction accuracy and quantifying uncertainty. Despite their potential, applicable general modeling frameworks to probabilistic approaches and DA are still limited because most modeling frameworks are based on a deterministic modeling approach. With increasing need for DA modeling platforms, a few frameworks such as openDA (Weerts et al., 2011) and PCRater applications (Karssenberg et al., 2010) have appeared recently (van Velzen, 2010). These approaches seem to provide innovative DA environments to overcome limitations of conventional deterministic modeling. However, there still remain cumbersome procedures such as development of model wrapper and further steps to use DA in more effective ways.

Over the last couple of decades, meanwhile, there have been improvements in modular modeling approaches to integrate modeling systems, including the modular modeling system (MMS) (Leavesley et al., 2002), object-oriented hydrologic modeling system (OHyMoS) (Ichikawa et al., 2000) and interactive component modeling system (ICMS) (Reed et al., 1999). These sorts of modular approaches provide a flexible platform on which various models and tools are integrated. Thus, modelers can develop various types of models for problem objectives, available data, and spatio-temporal scales of application by organizing registered modules in diverse ways (Lee et al., 2011).

OHyMoS is a hydrological modeling framework designed on the basis of the object-oriented programming concepts. Using OHyMoS as a computational library, users can develop their own element models and easily build a total simulation system model for hydrological simulations (Ichikawa et al., 2001). Unlike a process-based

modeling framework, OHyMoS benefits from its object-oriented feature to represent hydrological processes flexibly without any change of the main OHyMoS library. However, OHyMoS, like most other modular modeling approaches, is designed based on a deterministic approach. The original version of OHyMoS supports neither probabilistic simulation nor data assimilation.

In this chapter, MPI-OHyMoS is developed for supporting stochastic hydrologic simulations and data assimilation, while adapting all object-oriented features of original OHyMoS. Ensemble simulations are computed in parallel via the message passing interface (MPI), which can take advantage of the computational power of a high performance computing (HPC) system. Among the data assimilation methods, particle filtering (PF) is selected. The proposed framework is applied for uncertainty assessment of lumped and distributed hydrologic models in synthetic and real experiment cases.

This chapter is organized in the following way. Section 6.2 outlines basic features of MPI-OHyMoS: particle filtering, dual state-parameter estimation and parallelization for ensemble simulation. Section 6.3 illustrates DA processes in MPI-OHyMoS using a lumped hydrologic model. In Section 6.4, MPI-OHyMoS is implemented for the uncertainty assessment of a distributed hydrologic model in synthetic and real experiments. Section 6.5 summarizes the methodology and implementation results.

6.2 Features of MPI-OHyMoS

As MPI-OHyMoS is a stochastic and interactive version of OHyMoS, the basic concept of OHyMoS is reviewed briefly. OHyMoS is constructed as a set of dynamic elements communicating with each other based on object-oriented programming (Lee et al., 2011). As illustrated in Fig. 6-1, it provides an operation module, including the common functions required in hydrological simulations such as initialization of parameters and state variables, and setting the computational time steps and data exchange among element modules through input/output ports. Through OHyMoS, users can easily develop their own hydrologic modules by

connecting them to other modules and transferring data using predefined ports in the system library. Detailed information about OHyMoS and its implementations can be found and downloaded in at the web page of Hydrology and Water Resources Research Laboratory, Kyoto University (http:// hywr.kuciv.kyoto-u.ac.jp/ohymos/).

In MPI-OHyMoS, hydrologic modeling is implemented in the stochastic way. Fig. 6-2 shows how model ensembles are interactively assimilated in MPI-OHyMoS. Each ensemble member, representing a probable projection based on different parameters and state variables, is implemented independently. When a new observation arrives, the likelihood of ensemble members is estimated. In the resampling step, the whole information of each ensemble is renewed depending on its weight. In this way, ensembles can move to the regions with high conditional probability in each time step. Detailed features of MPI-OHyMoS are summarized below.

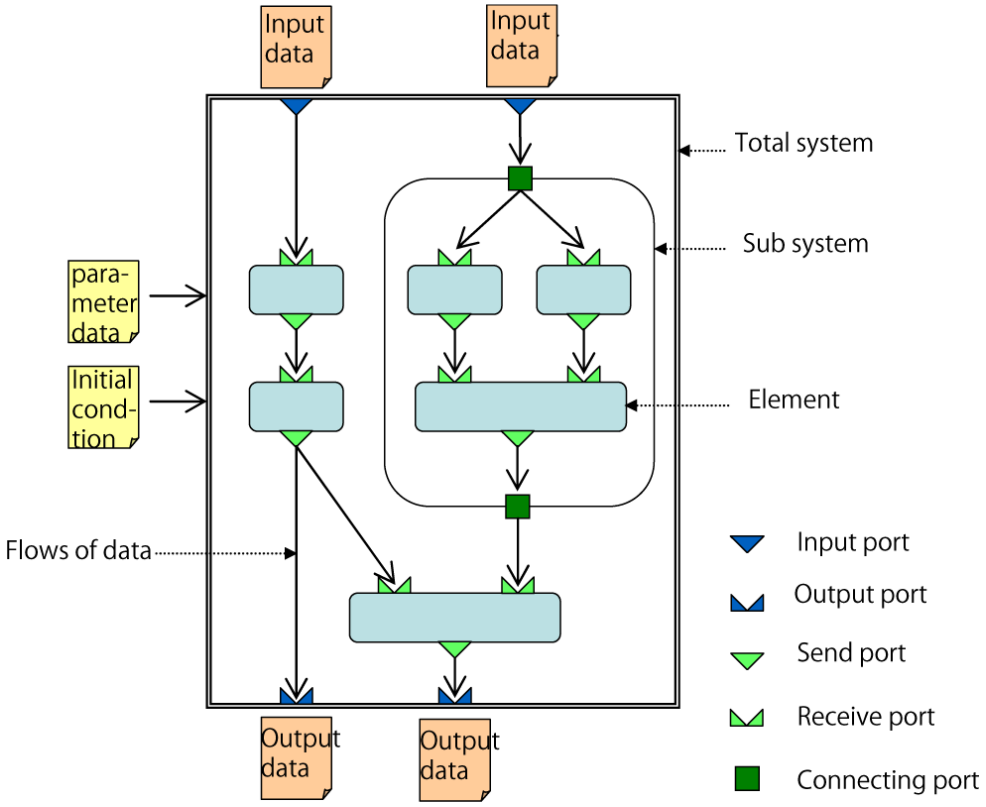

Fig. 6-1 The structure of original OHyMoS.

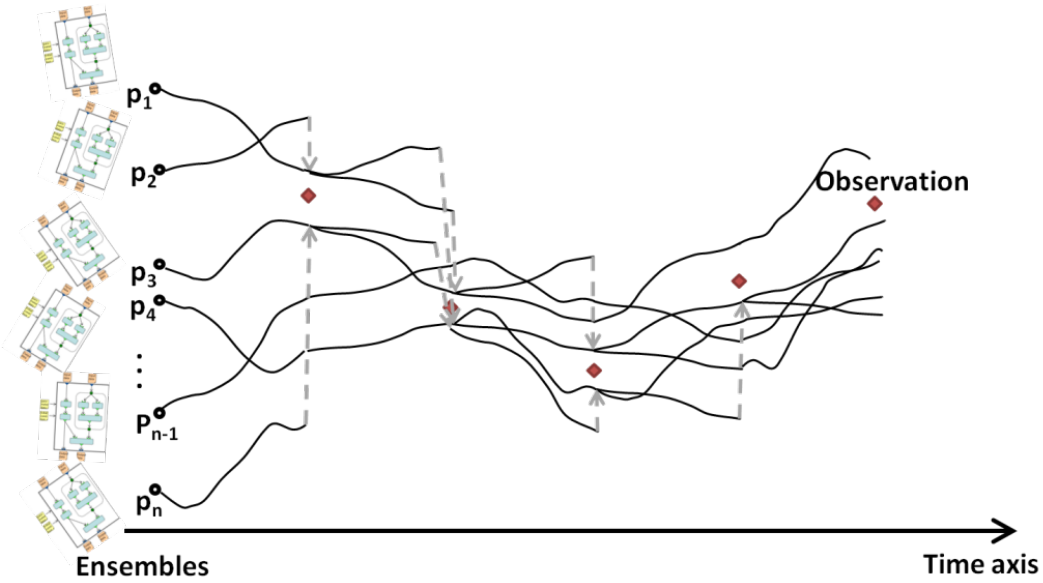

Fig. 6-2 Sequential data assimilation by MPI-OHyMoS

6.2.1 Particle filtering

Particle filtering (PF) is a Bayesian learning process that has the capability to handle non-linear, non-Gaussian state-space models. Unlike Kalman filter-based methods, PF performs updating on particle weights instead of state variables (Liu and Gupta, 2007), which has the advantage of reducing numerical instability, especially in physically based or process-based models. The key idea of PF is based on point mass representations of probability densities with associated weights (Ristic et al., 2004). To fix the notations, let us introduce x_t, which represents all target states at time t. Then, the posterior filtered density $p(x_t \mid y_{1:t})$ can be approximated as

$$p(x_t \mid y_{1:t}) \approx \sum_{i=1}^{n} w_t^i \delta(x_t - x_t^i) \tag{6-1}$$

where x_t^i and w_t^i denote the i^{th} posterior state ("particle") and its weight, respectively, $\delta(\cdot)$ denotes the Dirac delta function and $y_{1:t}$ denotes all available measurements. In typical circumstances, the recursive weight updating can be derived as follows:

$$w_t^i \propto w_{t-1}^i p(y_t \mid x_t^i) \tag{6-2}$$

where $p(y_t \mid x_t^i)$ is the likelihood of each particle x_t^i.

The SIS algorithm shown above is a Monte Carlo method that forms the basis for most particle filters. A common problem with the SIS algorithm is the degeneracy phenomenon: after a few iterations all but one particle will have negligible weight. The degeneracy phenomenon can be reduced by performing the resampling step whenever a significant degeneracy is observed.

In MPI-OHyMoS, a likelihood function is constructed as an independent element model to estimate the likelihood and weight of each particle, which can be combined with any element model and allow any user-defined density function.

6.2.2 Dual state-parameter updating

During the resampling step, information of different states and parameters is updated simultaneously. In the case of state updating, state variables, which are perturbed in the initial stage, are projected to the next time point by the state-space equation (e.g. hydrologic models) and updated in the resampling step. However, in the case of parameter updating, we need additional constraints because there is usually no time-evolution information.

To handle inference of the unknown parameters θ, kernel smoothing (Liu and West, 2001) is adapted to improve parameter identifiability. The smooth kernel density can be a mixture of Gaussian densities as follows:

$$P(\theta_t \mid y_{1:t-1}) \sim \sum_{i=1}^{n} w_{t-1}^i N(\theta_t \mid m_{t-1}^i, h^2 V_{t-1}^{\theta}) \tag{6-3}$$

where h is the variance reduction parameter and V_{t-1}^{θ} is the variance of parameter particles at time t-1 before resampling. The kernel locations m_{t-1}^i are specified by a shrinkage rule forcing the particles to be closer to their mean:

$$m_{t-1}^i = a\theta_{t-1}^i + (1-a)\bar{\theta}_{t-1} \text{ with } a = \sqrt{1-h^2} \tag{6-4}$$

where $\bar{\theta}_{t-1}$ is mean of parameter at time t-1. It can be verified that the mixture probability in Eq. (6-4) has a covariance matrix V_{t-1}^{θ} and that it does not increase over time (Liu and West, 2001). Several issues related with parameter estimation are

discussed in Appendix C. MPI-OHyMoS provides the kernel smoothing scheme as a basic option of parameter updating. The statistics of parameters can be estimated in the log scale, which will be shown in the distributed modeling case.

6.2.3 Parallelized ensemble simulation

MPI, a parallel computing protocol for a distributed memory system which is common in HPC, is used for the parallelization of the ensemble simulation and data assimilation in MPI-OHyMoS. Among variants of MPI libraries, openMPI (www.openmpi.org) and Boost library (www.boost.org) are selected. Note that MPI is different from OpenMP, commonly used in hydrology for loop parallelization in a single model, whose applicability is limited to a shared memory system.

6.3 Illustrative example of data assimilation via MPI-OHyMoS

In this section, an example is shown to illustrate the basic features and simulation processes of MPI-OHyMoS. A synthetic experiment is implemented using a linear reservoir model with an unknown initial condition and a model parameter.

6.3.1 Linear reservoir model

The linear reservoir model shown in Fig. 6-3 is based on the concept that a catchment behaves as a reservoir in which storage S is linearly related to outflow Q (US Army Corps. Eng. HEC, 1980). It can be described as:

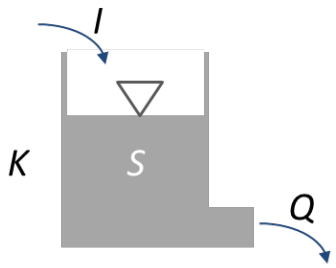

Fig. 6-3 A linear reservoir model.

$$S = KQ \tag{6-5}$$

$$\frac{dS}{dt} = I - Q \tag{6-6}$$

where K, called the storage coefficient, is a rate constant, t is the time, and I is inflow. For the computational implementation, a parameter K and the initial state S_0 should be specified. The state S should be stored at each time step as the initial condition of the next time step.

6.3.2 DA processes via MPI-OHyMoS

Fig. 6-4 illustrates processes of sequential data assimilation via MPI-OHyMoS in a linear reservoir model case. In this case, the total system of MPI-OHyMoS consists of two elements: a linear reservoir model and a likelihood function. At each time step, the linear reservoir model calculates the states S and Q using Eqs. (6-5) and (6-6). Because each ensemble has different model parameter and initial storage perturbed by random noises, n ensembles of the linear reservoir model result in different values of outflow Q. In the likelihood element, the likelihood of simulated outflow is estimated according to measurement outflow. Weights are then calculated and normalized such that $\sum_{i=1}^{n} w_k^i = 1$. Parameters and states are stored in the memory at each time step. In the resampling step, ensembles having large weight are duplicated to other ones. For example, in Fig. 6-4, Ensemble 2 is duplicated to Ensemble 1 between time step k and $k+1$. After the resampling step, Ensemble 1 has the same parameter and state with Ensemble 2. However, as random noises are added to parameter and state at each time step, Ensemble 1 and 2 result in slightly different outflows at time step $k+1$. In this way, state and parameter of ensembles are filtered at each time step. Estimated distributions of parameter and state represent posterior distribution.

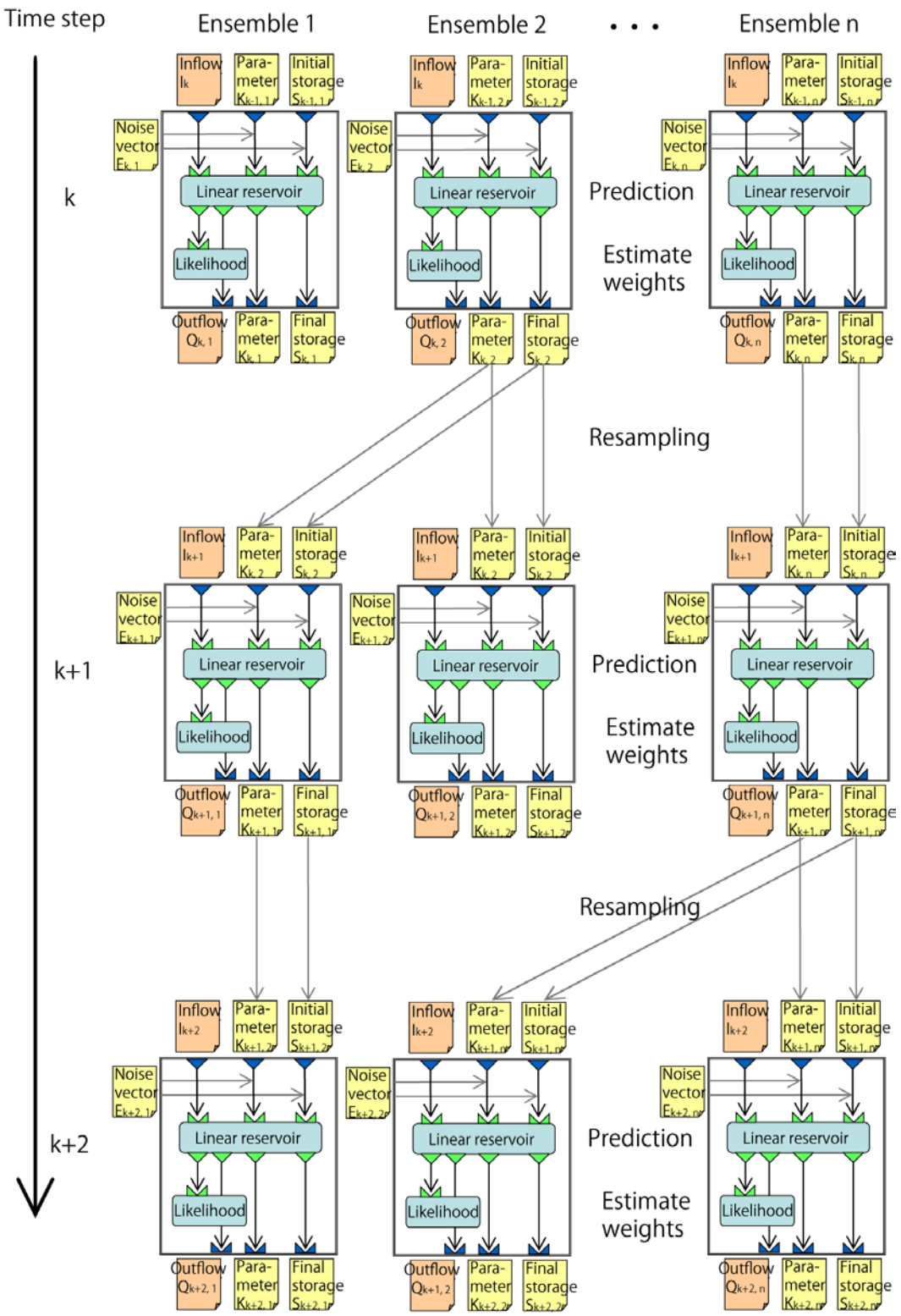

Fig. 6-4 Data assimilation processes of a linear reservoir model via MPI-OHyMoS.

6.3.3 Results of synthetic experiment

The synthetic experiment is implemented using a linear reservoir model to illustrate basic features of data assimilation in MPI-OHyMoS. Here we assume that the true values of parameters and initial states are unknown. Prior information on the ranges of parameters and initial conditions are shown in Table 6-1. Synthetic observation is calculated using synthetic true values, adding small perturbation generated from uniform distribution $U(-0.1, 0.1)$ as measurement error.

Fig. 6-5 shows two hundred ensemble simulations without PF. As shown in Fig. 6-5(a), the values of parameter K do not change during simulation. Ensemble discharge varies within large uncertainty bounds shown in Fig. 6-5(b). Fig. 6-6 shows ensemble simulations with PF. Parameter and state are updated using the synthetic observation every ten time intervals. The uncertainty bounds of parameter K and outflow reduce sharply via PF, showing a good agreement with the synthetic true. Note that the simulation is converged to synthetic true values quickly because the applied system is linear. A non-linear, non-Gaussian case is followed in the next section.

Table 6-1 Information of parameter and initial state.

Parameters and initial states	Synthetic true values	Ranges of parameter/state values for ensemble simulation
K_1	10	5~25
S_1^{ini}	20	5~25

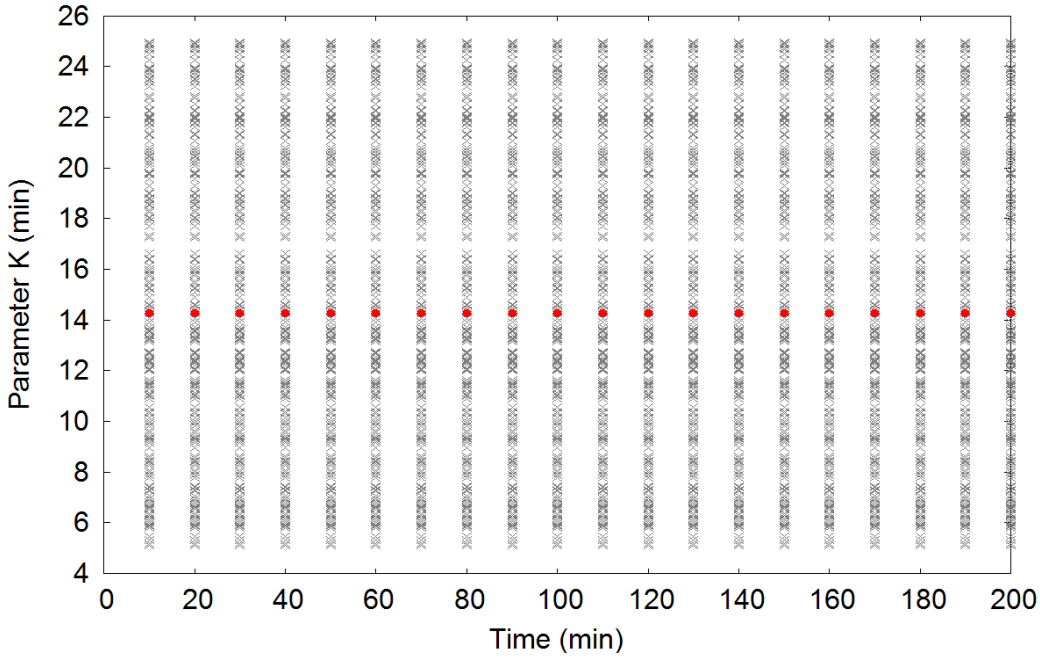

(a)

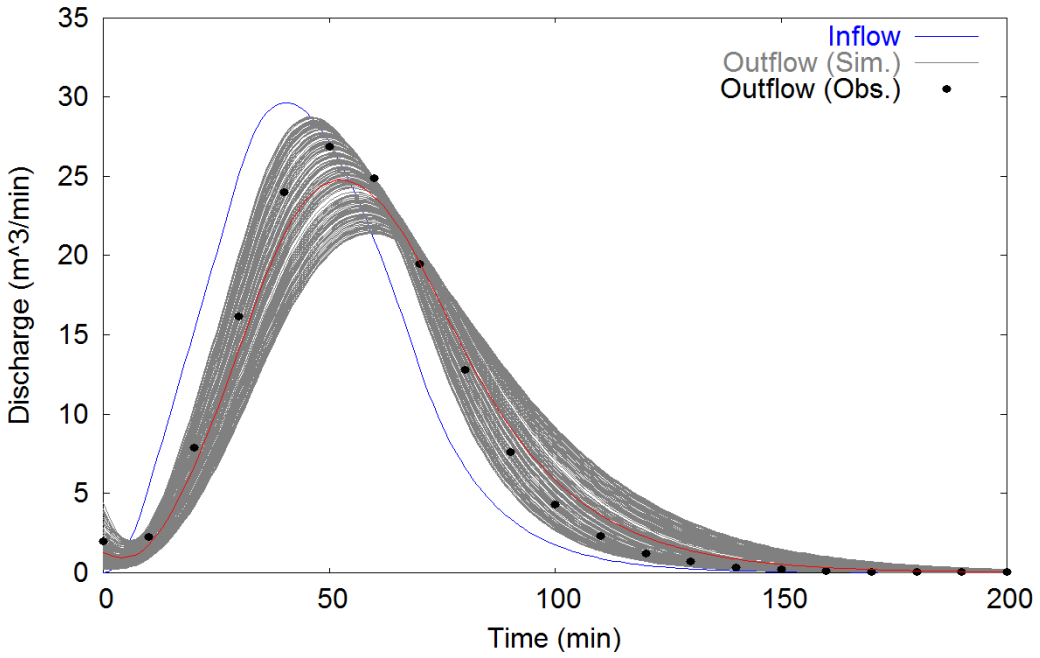

(b)

Fig. 6-5 Parallel simulations of the linear reservoir model without particle filtering by 200 ensembles. (a) Traces of parameter K. (b) Traces of inflow and outflow. Black dots represent synthetic observation. Grey lines represent 200 ensembles. A red line represents mean of ensembles. A blue line represents inflow.

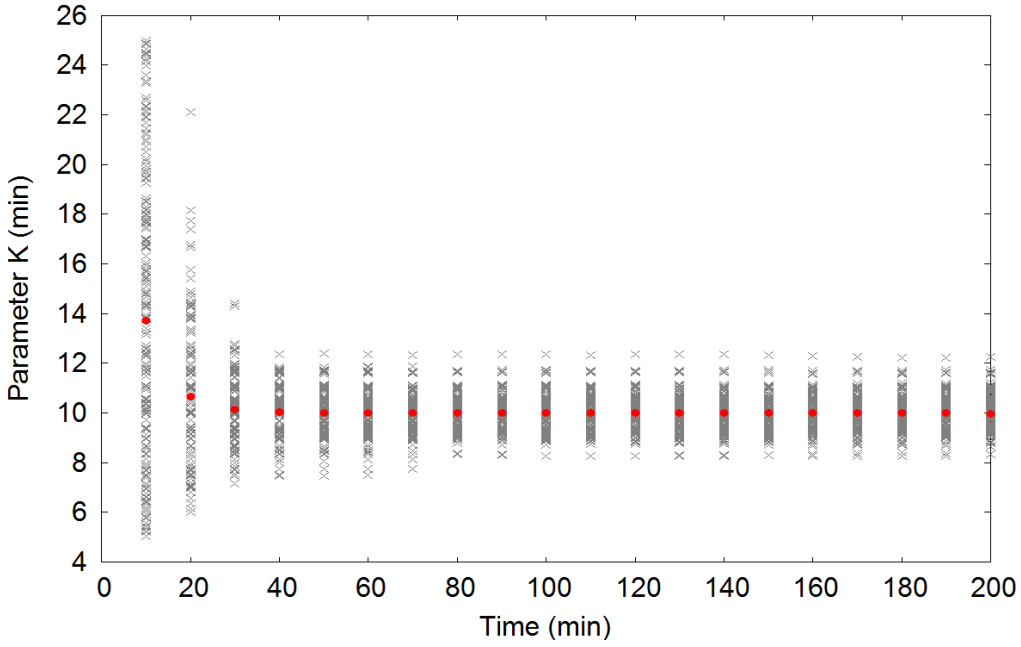

(a)

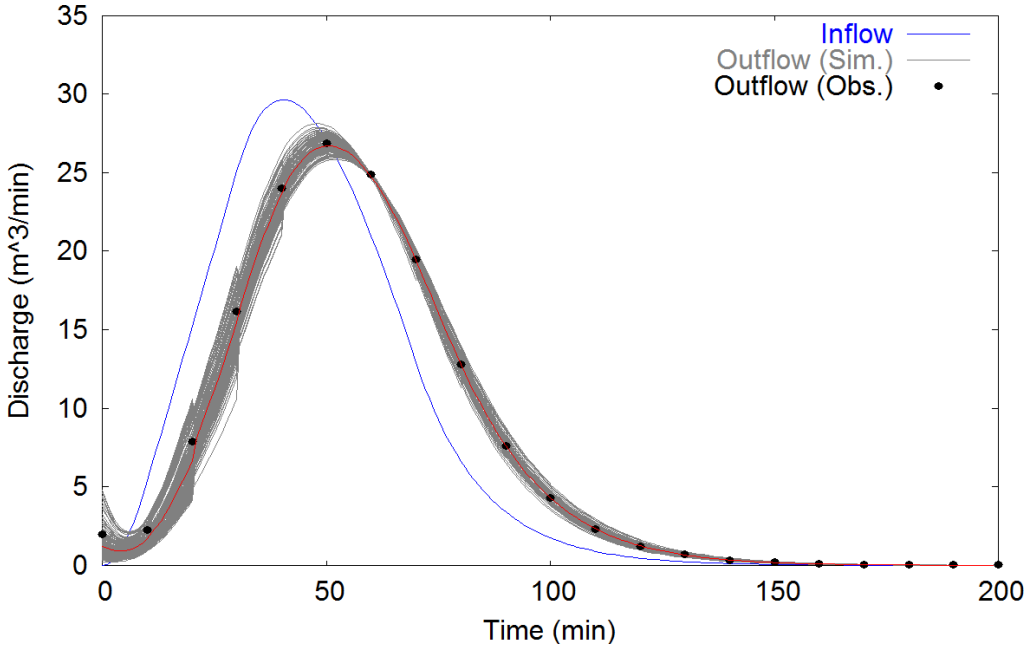

(b)

Fig. 6-6 Parallel simulations of the linear reservoir model with particle filtering by 200 ensembles. (a) Traces of parameter K. (b) Traces of inflow and outflow. Black dots represent synthetic observation. Grey lines represent 200 ensembles. A red line represents mean of ensembles. A blue line represents inflow.

6.4 Uncertainty assessment of a distributed hydrologic model

Synthetic and real experiments are implemented for uncertainty assessment of a fully distributed hydrologic model (Takasao and Shiiba, 1988; Ichikawa et al., 2001) to illustrate the applicability of MPI-OHyMoS.

6.4.1 Study area

The study area is the Maruyama River catchment in Japan with an area of about 909 km^2. Fig. 6-7 shows the streamflow gauging locations and rainfall measuring stations. Streamflow measurement at Fuichiba is used for data assimilation in both synthetic and real experiments. Land use consists of 37% forest, 10% savannas, and 53% crop land and natural vegetation (Hunukumbura, 2009).

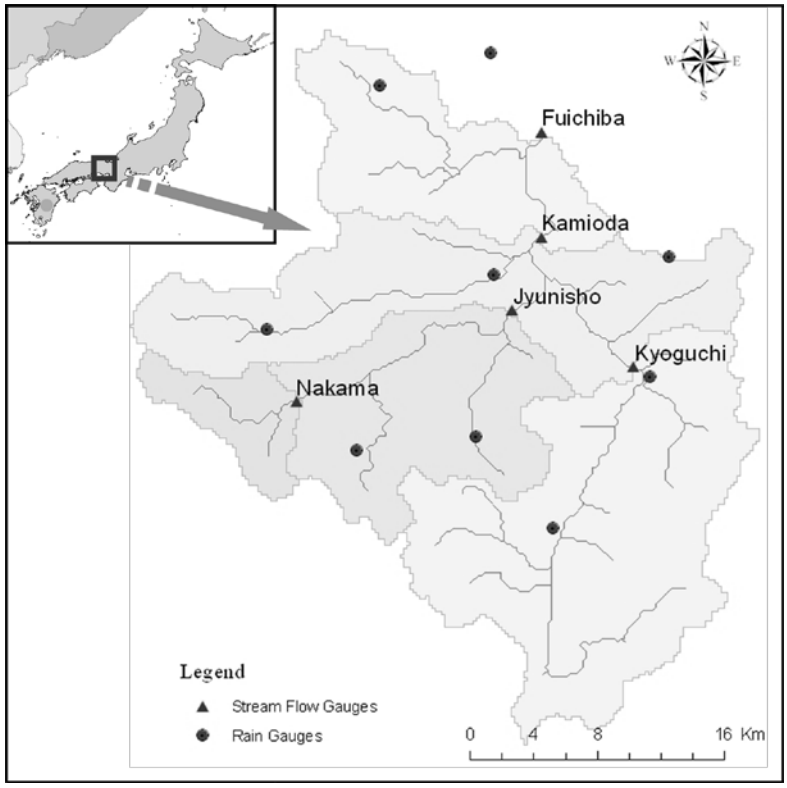

Fig. 6-7 The Maruyama River catchment (Hunukumbura, 2009).

6.4.2 A distributed hydrologic model

We construct a probabilistic distributed hydrologic model for the Maruyama River catchment based on three element modules: a hillslope runoff generation module, a river routing module, and a likelihood function. The hillslope and river routing modules were developed as elements of a deterministic distributed hydrological model using the kinematic wave theory in the previous study (Tachikawa et al., 2004). In this model, it is considered that the catchment consists of a number of rectangular slope elements which drain to the deepest gradient of its surrounding, as shown in Fig. 6-8.

Fig. 6-9 shows the flow process and the stage discharge relationship used in the hillslope model given in Eq. (6-7).

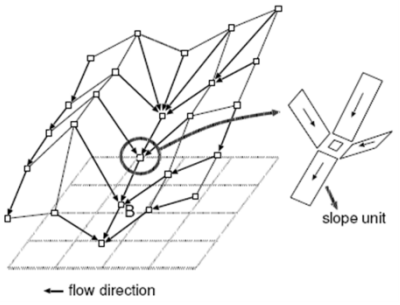

Fig. 6-8 Spatial flow movement.

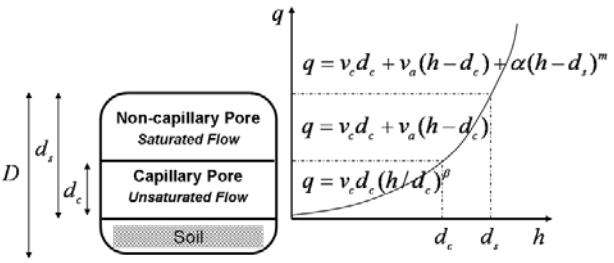

Fig. 6-9 Flow process in the hillslope model.

$$q = \begin{cases} V_c d_c (h/d_c)^{\beta} & 0 \le h \le d_c \\ V_c d_c + V_a (h - d_c) & d_c < h \le d_s \\ V_c d_c + V_a (h - d_c) + \alpha (h - d_s)^m & d_s < h \end{cases} \tag{6-7}$$

$$\frac{\partial h}{\partial t} + \frac{\partial q}{\partial x} = r(t) \tag{6-8}$$

where t is the time (s), x is space (m), and $r(t)$ is the rainfall intensity (mm/hour) to the slope element. The discharge per unit width q (m^2/s) is estimated by Eq. (7) combined with the continuity equation, Eq. (6-8), where $V_c = k_c i$ (m/s), $V_a = k_a i$ (m/s), $k_c = k_a / \beta$ (m/s), $\alpha = \sqrt{i} / n_{slope}$ ($m^{1/3}s^{-1}$), m=5/3, i is the slope unit gradient, k_c

(m/s) is the hydraulic conductivity of the capillary soil layer, k_a (m/s) is the hydraulic conductivity of the non-capillary soil layer, n_{slope} ($m^{-1/3}s$) is the roughness coefficient of the hillslope component. h (m) is the water stage, V_a and V_c are flow rates, and d_c and d_s are soil depth in the capillary pore and non-capillary pore, respectively. β is a parameter.

For channel routing, we use a one-dimensional kinematic wave equation as follows:

$$\frac{\partial h}{\partial t} + \frac{\partial q}{\partial x} = q_L \tag{6-9}$$

$$q = \alpha h^m \tag{6-10}$$

where h (m) is the channel water depth, q (m^2/s) the channel discharge per unit width, q_L is lateral inflow, $\alpha = \sqrt{i}/n_{river}$ ($m^{1/3}s^{-1}$), m =5/3 and n_{river} ($m^{-1/3}s$) is the roughness coefficient of the river component.

6.4.3 Model setup for data assimilation

The measurement error of the discharge is assumed as a Gaussian distribution, $N(0, \sigma^2_{obs_t})$. The standard deviation of the measurement error is chosen as:

$$\sigma_{obs_t} = \alpha_{obs} y_t + \beta_{obs} \tag{6-11}$$

In Eq. (6-11), y_t is observed discharge at time t. α_{obs} and β_{obs} are parameters representing uncertainty of observations.

The process noise is generated by a Gaussian distribution, $\varepsilon_{sim} \sim N(0, \sigma^2_{sim})$. The standard deviation of the process error is selected through sensitivity analysis. Then, the state variables of slope and river component in each grid are perturbed at each observation time step in a multiplicative manner as:

$$\hat{x}_t^j = (1 + \varepsilon_{sim}) x_t^j \tag{6-12}$$

where x_t^j and $\hat{x}_t^j$ are state variables before and after perturbation, respectively.

Among various parameters in the distributed hydrologic model, four parameters are selected for data assimilation. These parameters are d_c, k_a, n_{slope} and n_{river}.

The model setup uses 250 m grid resolution. The simulation time steps are six hundred seconds for the hillslope element and twenty seconds for the river routing element. Ensembles are updated hourly by the streamflow measurements at the Fuichiba gauging station. We use hourly observed rainfall from nine observation stations organized by the Ministry of Land, Infrastructure, Transport and Tourism in Japan (http://www1.river.go.jp/). Selected flood events are shown in Table 6-2. Event 3 is used for the synthetic experiment, while all events are used for the real experiment.

Table 6-2 Details of selected flood events in Fuichiba.

Flood Event	Date	Peak flow (m^3/s)	Initial flow of the event (m^3/s)
Event 1	10-20 Sep. 2001	715	42
Event 2	7-10 Sep. 2002	293	6
Event 3	19–24 Oct. 2004	4782	32

6.4.4 Synthetic experiment

The synthetic experiment is implemented using a distributed hydrologic model to demonstrate the applicability of MPI-OHyMoS for the missing data problem in complex cases and assess the identifiability of parameters. The basic procedures of the synthetic experiment in the distributed hydrologic model are the same in the lumped model case. Synthetic observation of streamflow is calculated by synthetic true values of parameters, shown in Table 6-3, adding small Gaussian noise.

For probabilistic modeling, the initial condition of states is perturbed by using noise from the uniform distribution, $\varepsilon_{ini} \sim U(0, \sigma_{ini}^2)$, in a multiplicative manner shown in Eq. (6-12). The applied value of σ_{ini} is 0.1. The standard deviation of process noise of states, σ_{sim}, is set as 0.01, which accounts for the predictive uncertainty of state variables. The process noise of parameters is controlled by kernel smoothing using

the information of ensemble mean and variance at the previous time step shown in Eqs. (6-3) and (6-4).

The statistics of parameter k_a are estimated in the log scale to cover wider ranges of uncertainty bounds compared to others. Parameters of observation error in Eq. (6-11), α_{obs} and β_{obs}, are set as 0.05 and 5, respectively. The size of ensembles is 1000.

The synthetic experiment is implemented in two separate simulations. In the preliminary stage, initial distributions of parameters are selected to cover ranges adopted in the previous study, while results of the preliminary stage are used as prior information in the second stage simulation. Values of synthetic true and uncertainty ranges of parameters at each stage are shown in Table 6-3.

Results of the preliminary stage of the synthetic experiment are shown in Fig. 6-10. Simulated streamflow, which is one-step-ahead prediction, shows good conformity with synthetic observation in terms of ensemble mean and distributions. Uncertainty of parameters lasts before the flood event as in the initial distributions and reduces sharply around the flood peak. Dual state-parameter updating via PF results in a reasonable estimation of parameters to cover synthetic true values within their posterior distributions. However, identifiability of parameters is different and the roughness coefficient of slope component shows diffusive distribution.

Results of the second stage are shown in Fig. 6-11. With reduced uncertainty ranges, traces of parameters show stable variations reaching synthetic true values according to sequential updating. Mean and confidence intervals of estimated parameters in the second stage are shown in Table 6-4. Identifiability of parameters is increased in the second stage with reduced initial probabilistic distributions. However, there seem to be asymptotic bounds where probabilistic distributions cannot be narrower, because the uncertainty of states and observations are considered simultaneously in data assimilation.

Table 6-3 Information of parameters in the synthetic experiment (Event 3).

Parameters	Synthetic true values	Initial ranges of parameters for ensemble simulation	
		Preliminary stage	Second stage
k_a (m/s)	0.006	0.001~0.1	0.001~0.01
d_c (m)	0.4	0.1~0.5	0.36~0.42
n_{river} ($m^{-1/3}s$)	0.038	0.015~0.055	0.3~0.4
n_{slope} ($m^{-1/3}s$)	0.33	0.15~0.55	0.035~0.043

Table 6-4 Mean and confidence intervals of estimated parameters in the second stage of the synthetic experiment (Event 3).

Parameters	Ensemble mean	Ranges of 60% confidence interval
d_c (m)	0.394	0.385~0.404
k_a (m/s)	0.0052	0.0048~0.0055
n_{slope} ($m^{-1/3}s$)	0.343	0.320~0.364
n_{river} ($m^{-1/3}s$)	0.0385	0.0369~0.040

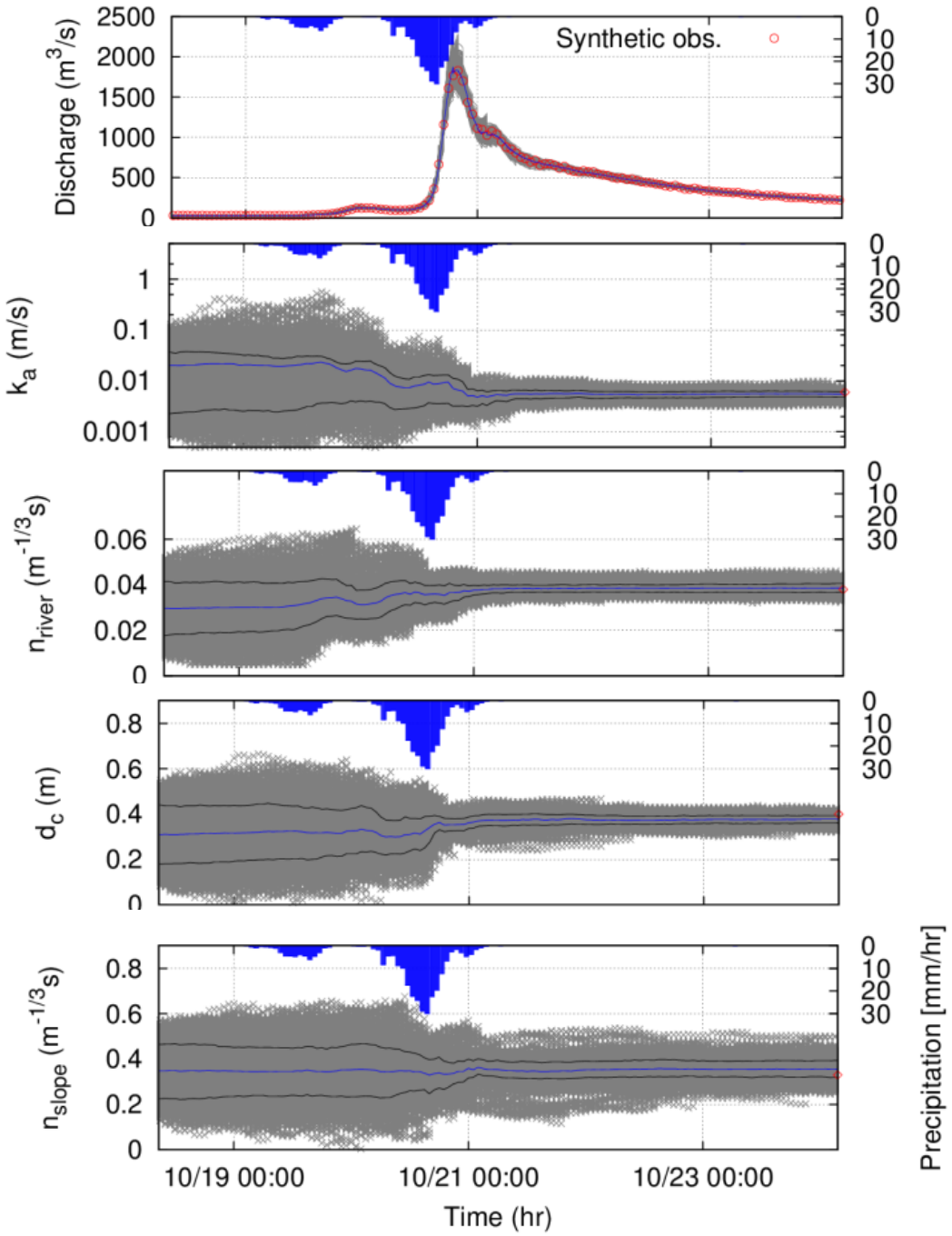

Fig. 6-10 Parallel simulations of the distributed hydrologic model with PF in the preliminary stage of the synthetic experiment (Event 3). Red dots represent synthetic observation. Grey lines represent traces of streamflow of ensembles. Grey dots represent traces of parameters of ensembles. Blue lines represent mean of ensembles. Black lines represent 60% confidence intervals.

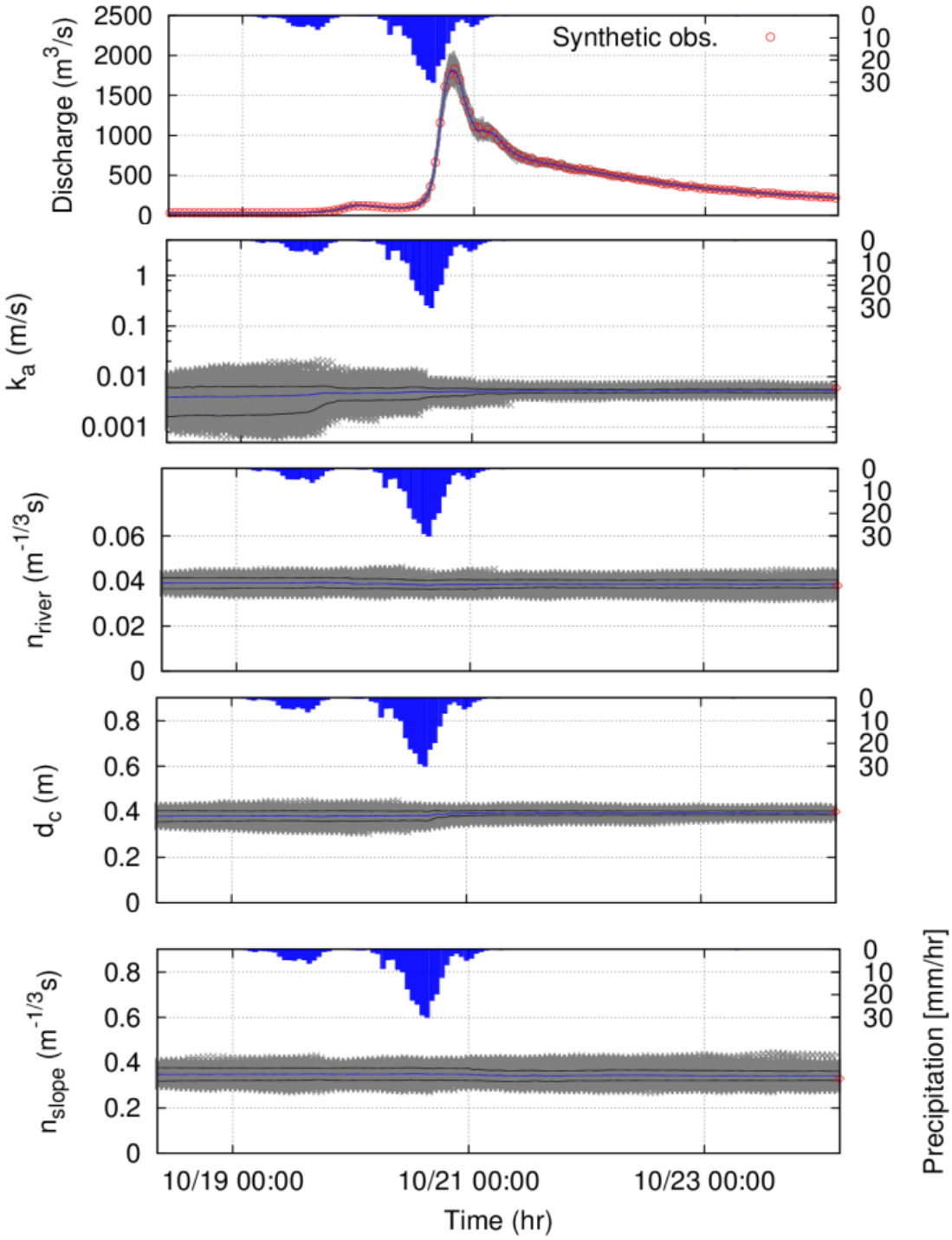

Fig. 6-11 Parallel simulations of the distributed hydrologic model with PF in the second stage of the synthetic experiment (Event 3). Red dots represent synthetic observation. Grey lines represent traces of streamflow of ensembles. Grey dots represent traces of parameters of ensembles. Blue lines represent mean of ensembles. Black lines represent 60% confidence intervals.

6.4.5 Real experiment

The real experiment is conducted in two stages using Event 1. The applicability of two-stage estimation is verified in simulations of Event 2 and 3, which are conducted using results of the preliminary stage as initial ranges of parameters. For parameter updating, k_a, d_c and n_{river} are selected excluding n_{slope} because the identifiability of n_{slope} is found to be relatively lower in the synthetic experiment.

In the preliminary stage, the initial ranges of parameters k_a, d_c and n_{river} are the same as in the synthetic experiment shown in Table 6-5, while the value of n_{slope} is set as 0.3 selected from the previous study (Lee et al., 2011; Kim et al., 2008). In the real experiment, the uncertainty of process and observation is assumed to be larger than that in the synthetic case. The standard deviation of process noise of states σ_{sim} is set as 0.05 and parameters of observation error α_{obs} and β_{obs} are set as 0.1 and 20, respectively. The standard deviation of initial states σ_{ini} is 0.3.

Simulation results of preliminary and second stages of Event 1 are shown in Figs. 6-12~6-13. As shown in Fig. 6-12, the uncertainty of parameters sharply reduces around the flood peak. Distribution of parameter k_a becomes narrow rapidly around the flood peak, while distribution of n_{river} shows smoothed movement. In the second stage, initial distribution of parameters is selected to cover 60% confidence intervals of the preliminary stage. As shown in Fig. 6-13, there is no rapid movement of parameter distribution during the second stage simulation leading to narrower posterior distribution, compared to the preliminary stage, whose estimated values are shown in Table 6-5.

Table 6-5 Mean and confidence intervals of estimated parameters in the second stage of the real experiment (Event 1).

Parameters	Ensemble mean	Confidence interval (60%)
k_a (m/s)	0.262	0.182~0.335
d_c (m)	0.174	0.152~0.196
n_{river} ($m^{-1/3}s$)	0.019	0.016~0.021

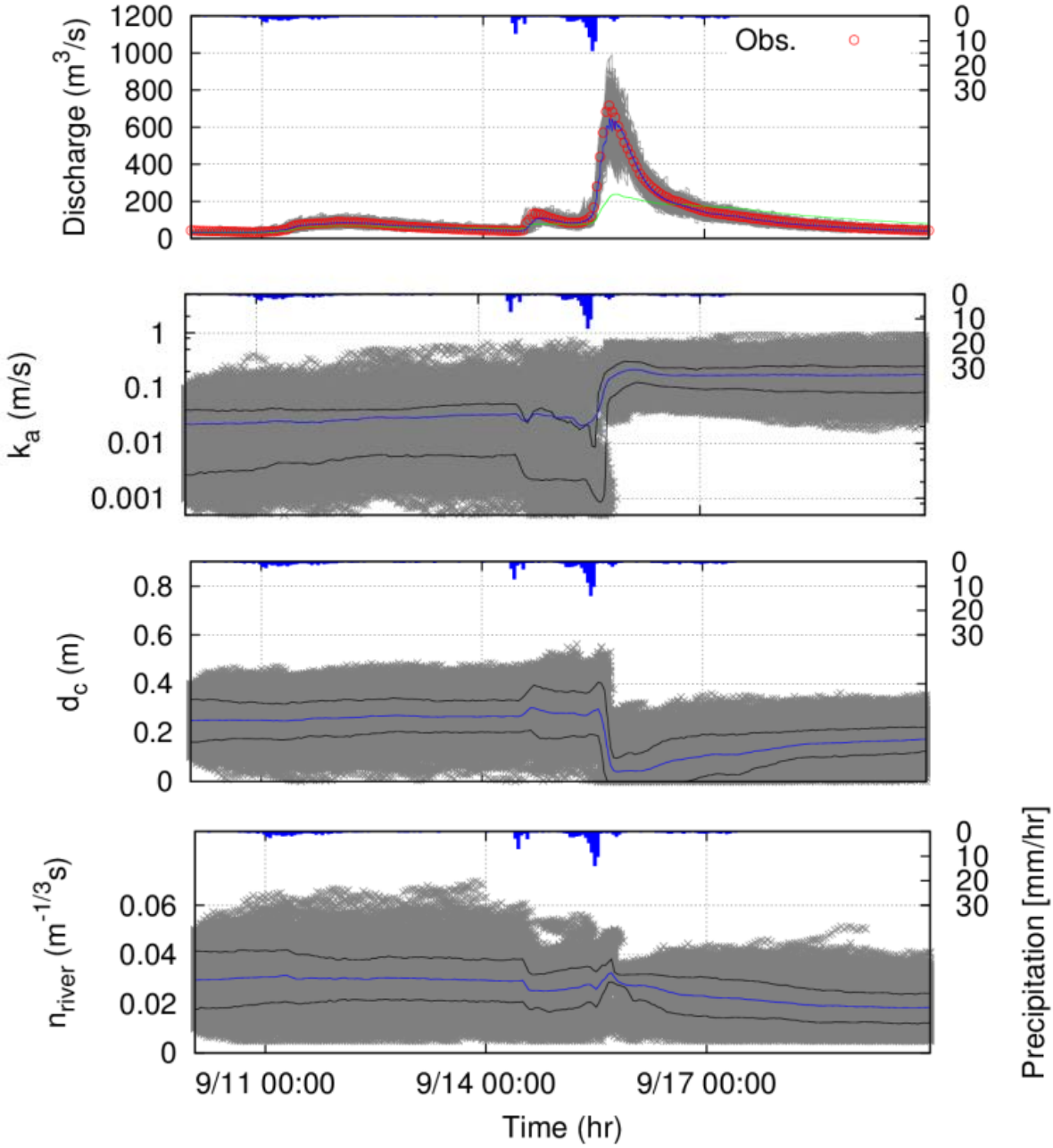

Fig. 6-12 Parallel simulations of the distributed hydrologic model with PF in the preliminary stage of the real experiment (Event 1). Red dots represent synthetic observation. Grey lines represent traces of streamflow of ensembles. Grey dots represent traces of parameters of ensembles. Blue lines represent mean of ensembles. Black lines represent 60% confidence intervals. Green lines represent deterministic modeling with parameters using mean of initial distribution.

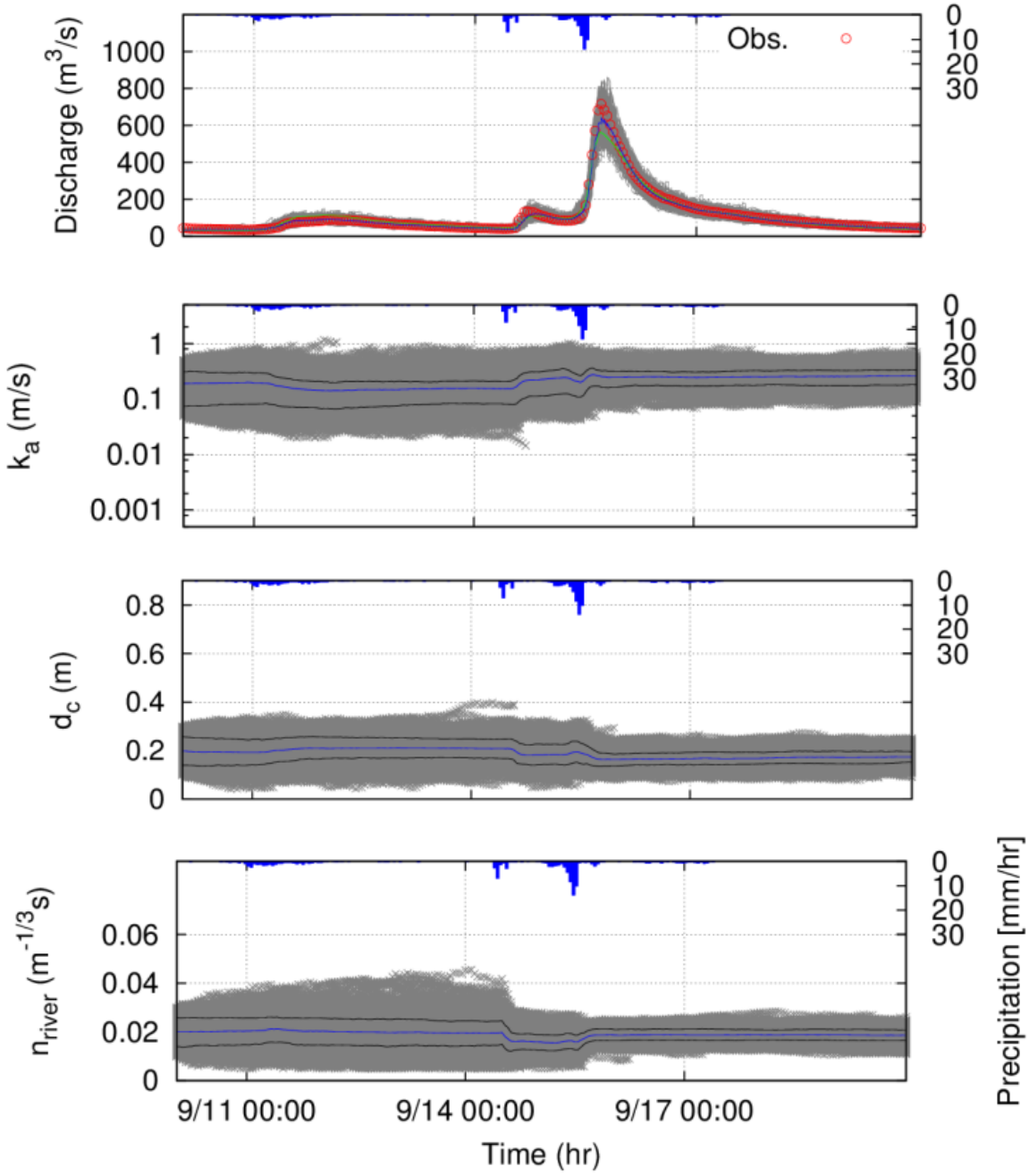

Fig. 6-13 Parallel simulations of the distributed hydrologic model with PF in the second stage of the real experiment (Event 1). Red dots represent synthetic observation. Grey lines represent traces of streamflow of ensembles. Grey dots represent traces of parameters of ensembles. Blue lines represent mean of ensembles. Black lines represent 60% confidence intervals. Green lines represent streamflow of deterministic modeling with parameters using mean of preliminary stage.

Streamflow prediction via PF is compared with the deterministic modeling case using mean of initial distribution or posterior of the preliminary stage. It is seen that the deterministic streamflow simulation is improved in the second stage.

Simulation results of Events 2 and 3 are shown in Figs. 6-14~6-15. In these cases, the initial conditions of parameters are adopted from the posterior estimated in Event 1 to assess the applicability of the parameters for the different flood events. In the results of both cases, the traces of parameter distributions show stable movement reaching narrow posteriors within the initial bounds. One-step-ahead prediction of streamflow also results in reliable discharge hydrographs in both cases. Note that the magnitudes of observed flood peak are quite different in each case.

Model performance is summarized in Table 6-6 using two indices: NSE and RMSE. The statistics show the improvement of the model performance via PF in all events compared to deterministic modeling cases. Parameter distributions estimated by PF at Event 1 result in good performance in Event 3, whose peak flood is about six times higher than Event 1. In Event 3, deterministic modeling presents improved performance, demonstrating transferability of the parameters for an unexperienced high flood. However, application into a smaller flood (Event 2) shows limited performance. Due to uncertainties coming from hydrologic models and observations, optimal parameters may change according to the magnitude of flood events and initial conditions. The results of deterministic modeling show that parameters estimated at large events (Event 1) may not be appropriate for small events (Event 2) or vice versa. This situation is found frequently in numerous hydrologic modeling cases. However, probabilistic approach and dual state-parameter updating could compensate the uncertainty of model structures.

Table 6-6 Summary of model performance for real experiment.

	Deterministic modeling		Particle filtering	
	NSE	RMSE (m^3s^{-1})	NSE	RMSE (m^3s^{-1})
Event 1	0.96	23	0.98	16
Event 2	-0.40	93	0.81	33
Event 3	0.94	217	0.98	117

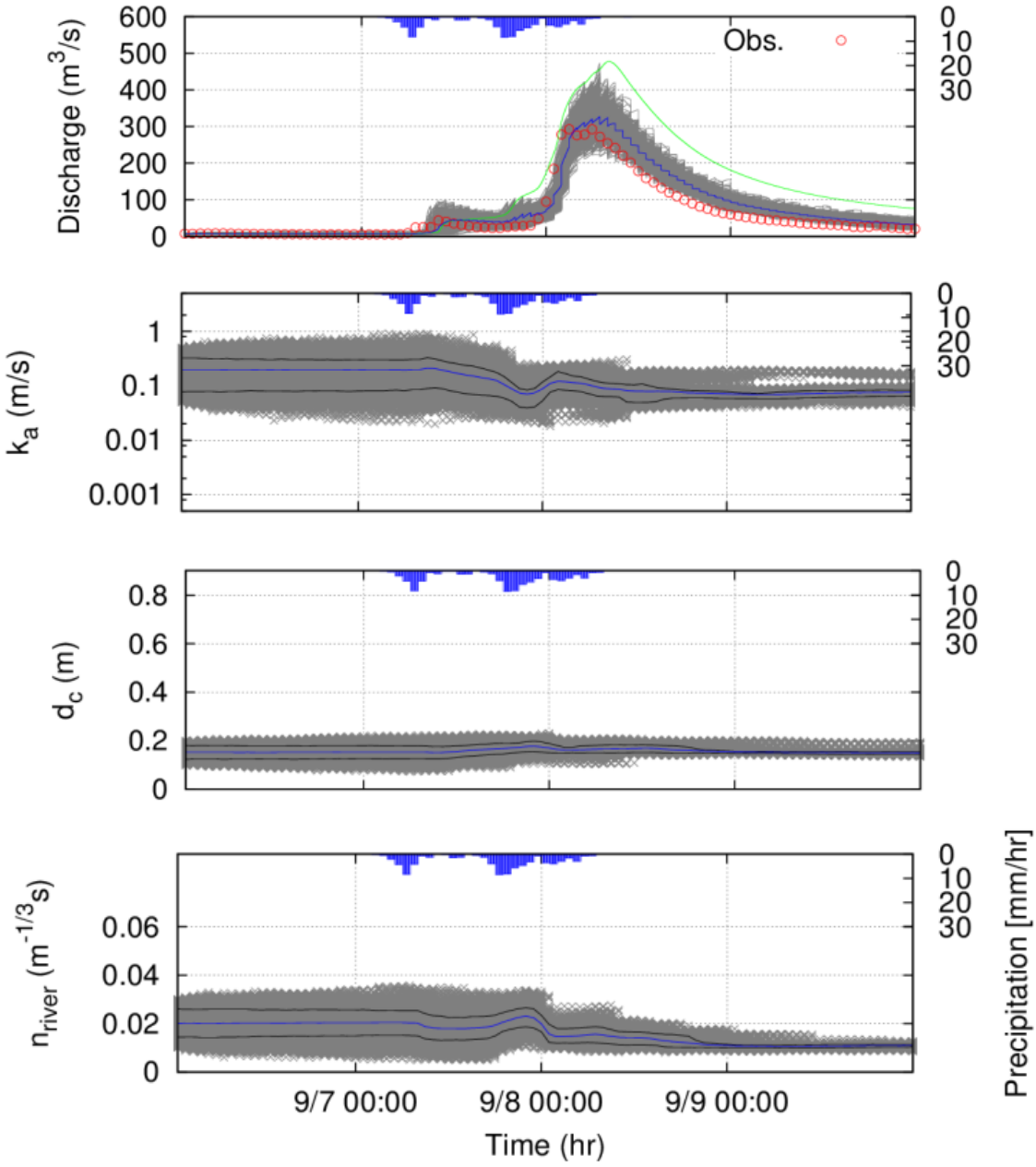

Fig. 6-14 Parallel simulations of the distributed hydrologic model with PF in the real experiment (Event 2). Red dots represent synthetic observation. Grey lines represent traces of streamflow of ensembles. Grey dots represent traces of parameters of ensembles. Blue lines represent mean of ensembles. Black lines represents 60% confidence intervals. Green lines represent streamflow of deterministic modeling with parameters using results of Event 1.

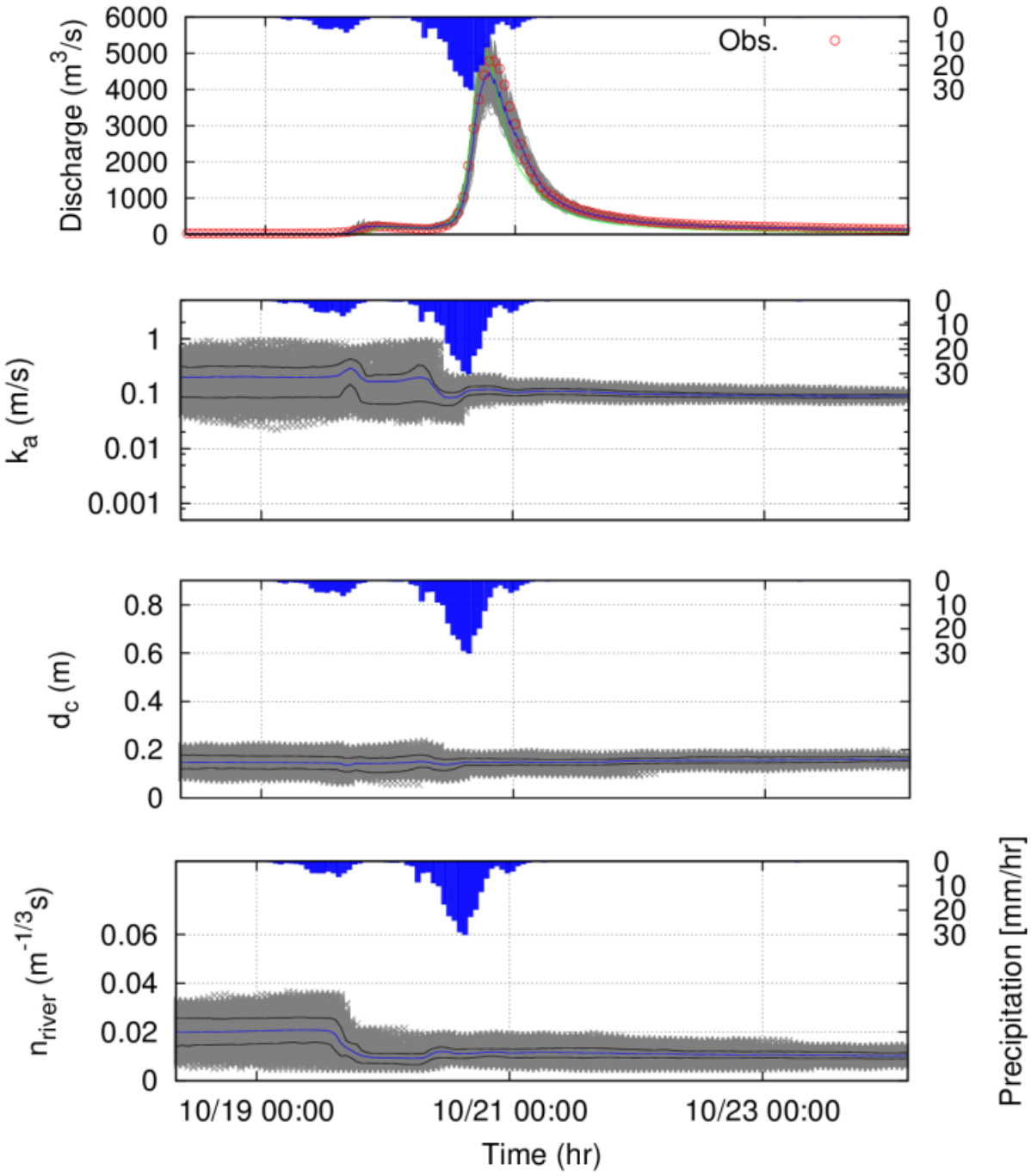

Fig. 6-15 Parallel simulations of the distributed hydrologic model with PF in the real experiment (Event 3). Red dots represent synthetic observation. Grey lines represent traces of streamflow of ensembles. Grey dots represent traces of parameters of ensembles. Blue lines represent mean of ensembles. Black lines represents 60% confidence intervals. Green lines represent streamflow of deterministic modeling with parameters using results of Event 1.

6.5 Conclusions

MPI-OHyMoS was developed as a hydrologic modeling framework for stochastic simulation and data assimilation. The flexible framework provided particle filtering, dual state-parameter updating and kernel smoothing to consider various sources of uncertainty in hydrologic modeling. Ensemble simulation was parallelized by MPI taking advantage of a high performance computing (HPC) system. Structure and implementation processes of data assimilation via MPI-OHyMoS were shown using a simple lumped model.

The applicability of MPI-OHyMoS was demonstrated using different hydrologic models such as lumped and distributed models. A synthetic experiment of a linear reservoir model and a distributed hydrologic model showed the dual state-parameter updating scheme of MPI-OHyMoS could be conducted properly for missing data problems. Especially, identifiability of model parameters was evaluated by two stage simulation in the distributed modeling case. The roughness coefficient of the slope component showed diffusive probabilistic distribution in the preliminary simulation. However, further study is needed for various conditions.

In real experiment cases of the distributed hydrologic model, simulated discharge via particle filtering showed good conformity with observation. Uncertainty bounds of ensembles were also reduced significantly. The assimilated results could be used to improve streamflow forecasting.

Despite their potential to estimate and mitigate uncertainty for non-linear, non-Gaussian models, implementation of sequential data assimilation including the particle filters has been limited due to lack of general modeling frameworks. MPI-OHyMoS is expected to make it easy to build a stochastic hydrologic model and to support data assimilation as a general modeling framework. In the future, we plan to improve MPI-OHyMoS in terms of parameter estimation methods and flexible assimilation control. The software framework developed in this paper can be obtained from the authors by request via email.

Chapter 7

Conclusions

The main objectives of this thesis were as follows:

1. Development of a dual state-parameter updating scheme (DUS) based on the SMC methods to estimate both state and parameter variables of a lumped hydrologic model.

2. Development of a robust particle filtering approach for considering different response times of internal state variables in a distributed hydrologic model.

3. Comparison of performance of ensemble Kalman filtering and particle filtering for short-term streamflow forecasting using a distributed hydrologic model.

4. Development of a hydrologic modeling framework for data assimilation: MPI-OHyMoS.

In **Chapter 3**, the sequential Monte Carlo (SMC) filters were applied to a conceptual hydrologic model, the storage function model, using state only updating and the dual state-parameter updating scheme. The river discharge forecast via the SMC filters was compared with observations. The forecast provided by the dual state-parameter updating scheme was superior to that of state only updating and deterministic modeling in terms of the model accuracy criteria, a scatter diagram, and simulated hydrographs. In the dual state-parameter updating scheme, parameter inference was performed by the kernel smoothing method. A significant reduction of parameter

uncertainty was observed for all parameters after the first flood peak, and estimated parameter distributions showed good conformity with off-line optimum. Performance results of SIR and the RPF showed similar forecasting accuracy, while ASIR resulted in a slightly higher number of errors than others. However, RMSE statistics of three SMC filters presented stable results when the number of particles was over 1,000.

In **Chapter 4**, a lagged particle filtering approach was proposed as a framework to deal with the delayed response, which originates from different time scales of hydrologic processes in a distributed hydrologic model. The regularized particle filter with the MCMC move step was implemented to preserve sample diversity under the lagged filtering approach. As a process-based distributed hydrologic model, WEP was implemented to illustrate the strength and weakness of the lagged regularized particle filter (LRPF) compared to SIR for short-term streamflow forecast. Two particle filters showed significantly improved forecasts compared to deterministic modelling cases in different simulation periods. Various ranges of process noise related to soil moisture were simulated for varying lead times. While SIR has different values of optimal process noise and shows sensitive variation of confidence intervals according to the process noise, the LRPF shows consistent forecasts regardless of the process noise assumption. Due to the preservation of particle diversity by the kernel, the LRPF showed enhanced forecasts, especially when the discharge changed sharply in a short time (the year 2007) and flood peak was high (the year 2004). However, the relatively large perturbation by the kernel could produce negative effects when the flood peak was relatively small and the hydrograph varied smoothly (the year 2003).

In **Chapter 5**, two sequential data assimilation methods, the ensemble Kalman filter and the particle filter, have been assessed for short-term streamflow hindcasting with a distributed hydrologic model, WEP. The ensemble square root filter and the regularized particle filter were implemented to avoid flaws associate with

conventional methods. The updating of state variables was performed through a lag-time window to consider lag and response times among internal hydrologic processes in a distributed hydrologic model. The EnSRF and the RPF were applied to two small catchments in Japan and Korea to assess the performance of the two methods. Ensembles perturbed by the noise of variation in soil moisture content were assimilated by streamflows observed at each outlet. In the case of the Katsura River catchment in Japan, in the predictions of both the EnSRF and the RPF improved when the lag time increased. Updated ensembles produced improved streamflow predictions for lead times of up to 15 hours. Without a lag-time window, the predictions became unstable in terms of means and confidence intervals. In the sensitivity analysis of the ensemble number, no significant variation in model efficiency was detected with variation in ensemble number. The results of this study indicate that the RPF performed better than the EnSRF even when the number of ensembles was extremely low, but further study of this difference is required. In the case of the Gyeongancheon catchment in Korea, the predictions obtained with the EnSRF and the RPF were equivalent for lead times ranging from 5 to 14 hours, while the prediction accuracy of the RPF was superior to the EnSRF for other lead times.
In both catchments, a lag-time window contributed to improving performance of the EnSRF and the RPF, and the RPF yielded predictions equal to or better than those of the EnSRF in accuracy. In the case of the EnSRF, a decrease in model performance was observed for both catchments when the lead times were short (< 4 hours). Sequential data assimilation methods have significant potential for application to highly nonlinear and non-Gaussian problems, such as process-based distributed models. Therefore, further study should be focused on real-time and multi-site data assimilation for hydrologic forecasting for a large-scale catchment, for which a lag-time window may provide an essential framework.

In **Chapter 6**, MPI-OHyMoS was developed as an open software framework for stochastic simulation and data assimilation. The flexible framework provided particle filtering, dual state-parameter updating and kernel smoothing to consider various

sources of uncertainty in hydrologic modeling. Ensemble simulation was parallelized by MPI taking advantage of a high performance computing (HPC) system. The applicability of MPI-OHyMoS was demonstrated using different hydrologic models such as lumped and distributed ones. The synthetic experiment cases of a linear reservoir model and a distributed hydrologic model showed that the dual state-parameter updating scheme of MPI-OHyMoS could be conducted properly for the missing data problem. Especially, the identifiability of model parameters was evaluated by two stage simulations in the distributed modeling cases. The roughness coefficient of slope component showed diffusive probabilistic distribution in the preliminary simulation. However, the further study was needed for various conditions. In the real experiment of the distributed hydrologic model, simulated discharge via particle filtering showed good conformity with observation. Uncertainty bounds of ensembles were also reduced significantly. Assimilated results could be used to improve streamflow forecasting.

The SMC methods have significant potential for high non-linearity problems, especially for process-based distributed models in hydrologic investigation. However, the computational cost and lack of proper frameworks for distributed modelling in terms of methodology and software have been bottlenecks to their practical implementation. This thesis showed the SMC methods could be applied for hydrologic modelling to improve forecasting accuracy and identify uncertainty from various sources and the applicability of proposed methodologies was demonstrated in various case studies using different hydrologic models. The LRPF proposed in Chapter 4 is expected to be used as one of the frameworks for sequential data assimilation of process-based distributed modelling. The main benefits of the LRPF are the improved forecasts for rapidly varied high floods and the stability of confidence intervals for uncertainty of process noise. As shown in Chapter 5, the lag-time window concept could be extended to ensemble Kalman filtering to improve performances in distributed modelling. MPI-OHyMoS developed in Chapter 6 is expected to make it easy to build a stochastic hydrologic model and to support data assimilation as a general modeling framework.

Appendices

A. Methods of resampling

In this section, basic resampling methods such as multinomial, stratified, systematic, and residual resampling are described. Detailed descriptions are provided in Douc et al. (2005) and Ristic et al. (2004). Resampling involves a mapping of particles with weights into particles with uniform weights. To fix the notations, we use following notations: n is the particle number and N^i are the particle duplication counts, which means how many times a particle i is duplicated in the resampling step.

A.1 Multinomial resampling

Multinomial resampling is based on an idea at the core of the bootstrap method (Doucet et al., 2001), where the duplication counts $N^1,\ldots,N^n$ are defined according to the multinomial distribution $Mult(n; w^1,...,w^n)$. In practice, multinomial resampling is achieved by repeated uses of the inversion method:

1. Draw n independent uniforms U^i on the interval (0,1].
2. Sort U^i in ascending order.
3. Construct the cumulative sum of weights of random measure $\{x_k^i, w_k^i\}$ as $c^i = c^{i-1} + w_k^i \quad (i = 2,...,n)$.
4. Count the number of $U^j (j = 1,...,n)$ located between c^{i-1} and c^i . Set the number as N^i .

As best sorting algorithm has a complexity of $O(n \log n)$ this is a major limitation in practical applications. However, it is possible to implement the resampling procedure in *O(n)* operations by sampling n ordered uniforms using an algorithm based on order statistics (Ristic et al., 2004).

A.2 Stratified resampling

Stratified resampling is based on an idea of pre-partitioning the (0,1] interval into n disjoint sets $(0,1] = (0,1/n] \cup \cdots \cup (\{n-1\}/n,1]$ and drawing uniforms in each of these sub-intervals. The procedure of this method follows these steps:

1. Draw *n* independent uniforms U^i on the interval $(\{i-1\}/n, i/n]$

2. Construct the cumulative sum of weights of random measure $\{x_k^i, w_k^i\}$ as $c^i = c^{i-1} + w_k^i \quad (i = 2,...,n)$.

3. Count the number of $U^j (j = 1,...,n)$ located between c^{i-1} and c^i. Set the number as N^i.

A.3 Systematic resampling

Systematic resampling is an efficient scheme having computational simplicity and good empirical performance. The procedure of this method follows these steps:

1. Draw an independent uniforms U^1 on the interval (0,1/n].

2. Set $U^i = (i-1)/n + U^1$

3. Construct the cumulative sum of weights of random measure $\{x_k^i, w_k^i\}$ as $c^i = c^{i-1} + w_k^i \quad (i = 2,...,n)$.

4. Count the number of $U^j (j = 1,...,n)$ located between c^{i-1} and c^i. Set the number as N^i.

A.4 Residual resampling

Residual resampling is mentioned by Whitley (1994) and Liu and Chen (1998) as a method to decrease the variance due to resampling. In this approach, we have

$$N^i = \lfloor nw^i \rfloor + \overline{N}^i \tag{A-1}$$

where $\lfloor \ \rfloor$ denotes the integer part and $\overline{N}^1,...,\overline{N}^n$ are distributed according to the multinomial distribution $Mult(n-R; \overline{w}^1,...,\overline{w}^n)$ with $R = \sum_{i=1}^n \lfloor nw^i \rfloor$ and

$$\overline{w}^i = \frac{nw^i - \lfloor nw^i \rfloor}{n-R} \tag{A-2}$$

In practice, the multinomial counts $\overline{N}^1,...,\overline{N}^n$ from the residual multinomial distribution are generated as in the multinomial resampling procedure drawing $n-R$ independent uniforms.

B. Parallel programming of resampling

The resampling step is required to reduce the effects of degeneracy. However, it limits the opportunity to parallelize the computational implementation because all the particles must be combined. Therefore, effective programming is essential to reduce the computation time. In parallel computing via MPI, the resampling step is executed by communication commands such as combinations of "send" and "receive" functions between processes. It is the best practice to reduce the number of communications in MPI code because communication commands among processes need more computation time compared to individual computation in a process.

The duplication procedure suggested in this section is designed to minimize the number of communications among particles in the resampling step. Table B-1 shows matrices required in this procedure (with only n = 10 particles). N^i can be calculated by any resampling methods described in Appendix A. The "copytozero" vector denotes the real duplication counts by subtracting one for non-zero components in N^i. The "copyfrom" and "copyorder" vectors denote the address of source particles and the duplication order for receiving particles, respectively. The "copyaccum" vector is needed in sending particles. The duplication can be performed from non-zero components in "copytozero" to non-zero components in "copyfrom". The information required in MPI functions is provided in each matrix. Implementation code in C++ is shown in Table B-2. Note that any forms of data can be communicated by this "Resampling" function with Boost library.

Table B-1 Vectors for the effective duplication procedure (n = 10).

Particle no.	1	2	3	4	5	6	7	8	9	10
N^i	1	0	3	0	0	2	1	2	1	0
copytozero	0	0	2	0	0	1	0	1	0	0
copyaccum	0	0	0	0	0	2	0	3	0	0
copyfrom	0	3	0	3	6	0	0	0	0	8
copyorder	0	1	0	2	3	0	0	0	0	4

Table B-2 Implementation code of the effective duplication in C++.

```
#include <boost/mpi.hpp>
#include <boost/serialization/string.hpp>
namespace mpi = boost::mpi;
…
void Resampling()
{
…
t_rank=Getmyrank();          // the number of a particle
t_p_total=Getptotal();       // total number of particles

lf(t_rank!=0){
if(copytozero[t_rank]!=0){
                icpnmax=copytozero[t_rank];
                for(icpn=1;icpn<=icpnmax;icpn++){
                                isnd=copyaccum[t_rank]+icpn;
                                for(np=1;np<t_p_total;np++){
                                                if(copyorder[np]==isnd){
                                                                rcevp=np;
                                                                break;
                                                }
                                }
                                world.send(rcevp,0,stout_tst.str());
                }
}else if(arraycopy[t_rank]==0){
                sndp=copyfrom[t_rank];
                stout_tst.str("");              str_tst.clear();
                world.recv(sndp,0,str_tst);
                stout_tst << str_tst;
}
}
…
}
```

C. Parameter estimation methods in SMC

In this section, parameter estimation methods such as artificial evolution and kernel smoothing are described mainly focusing on stability of each method. The detailed descriptions on artificial evolution and kernel smoothing are provided in Liu and West (2001) and Chen et al. (2005). Discussion on other parameter estimation methods in SMC are also provided in Storvik (2002), Vo et al. (2004), Andrieu et al. (2005), Yang et al. (2008), and Kantas et al. (2009).

For both methods, the general state-space model is extended to the sample-based framework with fixed parameters θ. At time *k*, we have a combined sample

$$\{x_k^i, \theta_k^i : i = 1,...,n\} \tag{C-1}$$

and associated weights

$$\{w_k^i : i = 1,...,n\} \tag{C-2}$$

representing an importance sample approximation to the time *k* posterior $p(x_k, \theta \mid y_{1:k})$ for both parameter and state. Note that the *k* suffix on the θ samples indicate that they are from the time *k* posterior, not that θ is time-varying. The Monte Carlo approximation $\{\theta_k^i, w_k^i\}$ has mean $\overline{\theta}_k$ and variance matrix V_k^θ.

The approach of artificial evolution is to add small random perturbations to all the parameter particles under the posterior at each time point before evolving to the next.

$$\theta_k = \theta_{k-1} + \zeta_k \qquad \zeta_k \sim N(0, W_k^\theta) \tag{C-3}$$

where ζ_k is random noise, W_k^θ is the variance of parameter particles at time *k* before resampling. Pretending that parameters are in fact time-varying implies an artificial "loss of information" between time points, resulting in posteriors that are too diffuse relative to the theoretical posteriors for the actual fixed parameters. The undesirable "loss of information" can be easily quantified. In the evolution in Eq. (C-3) with the innovation ζ_k independent of θ_{k-1} as proposed, the implied prior $p(\theta_k \mid y_{1:k-1})$ has the correct mean $\overline{\theta}_k$ but variance matrix $V_{k-1}^\theta + W_k^\theta$. The loss of information is explicitly represented by the component W_k^θ. In practice, we can control the variance using following treatment as $W_k^\theta = s^2 V_{k-1}^\theta$ with a small tuning parameter *s*. When the

dimension of parameters is small, we can have good empirical performance with the adjusted *s*. However, when the dimension of parameters increase it is difficult to choose a proper tuning parameter *s* due to different identifiability of parameters.

In kernel smoothing, the Monte Carlo approximation is expressed by a kernel form

$$P(\theta_k \mid y_{1:k-1}) \sim \sum_{i=1}^{n} w_{k-1}^i N(\theta_k \mid \theta_{k-1}^i, W_k^\theta) \tag{C-4}$$

As shown above this is over-dispersed relative to "target" variance V_{k-1}^θ. To correct for the over-dispersion, the kernel method use the shrinkage rule pushing sample θ_{k-1}^i values towards their mean $\overline{\theta}_{k-1}$ before adding a small degree of noise implied by the normal kernel. This suggests that the artificial evolution method should be modified by introducing correlations between θ_{k-1} and the random noise ζ_k. Assuming a non-zero covariance matrix, note that the artificial evolution equation (C-3) implies

$$V^\theta(\theta_k \mid y_{1:k-1}) = V^\theta(\theta_{k-1} \mid y_{1:k-1}) + W_k^\theta + 2C(\theta_{k-1}, \zeta_k \mid y_{1:k-1}) \tag{C-5}$$

To correct to "no information lost" implies that we set

$$V^\theta(\theta_k \mid y_{1:k-1}) = V^\theta(\theta_{k-1} \mid y_{1:k-1}) = V_{k-1}^\theta \tag{C-6}$$

which then implies

$$C(\theta_{k-1}, \zeta_k \mid y_{1:k-1}) = -W_k^\theta / 2 \tag{C-7}$$

Hence, there must be a structure of negative correlations to remove the unwanted information loss effect. In the case of approximate joint normality of $(\theta_{k-1}, \zeta_k \mid y_{1:k-1})$, this would then imply the conditional normal evolution in which

$$p(\theta_k \mid \theta_{k-1}) = N(\theta_k \mid A_k\theta_{k-1} + (I - A_k)\overline{\theta}_{k-1}, (I - A_k^2)V_{k-1}^\theta) \tag{C-8}$$

where

$$A_k = I - W_k^\theta V_{k-1}^{\theta\ -1} / 2 \tag{C-9}$$

Although a generalized kernel form with complicated shrinkage patterns is available for shrinkage matrix A_k, we just consider the very special case in which the matrix W_k^θ is specified using a standard discount factor technique.

$$W_k^{\theta} = V_{k-1}^{\theta}(\frac{1}{\delta} - 1) \tag{C-10}$$

where is a discount factor in (0,1], typically around 0.95-0.99. In this case, $A_k = aI$ with $a = (3\delta - 1)/2\delta$ and the conditional evolution density above reduces

$$p(\theta_k \mid \theta_{k-1}) \sim N(\theta_k \mid a\theta_{k-1} + (1-a)\overline{\theta}_{k-1}, h^2 V_{k-1}^{\theta}) \tag{C-11}$$

where

$$h^2 = 1 - a^2 \tag{C-12}$$

so that

$$h^2 = 1 - \left((3\delta - 1)/2\delta\right)^2 \tag{C-13}$$

The mean and variance matrix of the implied marginal distribution $p(\theta_k \mid y_{1:k-1})$ are also $\overline{\theta}_{k-1}$ and V_{k-1}^{θ} .This shows that kernel smoothing for fixed model parameters removes the problem of information loss over time.

Bibliography

Andrieu C., Doucet, A., and Holenstein, R.: Particle Markov chain Monte Carlo methods, J. R. Statist. Soc. B, 72, Part 3, 269–342, 2010.

Andrieu C., Doucet, A., and Tadic, V.: On-line parameter estimation in general state-space models, in: Proc. the 44th Conference on Decision and Control, 2005.

Arulampalam, M. S., Maskell, S., Gordon, N., and Clapp, T.: A tutorial on particle filters for online nonlinear/non-Gaussian Bayesian tracking, IEEE Trans. Signal Proces., 50, 174-188, 2002.

Barbetta, S., Moramarco, T., Franchini, M., Melone, F., Brocca, L., and Singh, V. P.: Case study: improving real-time stage forecasting muskingum model by incorporating the rating curve model, J. Hydrol. Eng., 16, 540-557, 2011.

Beven, K. J.: Environmental modeling: an uncertain future?, Routledge, 2009.

Beven, K. J. and Binley, A. M.: The future of distributed models: model calibration and uncertainty prediction, Hydrol. Process., 6, 279–298, 1992.

Blöschl, G. and Sivapalan, M.: Scale issues in hydrological modelling: a review, Hydrol. Process., 9, 251-290, 1995.

Burgers, G., van Leeuwen, P. J., and Evensen, G.: Analysis scheme in the ensemble Kalman filter, Mon. Weather Rev., 126, 1719-1724, 1998.

Cappé, O., Moulines, E., and Ryden, T.: Inference in hidden Markov models, Springer, 2005.

Chen, T., Morris, J., and Martin, E.: Particle filters for state and parameter estimation in batch processes, J. Process Control, 15, 665-673, 2005.

Clark, M. P., Rupp, D. E., Woods, R. A., Zheng, X., Ibbitt, R. P., Slater, A. G., Schmidt, J., and Uddstrom, M. J.: Hydrological data assimilation with the ensemble Kalman filter: Use of streamflow observations to update states in a distributed hydrological model, Adv. Water Resour., 31, 1309-1324, 2008.

DeChant, C. M. and Moradkhani, H.: Improving the characterization of initial condition for ensemble streamflow prediction using data assimilation, Hydrol. Earth Syst. Sci., 15, 3399-3410, doi:10.5194/hess-15-3399-2011, 2011.

Del Moral, P.: Feynman-Kac formulae: genealogical and interacting particle systems with applications, Springer, 2004.

Douc, R., Cappe, O., and Moulines, E.: Comparison of resampling scheme for particle filtering, in: Proc. the 4th International Symposium on Image and Signal Processing, 64-69, 2005.

Doucet, A., de Freitas, N., and Gordon, N. (Eds.): Sequential Monte Carlo methods in practice, Springer, 2001.

Evensen, G.: Sequential data assimilation with a nonlinear quasi-geostrophic model using Monte Carlo methods to forecast error statistics, J. Geophys. Res., 99, 10143-10162, 1994.

Evensen, G.: The ensemble Kalman filter: theoretical formulation and practical implementation, Ocean Dynamics, 53, 343-367, 2003.

Evensen, G.: Data assimilation: the ensemble Kalman filter, Springer, 2009.

Frei, M. and Künsch, H. R.: Sequential state and observation noise covariance estimation using combined ensemble Kalman and particle filters, Mon. Weather Rev., 140, 1476-1495, 2012.

Grayson, R. and Blöschl, G.: Spatial processes, organization and patterns, in: Spatial patterns in catchment hydrology: observations and modelling, Grayson, R. and Blöschl, G. (Eds.), Cambridge University Press, Cambridge, UK, 3-16, 2001.

Georgakakos, K. P.: A generalized stochastic hydrometeorological model for flood and flash-flood forecasting, Water Resour. Res., 22, 2096-2106, 1986.

Gilks, W. R. and Berzuini, C.: Following a moving target—Monte Carlo inference for dynamic Bayesian models, Journal of the Royal Statistical Society, B, 63, 127-146, 2001.

Giustarini, L., Matgen, P., Hostache, R., Montanari, M., Plaza, D., Pauwels, V. R. N., De Lannoy, G. J. M., De Keyser, R., Pfister, L., Hoffmann, L., and Savenije, H. H. G.: Assimilating SAR-derived water level data into a hydraulic model: a case study, Hydrol. Earth Syst. Sci., 15, 2349-2365, doi:10.5194/hess-15-2349-2011, 2011.

Gordon, N. J., Salmond, D. J., and Smith, A. F. M.: Novel approach to nonlinear/non-Gaussian Bayesian state estimation, Proc. Inst. Electr. Eng., 140, 107-113, 1993.

Han, E., Merwade, V., and Heathman, G. C.: Implementation of surface soil moisture data assimilation with watershed scale distributed hydrological model, J. Hydrol., 416–417, 98-117, 2012.

He, M., Hogue, T. S., Margulis, S. A., and Franz, K. J.: An integrated uncertainty and ensemble-based data assimilation approach for improved operational streamflow predictions, Hydrol. Earth Syst. Sci., 16, 815-831, doi:10.5194/hess-16-815-2012, 2012.

Hiemstra, P. H., Karssenberg, D., and van Dijk, A.: Assimilation of observations of radiation level into an atmospheric transport model: a case study with the

particle filter and the ETEX tracer dataset, Atmospheric Environment, 45, 6149-6157, 2011.

Hunukumbura, J. M. P. B.: Distributed hydrological model transferability across basins with different physio-climatic characteristics, Ph.D. thesis, Kyoto Univ., Japan, 2009.

Houtekamer, P. L. and Mitchell, H. L.: A sequential ensemble Kalman filter for atmospheric data assimilation, Mon. Weather Rev., 129, 123–137, 2001.

Ichikawa, Y., Murakami, M., Tachikawa, T., and Shiiba, M.: Development of a basin runoff simulation system based on a new digital topographic model, J. Hydraulic, Coastal and Environ. Engng. JSCE, 691, 43-52, 2001.

Ichikawa, Y., Tachikawa, Y., Takara, K. and Shiiba, M.: Object-oriented hydrological modeling system, in: Proc. 4th Int. Conference Hydroinformatics 2000, Iowa, USA, 2000.

Jeremiah, E., Sisson, S. A., Sharma, A., and Marshall, L.: Efficient hydrological model parameter optimization with sequential Monte Carlo sampling, Environmental Modelling and Software, 38, 283-295, 2012.

Jia, Y., Ding, X., Qin, C., and Wang, H.: Distributed modeling of landsurface water and energy budgets in the inland Heihe river basin of China, Hyrol. Earth Syst. Sci., 13, 1849-1866, 2009.

Jia, Y., Ni, G., Kawahara, Y., and Suetsugi, T.: Development of WEP model and its application to an urban watershed, Hydrol. Process., 15, 2175–2194, 2001.

Jia, Y. and Tamai, N.: Integrated analysis of water and heat balance in Tokyo metropolis with a distributed model, J. Japan Soc. Hydrol. Water Resour., 11, 150–163, 1998.

Johansen, A. M.: SMCTC: Sequential Monte Carlo in C++, J. Stat. Software, 30, 1-41, 2009.

Kalman, R. E.: A new approach to linear filtering and prediction problems, Trans. ASME. J. Basic Eng., 82, 35-45, 1960.

Kantas, N., Doucet, A., Singh, S. S., and Maciejowski, J. M.: An overview of sequential Monte Carlo methods for parameter estimation in general state-space models, in: Proc. 15th IFAC Symposium on System Identification, SYSID 2009, Saint-Malo, France, 2009.

Karssenberg, D., Schmitz, O., Salamon, P., de Jong, K., and Bierkens, M. F. P.: A software framework for construction of process-based stochastic spatio-temporal models and data assimilation, Environmental Modelling and Software, 25, 489-502, 2010.

Kim, H., Noh, S., Jang, C., Kim, D., and Hong, I.: Monitoring and analysis of hydrological cycle of the Cheonggyecheon watershed in Seoul, Korea, in: Proc. of International Conference on Simulation and Modeling, Nakornpathom, Thailand, 2005, C4–03, 2005a.

Kim, H. J., Yoon, S. K., Noh, S. J., and Jang, C. H.: The Cheonggye-cheon restoration project and hydrological cycle analysis, Water Engineering Research, 6, 179-187, 2005b.

Kim, S., Tachikawa, Y., and Takara, K.: Applying a recursive update algorithm to a distributed hydrologic model, J. Hydrol. Eng., pp. 336-344, 2007.

Kimura, T.: The flood runoff analysis method by the storage function model, The Public Works Research Institute, Ministry of Construction, Japan, 1961.

Kitagawa, G.: Monte-Carlo filter and smoother for non-Gaussian non-linear state-space models, J. Comput. Graph. Stat., 5, 1-25, 1996.

Kitanidis, P. K. and Bras, R. L.: Real-time forecasting with a conceptual hydrologic model 2. applications and results, Water Resour. Res., 16, 1034-1044, 1980.

Komma, J., Blöschl, G., and Reszler, C.: Soil moisture updating by ensemble Kalman filtering in real-time flood forecasting, J. Hydrol., 357, 228-242, 2008.

Kong, A., Liu, J. S., and Wong, W. H.: Sequential imputations and Bayesian missing data problems, J. Am. Stat. Assoc., 89, 278-288, 1994.

Leavesley, G. H., Markstrom, S. L., Restrepo, P. J., and Viger, R. J.: A modular approach to addressing model design, scale and parameter estimation issues in distributed hydrological modeling, Hydrol. Process., 16, 173-187, 2002.

Lee, G., Kim, S., Jung, K., and Tachikawa, Y.: Development of a large basin rainfall–runoff modeling system using the object-oriented hydrologic modeling system (OHyMoS), KSCE, Journal of Civil Engineering, 15, 595-606, 2011.

Leisenring, M. and Moradkhani, H.: Snow water equivalent prediction using Bayesian data assimilation methods, Stoch. Environ. Res. Risk Assess., 25, 253-270, doi: 10.1007/s00477-010-0445-5, 2011.

Li, Z. and Navon, I. M.: Optimality of variational data assimilation and its relationship with the Kalman filter and smoother, Quart. J. Roy. Met. Soc., 127, 661-683, 2001.

Li, B., Toll, D., Zhan, X., and Cosgrove, B.: Improving estimated soil moisture fields through assimilation of AMSR-E soil moisture retrievals with an ensemble Kalman filter and a mass conservation constraint, Hydrol. Earth Syst. Sci., 16, 105-119, doi:10.5194/hess-16-105-2012, 2012.

Liu, J. and Chen, R.: Sequential Monte-Carlo methods for dynamic systems, J. Am. Stat. Assoc., 93, 1032-1044, 1998.

Liu, Y. and Gupta, H. V.: Uncertainty in hydrologic modeling: toward an integrated data assimilation framework, Water Resour. Res., 43, W07401, doi: 10.1029/2006WR005756, 2007.

Liu, J. and West, M.: Combined parameter and state estimation in simulation-based filtering, in: Sequential Monte Carlo in practice, Doucet, A., de Freitas, N., and Gordon, N. (Eds.), Springer, 197-223, 2001.

Liu, Y., Weerts, A. H., Clark, M., Hendricks Franssen, H.-J., Kumar, S., Moradkhani, H., Seo, D.-J., Schwanenberg, D., Smith, P., van Dijk, A. I. J. M., van Velzen, N., He, M., Lee, H., Noh, S. J., Rakovec, O., and Restrepo, P.: Advancing data assimilation in operational hydrologic forecasting: progresses, challenges, and emerging opportunities, Hydrol. Earth Syst. Sci., 16, 3863-3887, 2012.

McMillan, H. K., Hreinsson, E. Ö., Clark, M. P., Singh, S. K., Zammit, C., and Uddstrom, M. J.: Operational hydrological data assimilation with the retrospective ensemble Kalman filter: use of observed discharge to update past and present model states for flow forecasts, Hydrol. Earth Syst. Sci. Discuss., 9, 9533-9575, doi:10.5194/hessd-9-9533-2012, 2012.

Montanari, M., Hostache, R., Matgen, P., Schumann, G., Pfister, L., and Hoffmann, L.: Calibration and sequential updating of a coupled hydrologic-hydraulic model using remote sensing-derived water stages, Hydrol. Earth Syst. Sci., 13, 367-380, 2009.

Montzka, C., Moradkhani, H., Weihermüller, L., Hendricks Franssen, H.-J., Canty, M., and Vereecken, H.: Hydraulic parameter estimation by remotely-sensed top soil moisture observations with the particle filter, J. Hydrol., 399, 410-421, 2011.

Moradkhani, H.: Hydrologic remote sensing and land surface data assimilation, Sensors, 8, 2986-3004, doi: 10.3390/s8052986, 2008.

Moradkhani, H., Hsu, K.-L., Gupta, H., and Sorooshian, S.: Uncertainty assessment of hydrologic model states and parameters: sequential data assimilation using the particle filter, Water Resour. Res., 41, W05012, doi: 10.1029/ 2004WR003604, 2005a.

Moradkhani, H., Sorooshian, S., Gupta, H. V., and Houser, P. R.: Dual state-parameter estimation of hydrological models using ensemble Kalman filter, Adv. Water Resour., 28, 135-147, 2005b.

Musso, C., Oudjane, N., and LeGland, F.: Improving regularized particle filters, in: Sequential Monte Carlo in practice, Doucet, A., de Freitas, N., and Gordon, N. (Eds.), Springer, 247-271, 2001.

Nie, S., Zhu, J., and Luo, Y.: Simultaneous estimation of land surface scheme states and parameters using the ensemble Kalman filter: identical twin experiments, Hydrol. Earth Syst. Sci., 15, 2437-2457, doi:10.5194/hess-15-2437-2011, 2011.

Noh, S. J., Tachikawa, Y., Shiiba, M., and Kim, S.: Applying sequential Monte Carlo methods into a distributed hydrologic model: lagged particle filtering approach with regularization, Hydrol. Earth Syst. Sci., 15, 3237-3251, doi:10.5194/hess-15-3237-2011, 2011a.

Noh, S. J., Tachikawa, Y., Shiiba, M., and Kim, S.: Dual state-parameter updating scheme on a conceptual hydrologic model using sequential Monte Carlo filters, Annual Journal of Hydraulic Engineering, JSCE, 55, 1-6, 2011b.

Noh, S. J., Tachikawa, Y., Shiiba, M., and Kim, S.: Sequential data assimilation for streamflow forecasting using a distributed hydrologic model: particle filtering and ensemble Kalman filtering, IAHS Red Book Publication, Floods: From Risk to Opportunity, accepted, 2012.

Oke, P. R., Sakov, P., and Corney, S. P.: Impacts of localisation in the EnKF and EnOI: experiments with a small model, Ocean Dynamics, 57, 32-45, 2007.

Pasetto, D., Camporese, M., and Putti, M.: Ensemble Kalman filter versus particle filter for a physically-based coupled surface-subsurface model, Adv. Water Resour., 47, 1-13, 2012.

Pitt, M. and Shephard, N.: Filtering via simulation: auxiliary particle filters, J. Am. Stat. Assoc., 94, 590-599, 1999.

Plaza, D. A., De Keyser, R., De Lannoy, G. J. M., Giustarini, L., Matgen, P., and Pauwels, V. R. N.: The importance of parameter resampling for soil moisture data assimilation into hydrologic models using the particle filter, Hydrol. Earth Syst. Sci., 16, 375-390, doi:10.5194/hess-16-375-2012, 2012.

Qin, C., Jia, Y., Su, Z., Zhou, Z., Qiu, Y., and Shen, S.: Integrating remote sensing information into a distributed hydrological model for improving water budget predictions in large scale basins through data assimilation, Sensors, 8, 4441–4465, doi: 10.3390/s8074441, 2008.

Qin, J., Liang, S., Yang, K., Kaihotsu, I., Liu, R., and Koike, T.: Simultaneous estimation of both soil moisture and model parameters using particle filtering method through the assimilation of microwave signal, J. Geophy. Res., 114, D15103, doi: 10.1029/2008JD011358, 2009.

Rakovec, O., Weerts, A. H., Hazenberg, P., Torfs, P. J. J. F., and Uijlenhoet, R.: State updating of a distributed hydrological model with ensemble Kalman filtering: effects of updating frequency and observation network density on forecast accuracy, Hydrol. Earth Syst. Sci., 16, 3435-3449, doi:10.5194/hess-16-3435-2012, 2012.

Reed, M., Cuddy, S. M., and Rizzoli, A. E.: A framework for modeling multiple resource management issues - an open modelling approach, Environmental Modelling and Software, 14, 503-509, 1999.

Reichle, R. H., McLaughlin, D. B., and Entekhabi, D.: Variational data assimilation of microwave radiobrightness observations for land surface hydrology applications, IEEE Trans. Geosci. Remote Sensing, 39, 1708-1718, 2001.

Rings, J., Huisman, J. A., and Vereecken, H.: Coupled hydrogeophysical parameter estimation using a sequential Bayesian approach, Hydrol. Earth Syst. Sci., 14, 545-556, doi:10.5194/hess-14-545-2010, 2010.

Ristic, B., Arulampalam, S., and Gordon, N.: Beyond the Kalman filter: particle filters for tracking applications, Artech House, 2004.

Robert, C. P. and Casella, G.: Monte Carlo statistical methods, Springer, New York, 1999.

Salamon, P. and Feyen, L.: Assessing parameter, precipitation, and predictive uncertainty in a distributed hydrological model using sequential data assimilation with the particle filter, J. Hydrol., 376, 428-442, 2009.

Salamon, P. and Feyen, L.: Disentangling uncertainties in distributed hydrological modeling using multiplicative error models and sequential data assimilation, Water Resour. Res., 46, W12501, doi: 10.1029/2009WR009022, 2010.

Schaap, M. G., Leij, F. J., and van Genuchten, M. T.: ROSETTA: a computer program for estimating soil hydraulic parameters with hierarchical pedotransfer functions, J. Hydrol., 251, 163-176, 2001.

Seo, D.-J., Koren, V., and Cajina, N.: Real-time variational assimilation of hydrologic and hydrometeorological data into operational hydrologic forecasting. J. Hydrometeorol., 4, 627-641, 2003.

Seo, D.-J., Cajina, L., Corby, R., and Howieson, T.: Automatic state updating for operational streamflow forecasting via variational data assimilation, J. Hydrol., 367, 255-275, 2009.

Smith, P. J., Beven, K. J., and Tawn, J. A.: Detection of structural inadequacy in process-based hydrological models: a particle-filtering approach, Water Resour. Res., 44, W01410, doi: 10.1029/2006WR005205, 2008.

Storvik, G.: Particle filters for state-space models with the presence of unknown static parameters, IEEE Trans. Signal Proces., 50, 281-289, 2002.

Tachikawa, Y., Nagatani, G., and Takara, K.: Development of stage-discharge relationship equation incorporating saturated–unsaturated flow mechanism, Annual Journal of Hydraulic Engineering, JSCE, 48, 7-12, 2004.

Takasao, T. and Shiiba, M.: Incorporation of the effect of concentration of flow into the kinematic wave equations and its applications to runoff system lumping, J. Hydrol., 102, 301-322, 1988.

van Delft, G., El Serafy, G. Y., and Heemink, A. W.: The ensemble particle filter (EnPF) in rainfall-runoff models, Stoch. Environ. Risk Assess., 23, 1203-1211, 2009.

van Leeuwen, P. J.: Particle filtering in geophysical systems, Mon. Weather Rev., 137, 4089-4114, 2009.

van Velzen, N.: A generic software framework for data assimilation and model calibration, Ph.D. thesis, Delft University of Technology, Netherlands, 2010.

US Army Corps of Engineers, Hydrologic Engineering Center: hydrographs by single linear reservoir model, 1980.

Vo, B.-N., Vo, B.-T., and Singh, S.: Sequential Monte Carlo methods for static parameter estimation in random set models, in: Proc. Intelligent Sensers, Sensor Networks and Information Processing Conference, 2004.

Vrugt, J. A., ter Braak, C. J. F., Clark, M. P., Hyman, J. M., and Robinson, B. A.: Treatment of input uncertainty in hydrologic modeling: doing hydrology

backward with Markov chain Monte Carlo simulation, Water Resour. Res., 44, W00B09, doi:10.1029/2007WR006720, 2008.

Vrugt, J. A., ter Braak, C. J. F., Diks, C. G. H., and Schoups, G.: Hydrologic data assimilation using particle Markov chain Monte Carlo simulation: theory, concepts and applications, Adv. Water Resour., in press, 2012.

Vrugt, J. A., Gupta, H. V., Nuallain, B. O., and Bouten, W.: Real-time data assimilation for operational ensemble streamflow forecasting, J. Hydrolmeteorol., 7, 548-565, 2006.

Weerts, A. H., van Velzen, N., Verlaan, M., Sumihar, J., Hummel, S., El Serafy, G. Y. H., Dhondia, J., Gerritsen, H., Vermeer-Ooms, S., Loots, E., Markus, A., Kockx, A.: OpenDA: open source generic data assimilation environment and its application in geophysical process models, 2011 AGU Fall Meeting, 2011.

Weerts, A. H. and El Serafy, G. Y. H.: Particle filtering and ensemble Kalman filtering for state updating with hydrological conceptual rainfall-runoff models, Water Resour. Res., 42, W09403, doi: 10.1029/2005WR004093, 2006.

Whitaker, J. S. and Hamill, T. M.: Ensemble data assimilation without perturbed observation, Mon. Weather Rev., 130, 1913-1924, 2002.

Whitley, D.: A genetic algorithm tutorial, Stat. Comput., 4, 65-85, 1994.

Yang, X., Xing, K., Shi, K., and Pan, Q.: Joint state and parameter estimation in particle filtering and stochastic optimization, J. Control Theory Appl., 6, 215-220, 2008.

Zhou, Y., McLaughlin, D., and Entekhabi, D.: Assessing the performance of the ensemble Kalman filter for land surface data assimilation, Mon. Weather Rev., 134, 2128-2142, 2006.